# Oligodendrocyte Progenitor Cell Tiling

**Maria F. Ali**
Charlottesville, Virginia

B.S., The College of William and Mary, Williamsburg, Virginia, 2014

A Dissertation presented to the Graduate Faculty of the University of Virginia in Candidacy for the Degree of Doctor of Philosophy

Department of Biology

University of Virginia
June, 2021

**Abstract**

During vertebrate development, oligodendrocyte progenitor cells (OPCs) are specified from gliogenic precursors in the central nervous system (CNS) after neurogenesis. Following specification, OPCs begin a complex process termed tiling that results in OPCs becoming evenly dispersed and occupying non-overlapping territories throughout the CNS. Developmental OPC tiling is comprised of three main components, namely, migration, proliferation, and contact-mediated repulsion (CMR). A few foundational studies have thoroughly characterized these OPC tiling behaviors, however, little is known about how these behaviors interact to result in OPCs being evenly distributed throughout the CNS.

In this dissertation, I begin by providing a comprehensive review of the molecular mediators currently understood to influence the individual behaviors of OPC tiling. I then propose a unified theory of how OPC tiling behaviors interact to produce the emergent property of uniform OPC dispersal throughout the CNS. Then, using zebrafish as a vertebrate model, I demonstrate the first *in vivo* investigation into the role of the Met signaling pathway in regulating OPC tiling, primarily focused on its role in mediating migration and proliferation. Finally, I present evidence regarding other molecular mediators that contribute to developmental OPC tiling and delineate the open questions that remain in our understanding of OPC tiling.

This work fills a gap in our understanding of molecular signaling pathways involved in regulating developmental OPC tiling, which lays a foundation for future investigation into adult tiling and understanding OPC behaviors in disease and injury-response.

## Dedication

The journey of getting my PhD was the most challenging and most rewarding period of my life. I dedicate the work presented here, first and foremost, to the two most important people in my life, William and Francesca. You are the most incredible family that I could have asked for. The comfort of a happy and loving home made every failed experiment, every grant deadline, and every battle with imposter syndrome almost inconsequential. I dedicate this work to my family. My parents, Frank and Charleen, my brother, Christian, his fiancé, Monica, and my cugino, Joe. Thank you to my parents for teaching me that life is about finding the balance between professional excellence and enjoying every moment you get with your family. This work is dedicated to the incredible Williams-Thompson family that welcomed me with both arms open. Thank you Mama T, Annie, Marcus, B, Maya, Tyson, and Christian for always supporting me and cheering me on. This work is dedicated to the sister I found in Jabria, you are my inspiration for always seeking joy, patience, and a great time.

Beyond my incredible family and support group, this work would not have been possible without the sage wisdom and guidance of my mentor, Sarah Kucenas, and Laura Fontenas . You both showed me such kindness and patience in teaching me every aspect of doing zebrafish research. This work is dedicated to Brittany Martinez, my sister throughout this PhD journey. Thank you for teaching me what grace through struggle means and for being my ultimate science role model. Thank you to Gordon Laurie, who's consistent encouragement always reminded me that I am good enough to be a scientist. Thank you to Keisha John for being one of the first people to truly see me and push me to be better than I ever thought I could be.

Self-doubt is the ultimate impediment to the pursuit of a PhD. Thank you to everyone, both named and not, who helped me fight this battle against doubt and who helped me believe that I could accomplish my goal of becoming Dr. Ali.

## Table of Contents

## Table of Figures

# Chapter I

# Introduction

## Oligodendrocyte Progenitor Cell Tiling

During vertebrate development, oligodendrocyte progenitor cells (OPCs) are specified from gliogenic precursors in the central nervous system (CNS), which consists of the brain and spinal cord (Barres, et al., 1993; Dawson, et al., 2000). In the ventral spinal cord, OPCs are specified from ventral progenitor cells marked by expression of the basic helix-loop-helix transcription factor olig2 (Warf, et al., 1991; Noll & Miller, 1993; Lu, et al., 2000; Zhou, et al., 2001; Park, et al., 2002). Following specification, OPCs rapidly disperse throughout the CNS until they occupy distinct, non-overlapping territories (Cai, et al., 2005; Kirby, et al., 2006; De Biase, et al., 2017; Ravanelli, et al., 2018). This process of OPC dispersal is termed developmental OPC tiling and is comprised of three main components: migration, proliferation, and contact-mediated repulsion (CMR) (Kirby, et al., 2006; Hughes, et al., 2013). In the literature, the majority of investigations into OPC development focus on either how OPCs are specified or how OPCs differentiate into oligodendrocytes, the myelinating cells of the CNS (Richardson et al. 2006; Bergles and Richardson 2015; Kearns et al. 2015; Crawford et al. 2016; Nishiyama et al. 2016; Chapman et al. 2018; Ravanelli et al. 2018; Hayashi and Suzuki 2019; Kuhn et al. 2019; Perlman et al. 2020). These studies, while necessary for identifying markers of OPCs and investigating OPC injury-response, leave out a critical window of OPC development where OPCs exhibit foundational tiling behaviors that persist throughout their life in the CNS.

Based on the abundance of studies and proposed mediators of OPC tiling behaviors, it is clear that a comprehensive understanding of the molecular mediators that guide OPC development is needed to understand how individual molecular mediators influence individual OPCs to produce a population of cells that is evenly

dispersed throughout the spinal cord. For this dissertation, I will focus on the conserved mechanism across vertebrates of OPC specification from ventral progenitors in the pMN domain of the spinal cord (Warf, et al., 1991; Noll & Miller, 1993; Zhou, et al., 2001; Park, et al., 2007). Ventral progenitors of OPCs are marked by their expression of the transcription factor olig2, which then upregulate expression of sox10 beginning around 36 hour post fertilization (hpf) in zebrafish, embryonic day 12.5 (E12.5) in mouse, and 10 weeks gestational age in human fetal development (Lu et al. 2000; Zhou et al. 2001; van Tilborg et al. 2017).

While much remains unclear about how individual mediators are regulating this process, there are a few conclusions I can draw from what we currently know about OPC tiling. OPC tiling begins immediately following OPC specification with OPCs migrating out of the pMN domain. From the moment OPCs are specified, it is clear that OPCs exhibit CMR from evidence demonstrating that OPC processes retract even after contact with its own processes (Kirby, et al., 2006; Huang, et al., 2020). Following initial migration, OPCs begin to proliferate. Newly born daughter cells exhibit CMR and migrate rapidly away from one another as they continue their migratory journey to their designated niche within the spinal cord. As OPCs begin to occupy their designated territories, axon-OPC interactions also influence OPC proliferation (Jepson, et al., 2012). As the population of OPCs throughout the spinal cord grows, OPCs begin to become evenly distributed with CMR actively facilitating a consistent minimum distance between neighboring OPCs. Ultimately, OPCs reach a steady-state of dispersal throughout the spinal cord that is maintained through the same developmental tiling behaviors of migration, proliferation, and CMR, as well as, apoptosis in adult OPC tiling (Hughes, et al., 2013; Birey, et al., 2017).

Given this framework for how OPC tiling behaviors are related to each other during development, new investigations are needed that take a comprehensive approach to understanding how the molecular mediators of each of these processes are related to

each other. In this introductory chapter, I will review what is known about mediators of the developmental OPC tiling behaviors of migration, proliferation, and CMR. I will then propose a model for how each of the developmental tiling behaviors interact to achieve OPC dispersal. In subsequent chapters, I will discuss the work I have done to identify mediators of these developmental tiling behaviors and the work left to be done to understand how these pathways are interacting to influence OPC behaviors during developmental tiling.

**Chemotactic signals that influence directional OPC migration**

The bulk of the investigation into mediators of OPC migration have focused on the contributions of chemoattractant and chemorepellent secreted molecules within the developing spinal cord in promoting directional OPC migration (Sugimoto, et al., 2001; Spassky, et al., 2002; Tsai, et al., 2002; Yan & Rivkees, 2002; Jarjour, et al., 2003; Lalive, et al., 2005; Tsai, 2006; Ohya, et al., 2007; Frost, et al., 2009; Mela & Goldman, 2013). The numerous signals identified as modulators of OPC migration were described as a molecular orchestra in a 2005 review and work done since then has continued to make the orchestra of chemotactic signals more complex (De Castro & Bribián, 2005). In brief, chemoattractant molecules that have been shown to induce positive directional migration of pMN derived OPCs include bFBF (basic fibroblast growth factor), PDGF (platelet derived growth factor), HGF (hepatocyte growth factor), 2-AG (endocannabinoid 2-arachidonoylglycerol), and Cxcl12 (C-x-c motif chemokine ligand 12) (Yan and Rivkees 2002; Ohya et al. 2007; Frost et al. 2009; Mela and Goldman 2013; Sanchez-Rodriguez et al. 2018; Watson et al. 2020). Figure 1-1A provides a comprehensive overview of the signaling pathways reported to be involved in regulating chemotactic behaviors in OPCs.

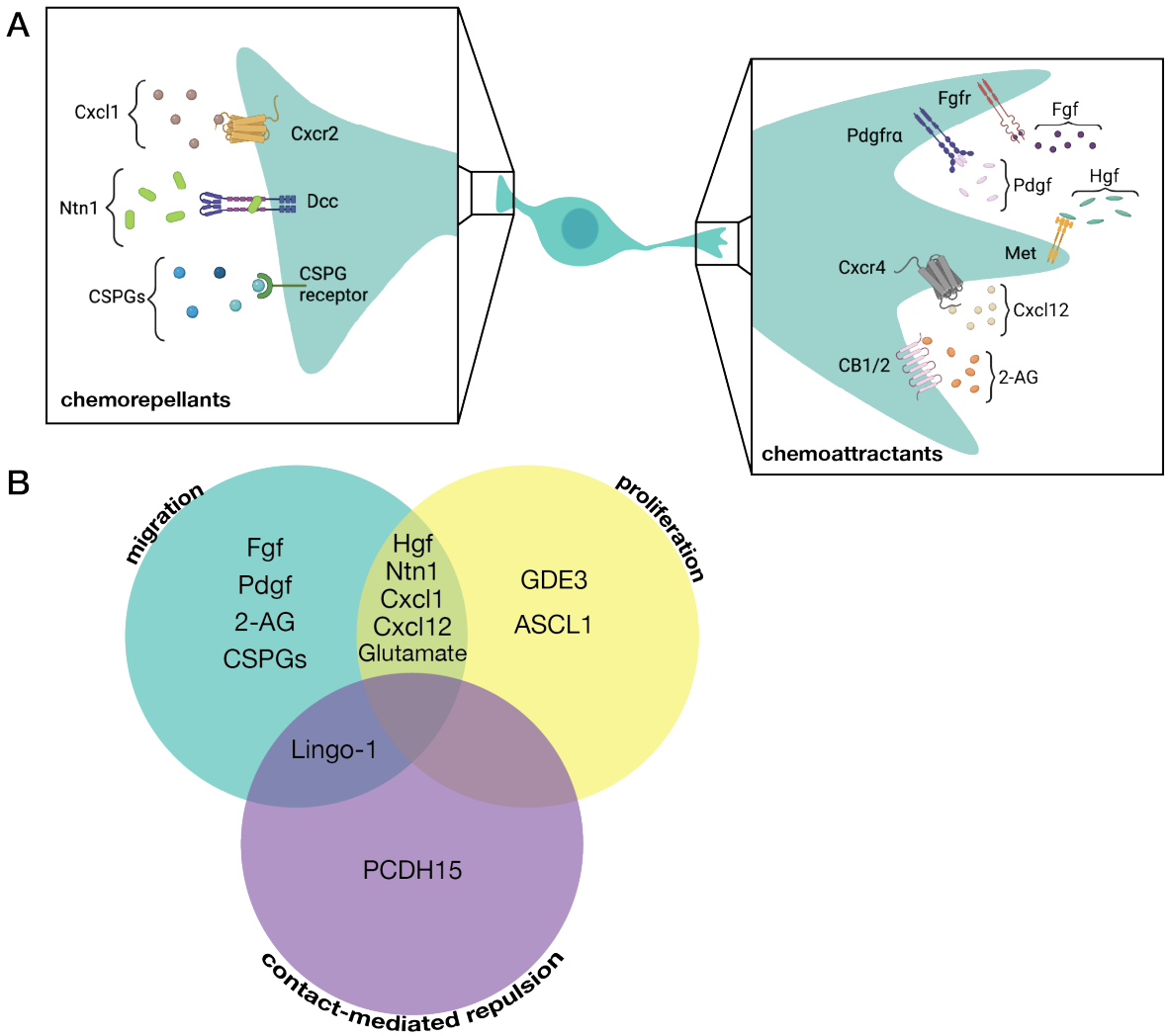


**Figure 1-1. Mediators of Oligodendrocyte Progenitor Cell Tiling.** (A) Diagram of a developing OPC in the spinal cord with chemotactic signaling molecules that guide either chemorepellent or chemoattractant migration. Chemoattractants include: Fibroblast growth factor (Fgf) signaling through its receptor Fibroblast growth factor receptor (Fgfr), Platelet derived growth factor (Pdgf) signaling through its receptor Platelet derived growth factor receptor alpha (Pdgfrα), Hepatocyte growth factor (Hgf) signaling through its receptor Mesenchymal-epithelial transition (Met), C-x-c motif chemokine ligand 12 (Cxcl12) signaling through its receptor C-x-c chemokine receptor 4 (Cxcr4), and 2-Arachidonoylglycerol (2-AG) signaling through its receptors Cannabinoid receptor type 1 and type 2 (CB1/2). Chemorepellents include: C-x-c motif chemokine ligand 1 (Cxcl1) signaling through its receptor C-x-c motif chemokine receptor 2 (Cxcr2), Netrin-1 (Ntn1) signaling through its receptor Deleted in colorectal carcinoma (Dcc), and Chondroitin Sulfate Proteoglycans (CSPGs) signaling through their cognate receptors. A cocktail of various CSPGs was used in this study, making it unclear exactly which CSPGs mediate this process. (B) Venn-Diagram demonstrating mediators that contribute to multiple tiling processes. GDE3 (Glycerophosphodiester

phosphodiesterase 3), ASCL1 (Achaete-Scute Family BHLH Transcription Factor 1), Lingo1 (Leucine-Rich Repeat and Immunoglobulin-like Domain Containing Nogo Receptor-Interacting Protein 1), PCDH15 (Protocadherin Related 15).

Chemorepellent molecules that either reverse or stop the directional migration of OPCs include Cxcl1 (C-x-c motif chemokine ligand 1), Ntn1 (Netrin-1), and CSPGs (chondroitin sulphate proteoglycans) (Tsai et al. 2002; Jarjour et al. 2003; Tsai 2006; Sun et al. 2017; Watson et al. 2020). These studies demonstrate that there are numerous chemotactic signals that influence OPC migration during development, but, the majority of studies that investigated mediators of OPC migration were conducted on OPCs in culture, which makes it difficult to discern exactly when these signaling pathways would be active during *in vivo* development. For example, the role of Met signaling was extensively shown to influence OPC migration and proliferation for OPCs in culture (Yan & Rivkees, 2002; Lalive, et al., 2005; Ohya, et al., 2007), however, mouse mutants for *Met* are embryonic lethal. Therefore, in Chapter III, I discuss the first *in vivo* investigation into the role of Met signaling in OPC tiling that I conducted utilizing zebrafish.

In the handful of *in vivo* studies that assess OPC migration in an altered chemotactic background, there was a population of OPCs that was still able to migrate (Tsai, et al., 2002; Tsai, 2006). This result indicates that different populations of OPCs respond to different chemotactic signals and a comprehensive approach to studying the combinatorial effects of these chemotactic signals is needed to parse out which populations of OPCs are sensitive to each chemokine. An intriguing possibility is that these chemotactic responses of OPCs are regulated by levels of receptor expression. It is possible that different subsets of OPCs express different combinations of these receptors at different timepoints and this differential expression can result in OPC dispersal that is evenly distributed throughout the CNS.

**Mitogenic mediators of OPC proliferation**

Following initial migration, OPCs exhibit robust proliferation in both the dorsal and ventral spinal cord. Numerous investigations have explored various mediators of OPC proliferation in response to demyelinating events and spinal cord injury (Patel, et al., 2012; L. Li, et al., 2018; Ying, et al., 2018; Adams, et al., 2020). However, only a handful of studies have sought to identify mediators of developmental OPC proliferation. The majority of proposed mediators of OPC proliferation have been identified for their contribution as both chemotactic and mitogenic signals for OPCs during development (Figure 1-1B). For example, Cxcl1 and Cxcl12 have opposite effects on OPC migration, but are both purported to stimulate OPC proliferation (Watson, et al., 2020). Additionally, the Met signaling pathway has been shown to promote OPC proliferation, which I explore further in Chapter III (Ohya, et al., 2007). In Chapter IV, I present evidence demonstrating that Ntn1 may also influence OPC proliferation.

Beyond these dual mediators of migration and proliferation, a handful of canonical mediators of proliferation have been identified, such as GDE3 (glycerophosphodiester phosphodiesterase 3), which negatively regulates OPC proliferation and ASCL1, a transcriptional regulator that is required to stimulate OPC proliferation (Kelenis, et al. 2018; Dobrowolski, et al. 2020). The identification of these mediators of OPC proliferation indicates that achieving the appropriate number of OPCs during development involves a complex balance of positive and negative modulators of OPC proliferation. Additionally, a recent study demonstrates that axon-OPC interactions also play a role in regulating OPC proliferation and that increased $Ca^{2+}$ signaling through AMPA-receptors at axon-OPC synapses directly increases OPC proliferation (Chen, et al., 2018). This feedback loop from neuronal signaling to increasing OPC proliferation indicates that the niche that OPCs occupy is also directly regulating the number of OPCs present. Taken together, these studies demonstrate that

OPC proliferation is regulated through intrinsic mediators during their initial migratory phase and by axon-glial signaling in the OPC niche following developmental migration.

**Proposed mediators of OPC contact-mediated repulsion**

The least investigated process of OPC tiling is CMR. Foundational studies demonstrated that OPCs retract their process and alter their direction of migration following contact with other OPCs (Kirby, et al., 2006; Hughes, et al., 2013). The majority of investigations into CMR have examined the role of CMR in the dispersal of various neuronal cell types during development (Noren & Pasquale, 2004; Egea & Klein, 2007; Grueber & Sagasti, 2010; Villar-Cerviño, et al., 2013). Canonical mediators of CMR are transmembrane proteins capable of bi-directional signaling, such as Eph-Ephrin signaling, Dscams (Down syndrome cell adhesion molecules), and Lingo1 (Leucine-Rich Repeat And Immunoglobulin-Like Domain-Containing Nogo Receptor-Interacting Protein 1) (Zimmer, et al., 2003; Noren & Pasquale, 2004; Millard, et al., 2007; Mayor & Carmona-Fontaine, 2010). Ephrin signaling and Lingo1 have been implicated in influencing axon-OPC interactions and OPC positioning (Prestoz, et al., 2004; Jepson, et al., 2012). In Chapter IV, I investigate a *lingo1a* mutant that demonstrates tiling defects consistent with what would be expected if *lingo1a* is involved in CMR. Additionally, in an RNA-seq experiment conducted by Dr. Andrew Latimer, OPCs were shown to uniquely express the zebrafish Dscam orthologs, *dscama* and *dscamb*. A recently published paper that conducted single-cell RNA-seq on OPCs derived from the human cortex found that *DSCAM* is uniquely enriched in these cells (Huang, et al., 2020). However, knock-down of *DSCAM* using shRNA showed no effect on OPC CMR (Huang, et al., 2020). In Chapter IV, I also demonstrate no change in OPC CMR in *dscama* mutants compared to wildtype. Intriguingly, however, Huang, et. al., found *PCDH15* to be uniquely expressed by OPCs and demonstrated that inhibiting PCDH15 resulted in a failure of OPCs to separate and migrate away from

each other following cell division (2020). This exciting new discovery lays the groundwork for investigating the contribution of CMR to OPC tiling by modulating this newly identified mediator of OPC CMR.

**Using zebrafish as a model for studying OPC tiling**

To study OPC tiling dynamics in the developing spinal cord, I utilize zebrafish as a vertebrate model. Zebrafish have a number of advantages compared to other model species because the rapid *ex utero* development of optically-transparent zebrafish embryos allows for non-invasive imaging of OPC tiling behaviors (Meyers, 2018). Additionally, the advent of CRISPR/Cas9 technology and the use of *Tol2* transposable elements to make transgenic zebrafish lines allows for the rapid investigation of OPC development utilizing genetic manipulations, such as gene knock-down, dominant negative inhibition of signaling, and fluorescent labeling of OPCs in the developing spinal cord (Kawakami, 2004; Hwang, et al., 2013).

In this dissertation, I demonstrate the contributions of various molecular mediators to OPC tiling behaviors. In Chapter III, I demonstrate the first *in vivo* investigation into the contribution of the Met signaling pathway to initiating OPC migration and show that Met is required for OPC migration and proliferation during the migratory phase of OPC tiling. Additionally, I identify that radial glia secrete the Met ligand, Hgf, in the spinal cord, which then causes OPCs to initiate migration. Characterization of the Met signaling pathway from the source of the ligand, Hgf, to the cell-autonomous expression of the Met receptor on OPCs during developmental tiling demonstrates the type of comprehensive approach that needs to be taken with other proposed mediators of tiling in order to fully understand the temporal regulation of the molecular mechanisms that drive OPC tiling. In Chapter IV, I demonstrate the contributions of novel mediators of OPC tiling behaviors, primarily focused on

proliferation and CMR. I present evidence that *lingo1a* is a novel mediator of OPC CMR. I also present evidence for a novel role of *ntn1* in mediating proliferation of OPCs.

Taken together, studies presented in this dissertation demonstrate novel mediators of OPC tiling that expand our understanding of glial tiling and spinal cord development.

# Chapter II

## Materials and Methods

Materials and methods presented in this chapter apply to all experiments presented in this dissertation and should be used as a reference for all subsequent chapters.

### Zebrafish Husbandry

All animal studies were approved by the University of Virginia Institutional Animal Care and Use Committee. Zebrafish strains used in this study were: AB*, *met*$^{uva38}$, *met*$^{fh534}$, *Tg(sox10(4.9):tagrfp)*$^{uva5}$,*Tg(olig2:egfp)*$^{vu12}$ (Shin, et al., 2003); *Tg(sox10(7.2):mrfp)*$^{vu234}$ (Kucenas, et al., 2008); *met*$^{egfp}$, *Tg(sox10(4.9):DNmet::IRES:egfp; cry:egfp)*$^{uva40}$; *Tg(olig1(5.3):DNmet::IRES:egfp; cry:egfp)*$^{uva39}$; *hgfa*$^{fh529}$ (Isabella, et al., 2020), *ftl*, *dscama*$^{-15bp}$, and *lingo1a*$^{uva28}$. Table 1 denotes abbreviations used for each mutant and transgenic line. Embryos were raised at 28.5°C in egg water and staged by hours or days post fertilization (hpf and dpf, respectively) (Kimmel, et al., 1995). Embryos of either sex were used for all experiments. Phenyl-thiourea (PTU)(0.004%) (Sigma) in egg water was used to reduce pigmentation for imaging. Stable, germline transgenic lines were used in all experiments.

**Table 1. Zebrafish lines used in this study and their genotypes**

| Full Name | Abbreviation | Reference |
|---|---|---|
| AB* | wildtype | |
| *Tg(olig2:egfp)*$^{vu12}$ | *olig2:egfp* | Shin et al. 2003 |
| *Tg(sox10(4.9):tagrfp)*$^{uva5}$ | *sox10:tagrfp* | Zhu et al. 2019 |
| *met*$^{fh555Tg}$ | *met*$^{egfp}$ | Ali et al. 2021 |
| *Tg(sox10(7.2):mrfp)*$^{vu234}$ | *sox10:mrfp* | Kucenas et al. 2008 |

| | | |
|---|---|---|
| *met*$^{uva38}$ | *met*$^{-/-}$ | Ali et al. 2021 |
| *Tg(sox10(4.9):DNmet::IRES:egfp; cry:egfp)*$^{uva40}$ | *sox10:DNmet* | Ali et al. 2021 |
| *Tg(olig1(5.3):DNmet::IRES:EGFP; cry:EGFP)*$^{uva39}$ | *olig1:DNmet* | Ali et al. 2021 |
| *hgfa*$^{fh529}$ | *hgfa*$^{-/-}$ | Isabella et al. 2020 |
| *met*$^{fh534}$ | *met*$^{fh534/fh534}$ | Ali et al. 2021 |
| *failure to launch* | *ftl*$^{-/-}$ | This dissertation |
| *dscama*$^{\perp 5bp}$ | *dscama*$^{\perp 5bp/\perp 5bp}$ | This dissertation |
| *lingo1a*$^{uva28}$ | *lingo1a*$^{-/-}$ | This dissertation |

**Generation of transgenic lines**

All constructs were generated using the Tol2kit Gateway-based cloning system (Kwan, et al., 2007). Vectors used for making the expression constructs were p5E-sox10(-4.9) (Carney, et al., 2006), p5E-olig1(-5.3) (Ali et al. 2021), pME-DNmet (Ali et al. 2021), p3E-IRES-EGFPpA, and pDestTol2pA2 destination vector (Kwan, et al., 2007).

To generate p5E-olig1, 5.3 kb of sequence immediately upstream of the *olig1* gene (Ensembl: ENSDARG00000040948) was amplified from wildtype genomic DNA using the following primers: forward 5'-GTATGAAGCCTCTTGGCACAG-3' and reverse 5'-CTGAAAAAAGATATTCAGAGAACATGG-3', as previously described (Auer et al. 2018). The resulting PCR product was subcloned into pENTR™ 5´-TOPO (Invitrogen) to generate a p5E entry for Gateway cloning and was verified by sequencing. The *olig1* promoter was created by Dr. Laura Fontenas.

To generate pME-DNmet, I used the Q5 Site-Directed Mutagenesis Kit (NEB) and generated site-specific mutations in *met* cDNA, which we generated used RT-PCR as

described below, using the following primers: forward 5'-CAACATCGACAAAATGACACCCTTCCCCTCTCTCATATCATCTCAG-3' and reverse, 5'-ACGAAGGTGGTGTTCAGGAGGATGAAGTGCTCTCCGCTGAAGC-3'. I confirmed the mutations using sequencing, then subcloned the cDNA containing the DNmet mutations into pME-MCS to generate a pME entry for Gateway cloning. p5E, pME, and p3E-IRES-EGFPpA vectors were ligated into destination vectors through LR reactions (Ashton, et al., 2012). Final constructs were amplified, verified by restriction digest, and sequenced to confirm the insertions. To generate stable transgenic lines, plasmid DNAs were microinjected at a concentration of 25 ng/μL in combination with 10 ng/μL *Tol2* transposase mRNA at the one-cell stage and screened for founders (Kawakami, 2004).

The *met*$^{fh555Tg}$ enhancer trap line was generated using the CRISPR/Cas9-mediated knock-in strategy described in (Kimura, et al., 2014). 1 nL of a cocktail of the following components was injected into one-cell stage embryos: 66.6 ng/μL each of 3 CRISPR guide RNAs targeting within or just upstream of the *met* 5' UTR (target sequences GGTCTCGGGATGGGATGCGA, GGTTCTCTCCGCAAACGCTG, and GGGTAAGCGGGTTCGCTGAT), 200 ng/μL Mbait gRNA, 20 ng/μL Mbait-hsp70-GFP plasmid, 800 ng/μL Cas9 protein (PNABio #CP02). Founders were screened for *GFP* expression replicating the known *met* expression pattern.

The *met*$^{fh534}$ allele was made using standard CRISPR/Cas9 mutagenesis protocol (Talbot & Amacher, 2014). One cell stage embryos were injected with 100 pg each of 2 CRISPR guide RNAs (target sequences GGTTCTGGCCATCTGGCTCG and GGCTTCGGCTGCGTGTTTCA) and 500 pg Cas9 protein, and F1 mutant animals were identified by sequencing. *met*$^{fh534}$ is a 25bp deletion starting at nucleotide

3275 of the coding sequence, resulting in a frameshift at amino acid 1093 and a premature stop at amino acid 1105. The *met*$^{fh555Tg}$ enhancer trap line and *met*$^{fh534}$ allele were generated in the lab of Dr. Cecilia Moens by Dr. Adam Isabella.

### *In vivo* imaging

Embryos were anesthetized with 0.01% 3-aminobenzoic acid ester (Tricaine), immersed in 0.8% low-melting point agarose and mounted in glass-bottomed 35 mm Petri dishes (Electron Microscopy Sciences). After mounting, the Petri dish was filled with egg water containing PTU and Tricaine. A 40X water objective (NA = 1.1) mounted on a motorized Zeis AxioObserver Z1 microscope equipped with a Quorum WaveFX-X1 (Quorum Technologies) or Andor CSU-W1 (Oxford Instruments) spinning disc confocal system was used to capture all images. Images were imported into MetaMorph (Molecular Devices) and/or ImageJ. Time-lapse images were analyzed using cell tracking software as previously described in (Wang, et al., 2018). All images were then imported in Adobe Photoshop and Illustrator. Adjustments were limited to levels, contrast, and cropping.

### Cell tracking software

The cell tracking software was generated in the lab of Dr. Guoqiang Yu by Dr. Yinxue Wang. For quantification and motility analysis of OPCs, we developed an automated software to detect and track motile cells in time-lapse imaging experiments of *olig2:egfp* embryos and larvae (Wang, et al., 2018). To correct for photobleaching, we normalized fluorescence intensity to an identical mean and an identical variance at all time points and to account for long-term image shift due to larval growth, we used global image registration. For intra-frame detection and segmentation of all cells, we applied the cell detection algorithm SynQuant to map the second-order derivative transformed intensity (Wang, et al., 2020). The under-segmentation and over-segmentation in intra-

frame detection were then corrected by imposing temporal consistency of segmentation, which was modeled as an optimization problem. Rapid motion was detected by testing regional intensity change and to link the detections, we adapted our established algorithm muSSP to a mixed motion model form (Wang, et al., 2019).

The motion patterns of all obtained traces were then analyzed to obtain a quantification of cell motility and to distinguish OPCs from other cells in the field of view. The distance traveled was calculated by adding up the magnitude of displacement between any two consecutive time points and the instantaneous velocity of any *olig2*$^{+}$ OPC was approximated by the average velocity between two consecutive time points, while the instantaneous speed was the magnitude of it. The overall average speed was the distance traveled divided by time period and we identified OPCs from neighboring cells by hypothesis testing on the instantaneous velocity. Assuming the majority of cells in the field of view were not moving, the null distribution was learned by fitting a multivariate Gaussian distribution to all instantaneous velocity values of the obtained traces. Any cell whose trace once had significantly high instantaneous velocity was identified as an OPC.

**Wholemount Immunohistochemistry**

Dechorionated embryos and larvae were fixed with 4% PFA for 1 hour at room temperature (RT), washed in PBSTX (1% Triton X-100, 1x PBS) for 5 min, followed by a 5 minute wash with DWTx (1% Triton X-100 in $DH_2O$), then permeabilized in acetone at RT for 5 min and at -20 °C for 10 min, followed by a 5 min wash with PBSTx. Embryos were then blocked in 5% goat serum/PBSTx for 1 hr, incubated in primary antibody with 5% goat serum/PBSTx for 1 hr at RT and overnight at 4°C. Embryos were washed extensively with PBSTx at RT and incubated in secondary antibody overnight at 4°C. After antibody incubation, embryos were washed extensively

with PBSTx and stored in PBS at 4°C until imaging. The following antibodies were used: rabbit anti-Sox10 (1:5000) (Binari, et al., 2013), Alexa Fluor 647 goat anti-rabbit IgG(H+L) (1:1000; ThermoFisher). Embryos were mounted in glass-bottomed Petri dishes for imaging as described above.

**Immunohistochemistry on sections**

Embryos and larvae were fixed in 4% PFA for 2 hr at RT. After fixation, the embryos were sectioned by embedding them in 1.5% agarose/30% sucrose and frozen in 2-methylbutane chilled by immersion in liquid nitrogen. We collected 20 µm transverse sections on microscope slides using a cryostat microtome. Sections were rehydrated in PBS for 1 hr and blocked with 5% goat serum/PBS for 1 hr at RT. Primary antibody incubation was done overnight at 4°C. Secondary antibody incubation was done for 2 hr at RT. Antibodies used were: rabbit anti-Sox10 (1:5000) (Binari, et al., 2013), mouse 3D4 anti-met (1:100; ThermoFisher), mouse anti-Zrf1 (1:1000; ZIRC), mouse anti-HGF (1:500; ABclonal), Alexa Fluor 647 goat anti-rabbit IgG(H+L)(1:1000), and Alexa Fluor 568 goat anti-mouse IgG(H+L) (1:1000). Sections were covered with Aqua-Poly/Mount (Polysciences). A 63X oil objective (NA = 1.4) mounted on a motorized Zeiss AxioObserver Z1 microscope equipped with a Quorum WaveFX-X1(Quorum Technologies) or Andor CSU-W1 (Andor Oxford Instruments) spinning disc confocal system was used to capture all images. Images were imported into Image J and Adobe Photoshop and Illustrator. Adjustments were limited to levels, contrast, and cropping.

***In situ* hybridization**

Larvae were fixed in 4% PFA at 4°C overnight and stored in 100% methanol at -20°C and processed for *in situ* RNA hybridization as previously described (Hauptmann & Gerster, 2000). Plasmids were linearized with appropriate restriction enzymes and cRNA preparation was carried out using Roche DIG-labeling reagents and RNA

polymerases (NEB). I used previously published probes for *olig2* (Park, et al., 2002), *ntn1a* (Vanderlaan, et al., 2005), *hgfa* (Haines, et al., 2004), and *mbpa*. *Mag, cldnk, cd59,* and *ntn1b* probes were generated using the following primers: *mag* (forward primer: 5'-CACGCACTCAGATGGGTACA-3', reverse primer: 5'-TAATACGACTCACTATAGGTTAAACTTTGAGCCCAGGAGC-3'), *cldnk* (forward primer: 5'-TCACAGCCTTCATCGGGAAC-3', reverse primer: 5'-TAATACGACTCACTATAGGTCCAGCAAACAGGCACAAG-3'), *cd59* (forward primer: 5'-GCCTGCTTGTCTGTCTACGA-3'; reverse primer: 5'-TAATACGACTCACTATAGAGGTGACGAGATTAGCTGCG-3'), and *ntn1b* (forward primer: 5'-CGTTACACTTACACCGTCCAC-3', reverse primer: 5'-TATAGTGAGTCGTATTAATTTCCGTTACACTTACACCGTCCAC-3') and t7 RNA polymerase. Sectioning was performed as described above and sections were covered with Aqua-poly/mount (Polysciences). Images were obtained using a Zeiss AxioObserver inverted microscope equipped with Zen, using a 63x oil immersion objective.

**Chemical treatments**

For glutamate inhibitor experiments, dechorionated *sox10:mrfp* larvae were treated from 24 hpf to 72 hpf with 1% Dimethyl Sulfoxide (DMSO) or DL-*threo*-β-Benzyloxyaspartic acid (DL-TBOA or TBOA) (Tocris) at either 0.2 or 0.4 mM in PTU egg water.

In our initial small molecule screen, dechorionated *olig2:egfp* larvae were treated with 10 μm kinase inhibitor in 1% DMSO in PTU egg water from 24 to 76 hours post fertilization (hpf). Kinase inhibitors used were 1 of 430 kinase inhibitors from the L1200 Kinase Inhibitor Library (Selleck Chem), MK-2461 (Selleck Chem), or Trichostatin-A (TSA) (Selleck Chem). Control siblings were treated with 1% DMSO in PTU egg water. The small molecule screen was conducted in triplicate.

For the EdU incorporation assay, larvae were treated with 0.4 mM EdU in 4% DMSO for 6 hours in PTU egg water at 28.5°C then fixed for 1 hr in 4% PFA at RT. Larvae were washed for 5 min with 1X PBSTX, 5 min in DWTX, then permeabilized with cold acetone for 10 min at −20 °C and stained for EdU using the Click-it EdU Cell Proliferation kit for Imaging with Alexa Fluor 647 dye (ThermoFisher), as detailed in the kit protocol. Click-it reaction was performed for 1 hr at RT and thoroughly washed overnight with PBSTX prior to imaging.

**Genotyping**

Genomic DNA was extracted using HotSHOT (hot sodium hydroxide and tris) and PCR was performed using GoTaq green master mix (Promega) (Truett, et al., 2000). The primers used for genotyping *met*$^{uva38}$ are as follows: forward 5'-ATCGTACGCATGTGTTCTTCAG-3' and reverse 5'-TGATGTCCGTGATGGAGATAAG-3'. The primers used for genotyping *met*$^{fh534}$ are as follows: forward 5'-AATCTCTGCCATGTTTTCCTGT-3' and reverse 5'-AGTCCAAAACTATCCCAAGCAA-3'. The primers used for genotyping *dscama*$^{\lrcorner 15bp}$ are as follows: forward 5'- GGCATCCCTACTAACCACACAT-3' and reverse 5'-AAGTGGAAGATCTGGAGAGTGC-3'. The primers used for genotyping *lingo1a*$^{uva28}$ are as follows: forward 5'- GCAAGAATCGAATCAAAACCAT-3' and reverse 5'-CTGGAACATGTAGTCCAGCAGA-3'.

**RT-PCR**

mRNA was extracted and cDNA synthesized as described previously (Peterson & Freeman, 2009) with the use of a RNA easy Mini kit (Qiagen) and High-capacity cDNA Reverse Transcription kit (Applied Biosystems) according to manufacturer instructions. Equal amounts of mRNA were used for cDNA synthesis, and PCR was performed

using GoTaq green master mix (Promega). The following primers were used: *ef1a* forward: 5'-GAGACTGGTGTCCTCAAGCC-3' and reverse: 5'-CCAACGTTGTCACCAGGAGT-3', and *met*$^{mva38}$ forward: 5'-ATCGTACGCATGTGTTCTTCAG-3' and reverse: 5'-TGATGTCCGTGATGGAGATAAG-3'.

**Morpholino injections**

*Netrin1a* and *b* morpholinos (MOs) were obtained from Gene Tools, LLC: *ntn1a*-202, 5'-GCATCAGAGACTCTCAACATCCTCG-3' and *ntn1b*-202, 5'-CGCACGTTACCAAAATCCTTATCAT-3'. MOs were suspended in sterile $dH_2O$ and injected into wildtype embryos at 0.6 mM for *ntn1a* and *b* individually or 0.4 mM for each MO when injected together.

**TUNEL Assay**

Embryos were fixed and sectioned as described above. Sections were fixed for 10 minutes with 1% PFA at RT, washed for 2x 5 minutes with 1X PBS, incubated for 5 minutes in Ethanol:Acetic Acid (2:1) at -20°C, then washed again for 2x 5 minutes with 1X PBS. Sections were then equilibrated for 60 minutes with $ddH_2O$, then incubated in TdT enzyme for 60 mins at 37°C, followed by 3x 1 min PBS washes. Anti-DIG antibody was applied for 30 min in the dark then washed continuously for 40 minutes with PBS and mounted with Vecta-shield (Vector Labs).

**Statistical Analysis**

GraphPad PRISM 9 software was used to plot data and perform statistical analyses. Pairwise comparison *p*-values involving only 2 groups were calculated using a Student's two-tailed *t*-test. Pairwise comparison *p*-values involving more than 2 groups were calculated using a one-way ANOVAs followed by Dunnett's Multiple Comparison tests

or Tukey's Multiple Comparison test. The data in plots and the text are presented as means ± SEM.

# Chapter III

## The Met Signaling Pathway in Oligodendrocyte Progenitor Cell Tiling


### Abstract

Oligodendrocyte progenitor cells (OPCs) are a group of highly motile cells in the central nervous system (CNS) that migrate rapidly until they occupy distinct, non-overlapping domains throughout the CNS. This migration is part of the overall developmental OPC process termed tiling that is comprised of migration, proliferation, and contact-mediated repulsion. Using live *in vivo* imaging in zebrafish larvae in combination with various molecular genetic techniques, I demonstrate that the Met signaling pathway, comprised of the ligand, hepatocyte growth factor (Hgf), and the receptor, Met, is required for two aspects of OPC tiling: migration and proliferation. By utilizing zebrafish as a vertebrate model, I conducted the first *in vivo* investigation into the role of Met signaling and OPC tiling.


### Introduction

During vertebrate spinal cord development, OPCs are specified from ventral gliogenic precursors (Warf et al. 1991; Lu et al. 2000; Dimou et al. 2008; Ravanelli et al. 2018). Immediately following specification, these cells undergo a process termed tiling where they actively disperse throughout the spinal cord, ultimately forming non-overlapping domains with neighboring OPCs (Hughes, et al., 2013; De Biase, et al., 2017). Although tiling is a behavior that has been extensively studied in the context of neuronal development, very few studies have characterized these events in glia (Cameron & Rao, 2010; Grueber & Sagasti, 2010; Villar-Cerviño, et al., 2013; Nichols, et al., 2018). The process of OPC tiling is comprised of three main cellular behaviors: migration, proliferation, and contact-mediated repulsion. Though the phenomenon of OPC tiling is well-described, the molecular mediators of this process remain largely

unknown. What has been identified are a number of chemoattractant or chemorepellent molecules that influence OPC migration (Spassky, et al., 2002; Tsai, et al., 2002; Jarjour, et al., 2003; Tsai, 2006). In this study, I sought to identify, in an unbiased manner, molecular mediators that govern the initial migration of OPCs during developmental tiling. Using an unbiased small molecule screen, I identified several pathways, including Met signaling, as essential mediators of OPC migration.

Previous *in vitro* studies revealed that hepatocyte growth factor (Hgf), the ligand for Met, acts as a chemotactic signal for OPCs (Yan & Rivkees, 2002; Lalive, et al., 2005; Ohya, et al., 2007). Met, also known as scatter factor receptor or Hgf receptor, is a widely studied receptor tyrosine kinase that is involved in a number of morphogenetic processes during embryogenesis, including regulating cellular migration and motility (Soriano, et al., 1995; Prat, et al., 1998; Birchmeier & Gherardi, 1998; Viticchiè, et al., 2015; J. Zhang & Babic, 2015). In particular, OPCs in culture, upon application of Hgf, exhibit increased migration and proliferation (Yan & Rivkees, 2002; Lalive, et al., 2005; Ohya, et al., 2007). Additionally, it is well documented that OPCs express the c-Met receptor (Kilpatrick, et al., 2000; Lalive, et al., 2005; Ohya, et al., 2007; Mela & Goldman, 2013). Though these studies established foundational work supporting Met as a possible mediator of OPC migration, further investigation into the role of Met signaling in regulating developmental OPC migration *in vivo* were impeded because mouse *Met* mutants are embryonic lethal.

In order to study the role of Met signaling *in vivo,* I utilized zebrafish as a vertebrate model. Because zebrafish embryos receive maternal mRNAs, including *met* mRNA from their mother (Latimer & Jessen, 2008), zebrafish *met* mutants are able to successfully complete embryogenesis and can therefore be used to investigate later developmental processes, including OPC migration. In fact, many recent studies have used zebrafish embryos and larvae lacking Met function to study a number of

development processes including motor axon targeting and migratory muscle precursor migration (Talbot, et al., 2019; Nord, et al., 2019; Isabella, et al., 2020).

Here, I describe the identification of the Met receptor as an essential mediator of OPC migration. Using a combination of pharmacological and genetic manipulations with *in vivo,* time-lapse imaging and a new software to analyze OPC migration dynamics, I demonstrate that Met signaling is required for the initial, dorsal migration of OPCs during development of the vertebrate spinal cord. Furthermore, by modulating Met signaling using cell-specific drivers, I show that Met signaling acts cell-autonomously within OPCs. Together, my results demonstrate that Met signaling regulates initial OPC migration during developmental tiling.

## Results

### Met inhibition impairs developmental OPC migration

While the phenomena of OPC migration and tiling are well known, few mediators of this process have been identified. Therefore, to identify molecular mediators of OPC tiling, I conducted an unbiased kinase inhibitor screen in zebrafish embryos and larvae. To do this, I treated *olig2:egfp* zebrafish embryos*,* where *olig2* regulatory sequences drive expression of GFP in motor neurons and oligodendrocyte lineage cells (OLCs), with 1% DMSO as a control, 0.2 μM Trichostatin A (TSA) in 1% DMSO, or 10 μM of 1 of 430 kinase inhibitors from the Selleck Kinase Inhibitor Library in 1% DMSO. I used TSA as a positive control because it is a histone deacetylase (HDAC) inhibitor that blocks OPC specification and, therefore, embryos treated with this compound would not exhibit OPC migration into the dorsal spinal cord (Cunliffe & Casaccia-Bonnefil, 2006) (Figure 3-1A and B). I treated the embryos from 24 hours post fertilization (hpf), which is prior to OPC specification, until 76 hpf, which is during the middle-to-late migratory phase of these cells. By treating prior to OPC specification, I sought to identify molecular mediators that affect OPC migration,

but do not block OPC specification. If I observed a complete absence of OPC migration, similar to that which occurs in the presence of TSA, then it is possible that the small molecule affected either OPC specification or migration. However, if I saw defects in migration, but there were still OPCs present, then the kinase inhibitor likely did not affect specification.

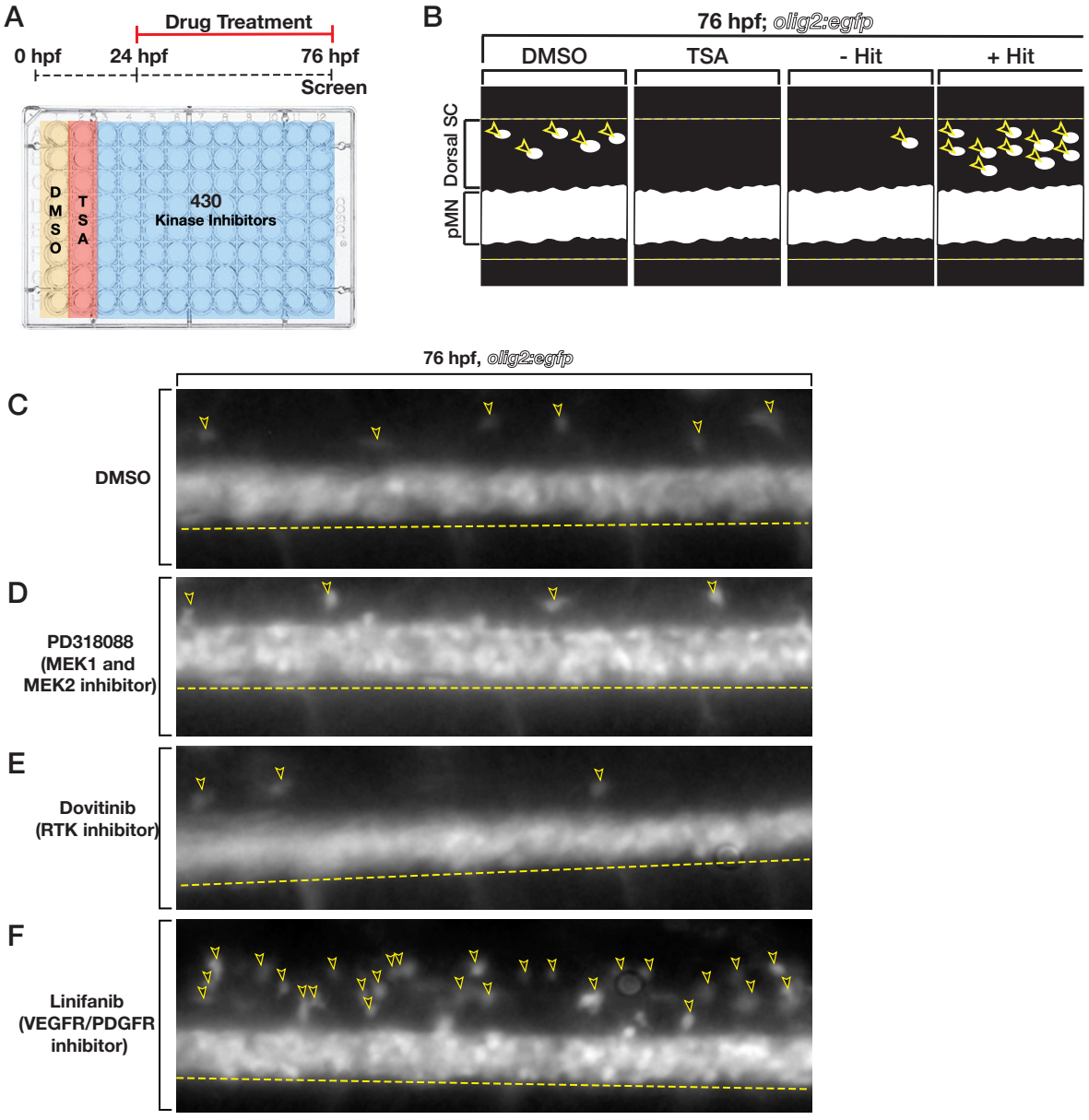


**Figure 3-1. Kinase inhibitor screen identifies small molecules that alter OPC migration.** (A) Schematic of the kinase inhibitor screen and treatment paradigm that tested 430 kinase inhibitors for developmental OPC migration defects. Trichostatin A (TSA), which inhibits OPC specification, was used as a positive

control. (B) Cartoon of a lateral view of 76 hpf *olig2:egfp* larvae spinal cord showing DMSO (negative control), TSA (positive control), and examples of possible hits: reduced OPCs in the dorsal spinal cord (SC) and increased OPCs in the dorsal SC. pMN denotes pMN domain. (C-F) Low magnification images of lateral views of 76 hpf *olig2:egfp* larvae spinal cords treated with (C) DMSO, (D) PD318088 (Mitogen-activated protein kinase kinase 1 (MEK1) and MEK2 inhibitor), (E) Dovitinib (Receptor Tyrosine Kinase (RTK) inhibitor), and (F) Linifanib (Vascular endothelial growth factor receptor (VEGFR)/PDGFR inhibitor). Arrowheads denote OPCs. Yellow dashed lines mark the extent of the spinal cord.

At 76 hpf, I first screened drug-treated larvae to confirm that overall larval morphology was indistinguishable compared to DMSO-treated larvae. I then individually screened drug-treated larvae for changes in OPC migration by looking for either an increase or decrease in the number of *olig2*$^+$ cells in the dorsal spinal cord compared to DMSO-treated controls (Figure 3-1B). From our screen of 430 kinase inhibitors, I identified 19 compounds that resulted in increased numbers of OPCs in the dorsal spinal cord, and 35 compounds that resulted in decreased numbers of OPCs in the dorsal spinal cord. Figure 3-1C-F contains examples of hits that either increased or decreased OPC numbers. One exciting "hit" was in larvae treated with MK2461, a c-Met inhibitor, in which I observed a decrease in the number of OPCs in the dorsal spinal cord (Figure 3-2).

To confirm the reduction in migrating OPCs I observed during MK2461 treatment, I used *in vivo,* time-lapse imaging in 55 hpf *olig2:egfp* larvae (Figure 3-2A). In these movies, I see a significant reduction in the number of dorsally migrating OPCs (Figure 3-2A). However, we did observe active OPC migration in the ventral spinal cord, indicating that OPCs are specified, but exhibit migration defects (Figure 3-2A). For quantification and motility analyses of OPCs, in collaboration with the Yu Lab and Virginia Tech, we developed an automated software to detect and track motile *olig2*$^+$ OPCs distinct from *olig2*$^+$ cells in pMN domain, which contains a mixture of motile OPCs and non-motile motor neuron cells and precursors (Wang, et al., 2018). Using this cell tracking software, I assessed the migratory behaviors of OPCs in time-lapse movies from 55 to 74 hpf. From these analyses, I found that the number of migratory

OPCs was significantly reduced in MK2461-treated larvae compared to control larvae ($p < 0.0001$) (Figure 3-2B). Specifically, I observed significantly reduced numbers of dorsally, but not ventrally, migrating OPCs in MK2461-treated larvae compared to DMSO-treated controls in a 3-somite window ($p < 0.0001$) (Figure 3-2C and D).

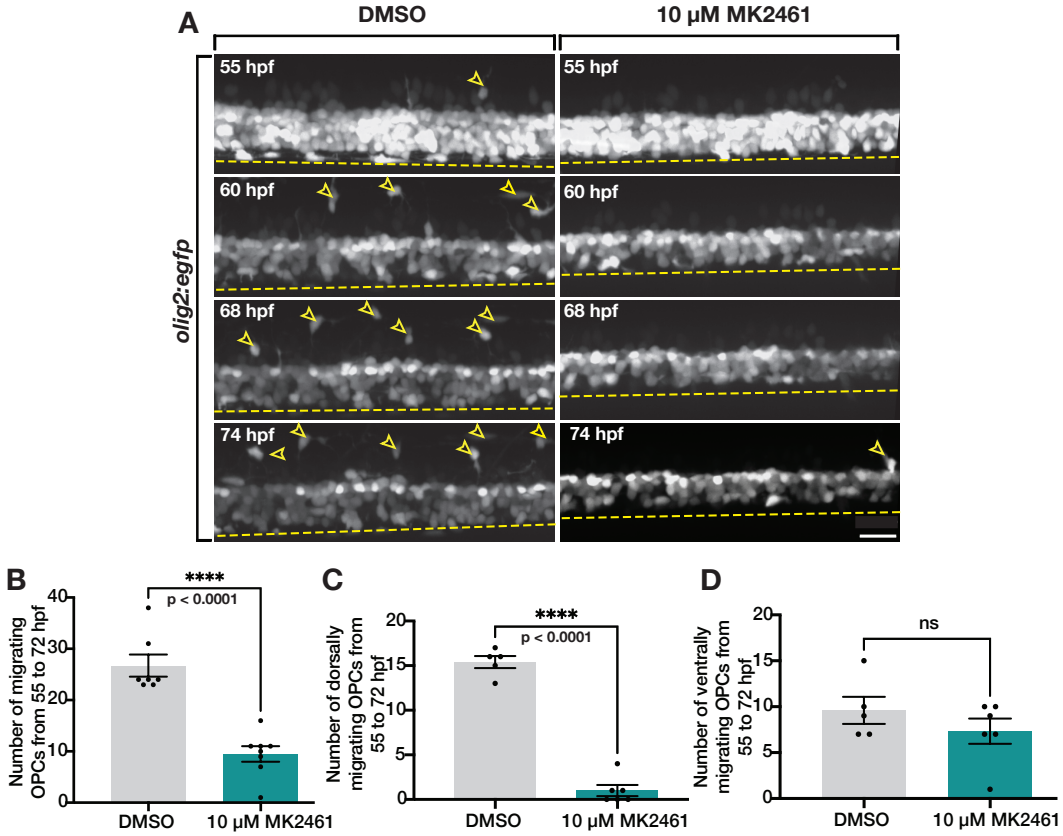


**Figure 3-2. Kinase inhibitor screen identifies Met as mediator of dorsal OPC migration.** (A) Images taken from 18 hour time-lapse movies of DMSO and MK2461-treated 55 hpf *olig2:egfp* larvae. Yellow arrowheads denote dorsally migrating OPCs. Yellow dashed line denotes ventral edge of the spinal cord. (B-D) Quantifications taken from time-lapse movies of DMSO (n = 7) and MK2461-treated (n = 7) larvae in (A). Mean with SEM. Statistical test: Student's t-test. Scale bar, 20 μm.

I next wanted to determine if treatment with MK2461 altered other aspects of OPC migration, including velocity and distance traveled. To do this, I used our cell-tracking software to analyze our time-lapses, like those shown in Figure 3-2A, for the velocity and distance traveled of individually migrating OPCs. In general, MK2461-treatment did not alter velocity or distance traveled when looking at all OPCs compared

to control larvae (Figure 3-3). However, the dorsally migrating, and not the ventrally migrating, OPCs traveled a shorter distance compared to DMSO-treated control larvae ($p = 0.0069$) (Figure 3-3C and E). The average velocity of migration for dorsally and

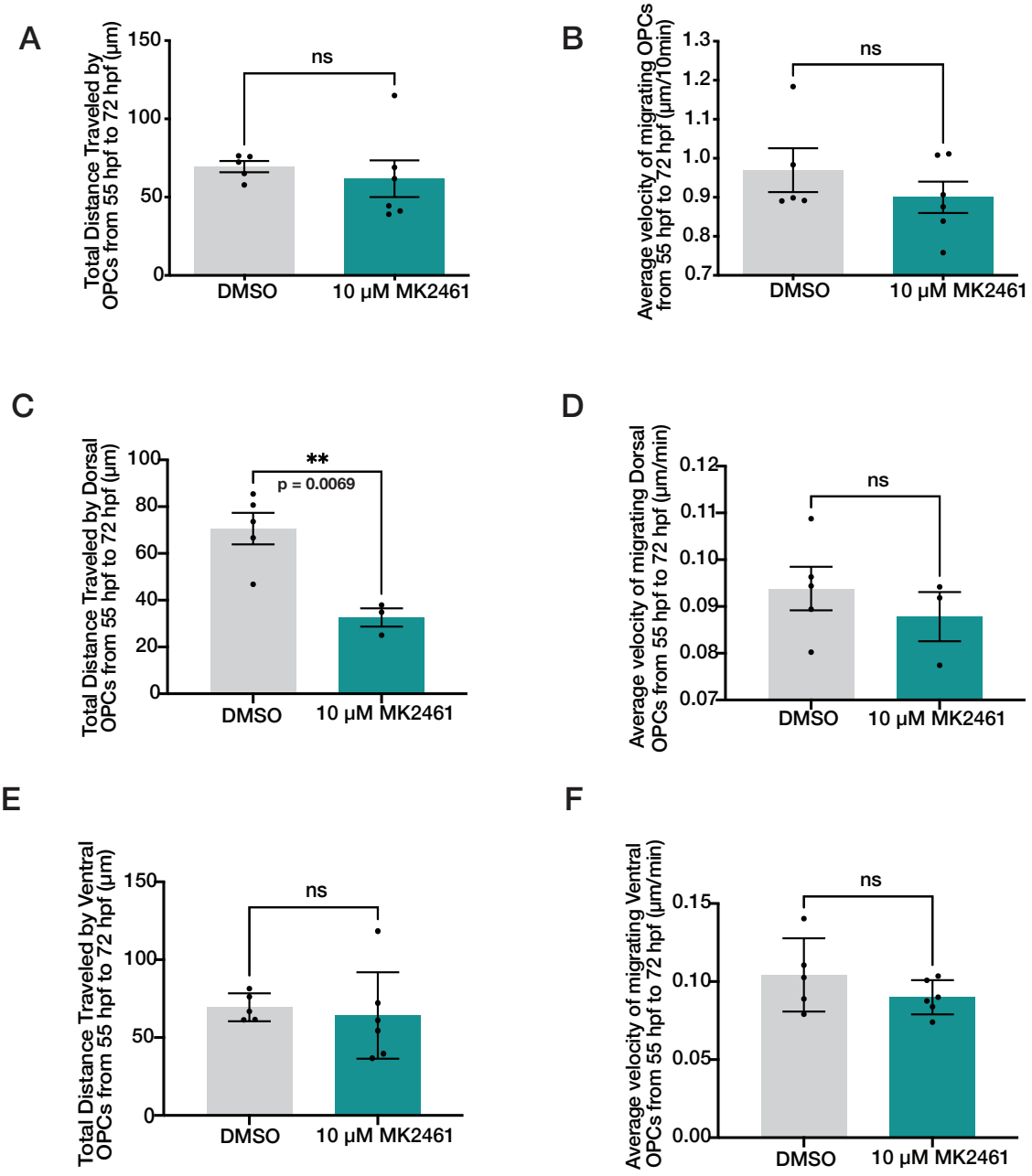


**Figure 3-3. Met inhibition alters the distance that dorsal OPCs migrate.** (A-F) Quantifications taken from time-lapse movies of DMSO (n = 7) and MK2461-treated (n = 7) larvae in (Figure 1C). Mean with SEM. Statistical test: Student's t-test.

ventrally migrating OPCs was not affected by MK2461 treatment (Figure3-3D and F). It is likely that because there were fewer dorsally migrating OPCs, those that did migrate dorsally did not have to travel as far to avoid neighboring OPCs, which would result in a shorter distance travelled. Taken together, I observed that treatment with MK2461 resulted in a reduction in the number of OPCs that migrate dorsally during development and Met, therefore, is a mediator of OPC dynamics during development.

**Zebrafish OPCs express Met**

Previous *in vitro* studies of mouse and rat OPCs used antibody labeling to show that OPCs express the Met receptor (Kilpatrick, et al., 2000; Lalive, et al., 2005; Ohya, et al., 2007; Mela & Goldman, 2013). Therefore, I wanted to determine if zebrafish OPCs also express Met. To investigate Met expression in OLCs, I used the c-Met 3D4 antibody to label $Met^+$ cells in conjunction with an antibody specific to zebrafish sox10 to label 3 days post fertilization (3 dpf) *olig2:egfp* zebrafish larvae to observe c-Met expression in OLCs. I then imaged transverse sections through the spinal cord of antibody-labeled larvae and observed $Met^+/sox^+/olig2^+$ cells in the spinal cord (Figure 3-4A). Interestingly, not all $sox10^+/olig2^+$ cells were $Met^+$, indicating that there are populations of both $Met^+$ and $Met^-$ OLCs (Figure 3-4A).

To confirm these findings, I used a new enhancer trap transgenic line, $met^{egfp}$, where eGFP is under *met* regulation due to CRISPR-targeted insertion immediately upstream of the endogenous *met* gene, to asses *met* expression in OLCs from 48 to 96 hpf (Kimura, et al., 2014). To label OLCs, I labeled $met^{egfp}$ embryos and larvae with our sox10 antibody (Figure 3-4B). I then imaged the spinal cord and quantified the number of $met^+/ sox10^+$ cells. I found that at 48 hpf, just prior to OPC migration, a large percentage of $sox10^+$ OPCs were $met^+$ (78.95%) (Figure 3-4C). By 55 hpf, only 64.68% of $sox10^+$ OPCs were $met^+$ and this level of $met^+$ OPCs stayed roughly constant through 72 hpf, where 61.76% were $met^+$ (Figure 3-4C). The consistent expression of *met* in the

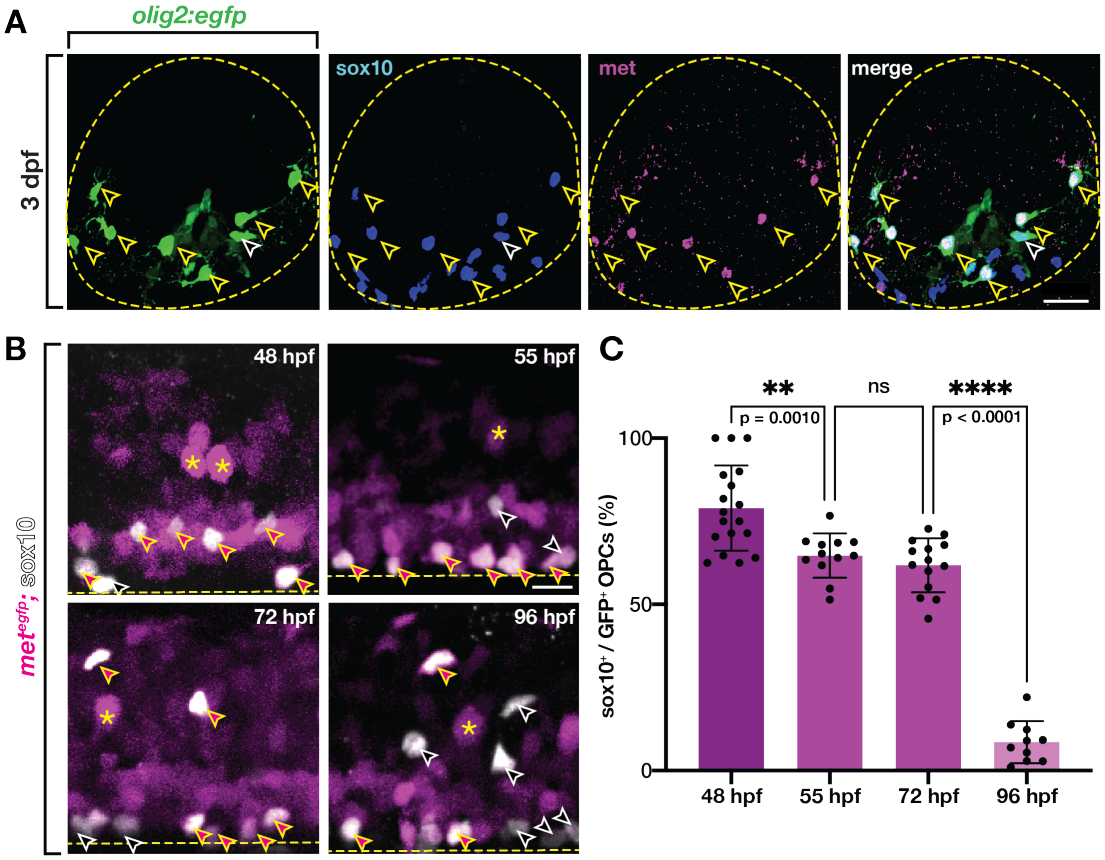


**Figure 3-4. Zebrafish OLCs express Met.** (A) Transverse sections of a 3 dpf *olig2:egfp* larvae spinal cord labeled with antibodies to sox10 (blue) and Met (magenta). Yellow open arrowheads denote Met$^+$ OLCs. White arrowheads denote Met$^-$ OLCs. Yellow dashed circle denotes boundary of the spinal cord. (B) Lateral view of *met*$^{egfp}$ spinal cords at 48, 55, 72, and 96 hpf labeled with a sox10 antibody. Asterisks denote examples of *met*$^+$ motor neurons. Magenta-filled yellow arrowheads denote sox10$^+$/*met*$^+$ OPCs, white arrowheads denote sox10$^+$/*met*$^-$ OLCs. Yellow dashed line denotes ventral edge of the spinal cord. (C) Percentage of OPCs that are sox10$^+$ and *met*$^{egfp+}$ in 322 µm of spinal cord at 48 hpf (n = 18), 55 hpf (n = 12), 72 hpf (n = 14), and 96 hpf (n = 10). Mean with SEM. Statistical test: 1-way ANOVA with Tukey's Multiple Comparison Test. Scale bars, 10 µm (A), 20 µm (B).

majority of OPCs from 55 to 72 hpf is consistent with the major migratory period of OPCs, which occurs during the same time window. By 96 hpf, when most OLCs have completed their migration and many are initiating myelination of spinal cord axons, the population of OLCs that expressed *met* was decreased significantly to 8.56% (Figure 3-4C). These findings are consistent with previous investigations demonstrating that OPCs must down-regulate expression of Met in order to differentiate into

oligodendrocytes (Ohya, et al., 2007). From these expression studies, I conclude that zebrafish OPCs express Met.

**Met inhibition reduces OPC numbers**

Because I observed Met expression in migratory OPCs, I next sought to more closely investigate the effect of MK2461 on their migration. First, I conducted a dose response curve using the same treatment paradigm as the drug screen described above by treating 24 hpf *olig2:egfp* larvae with a 1% DMSO control or increasing doses of MK2461 in 1% DMSO and quantified the number of *olig2*$^{+}$ OPCs in the dorsal spinal cord at 76 hpf. I found that increasing doses of MK2461 resulted in decreasing numbers of OPCs in the dorsal spinal cord of *olig2:egfp* larvae at 76 hpf compared to DMSO-treated larvae ($p < 0.0001$) (Figure 3-5A). To more directly assay the positioning and number of OPCs in control and drug-treated larvae, I used serial sectioning in 76 hpf *olig2:egfp;sox10:mrfp* larvae treated with 1% DMSO or MK2461 in 1% DMSO and quantified the number and location of *olig2*$^{+}$/*sox10*$^{+}$ cells (Figure 3-5B). These studies revealed that the overall number of OLCs was reduced in the spinal cord of MK2461-treated larvae when compared to controls (Figure 3-5C), and the decrease affected both the number of dorsal and ventral OLCs ($p < 0.0001$) (Figure 3-5D and E).

Interestingly, I saw an increase in the number of OLCs in the pMN domain in larvae treated with MK2461, which indicates that OPCs were specified in MK2461-treated larvae and that the migration defect I observed was not simply due to perturbed specification ($p = 0.0349$) (Figure 3-5F). Additionally, in contrast to our earlier studies in whole larvae where I observed that ventral OLCs were unaffected by MK2461 treatment, I saw a significant reduction in this population when I assessed their location in serial sections ($p < 0.0001$) (Figure 3-5E). I believe this occurred because it is much more difficult to observe ventral OLCs in whole-mount *olig2*:*egfp* larvae. Additionally, the overall of reduction of OLCs in MK2461 could be the result of reduced

proliferation in OPCs, as Met is also implicated in regulating OPC proliferation in *in vitro* studies using OPC cell culture (Ohya, et al., 2007).

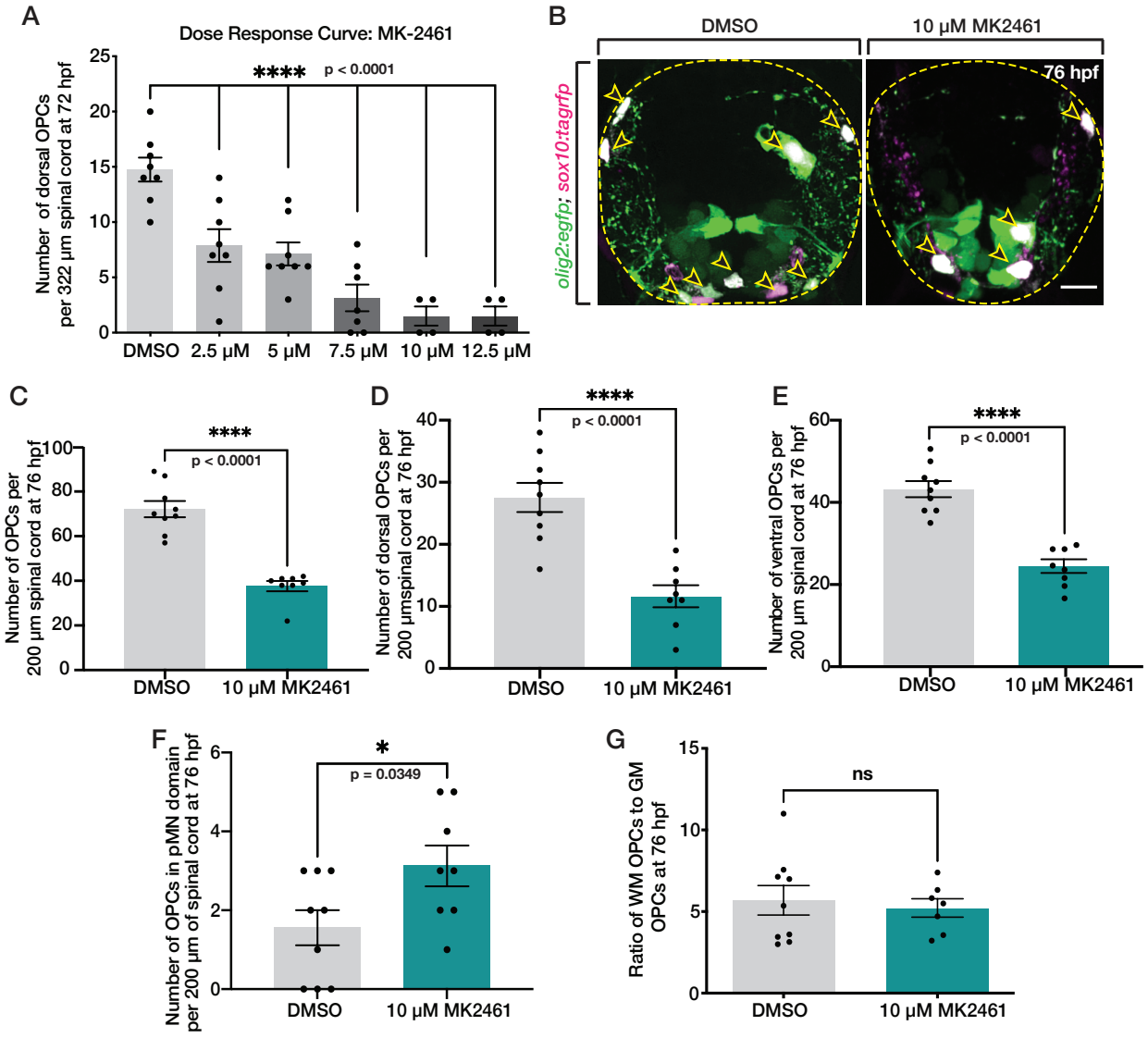


**Figure 3-5. Met receptor inhibition decreases the number of OLCs in spinal cord.** (A) Dose-response curve of the number of OLCs in the dorsal spinal cord of larvae treated from 24 hpf to 3 dpf with 1% DMSO (n = 8) or MK2461 in 1% DMSO in the following doses: 2.5 µM (n = 8), 5 µM (n = 8), 7.5 µM (n = 7), 10 µM (n = 4), and 12.5 µM (n = 4). Statistical test: 1-way ANOVA with Dunnett's Multiple Comparison Test. (B) Transverse sections of 76 hpf *olig2:egfp;sox10:tagrfp* larvae treated with 1% DMSO or 10 µM MK2461 in 1% DMSO from 24 hpf to 3 dpf. Yellow open arrowheads denote *sox10*$^{+}$*/olig2*$^{+}$ OLCs. (C-G) Quantifications of *olig2*$^{+}$*/sox10*$^{+}$ OLCs from serial sections of *olig2:egfp;sox10:tagrfp* larvae treated with 1% DMSO (n = 9) or 10 µM MK2461 in 1% DMSO (n = 8) from 24 hpf to 3 dpf. Mean with SEM. Statistical test: Student's t-test was used in C-G. Scale bar, 10 µm.

Finally, a growing body of literature suggests that there are functionally different subsets of OPCs and that these subsets may have an affinity for specific regions of the CNS, such as the gray matter (GM) or white matter (WM) (Dawson et al. 2000; Birey and Aguirre 2015; Viganò and Dimou 2016; Spitzer et al. 2018; Kelenis et al. 2018). Therefore, I wanted to quantify the distribution of OPCs by comparing the ratio of WM to GM in DMSO- and MK2461-treated zebrafish larvae (Figure 3-5G). Overall, there was no difference in the WM to GW OPC distribution, indicating that Met inhibition does not affect overall positioning of OPCs. Taken together, I conclude that Met mediates OPC migration during development and potentially OPC proliferation, but does not affect OPC specification or distribution.

**Met is required for initial developmental OPC migration**

Given the migration phenotype I observed with the c-Met inhibitor, MK2461, and the expression pattern of Met in zebrafish OLCs, I sought to further investigate Met as a mediator of OPC migration during development using CRISPR/Cas9 mutagenesis (Hwang, et al., 2013; Hruscha, et al., 2013). Using CHOPCHOP, I generated a guide RNA (gRNA) specific to exon 2 of the zebrafish *met* coding sequence (Labun, et al., 2019). Using this synthesized gRNA, I injected one-cell embryos with the gRNA for *met* and Cas9 protein and grew potential founders to adulthood. I then outcrossed putative founders and screened for frameshift mutations in their offspring and identified a founder with a mutation that resulted in a 16 base pair insertion into the second exon of *met* that results in an early stop codon (Figure 3-6A). This mutation causes the premature termination in the beta chain of the sema domain resulting in a truncated polypeptide that would be functionally unable to homodimerize upon Hgf binding and, therefore, would be unable to initiate downstream signaling

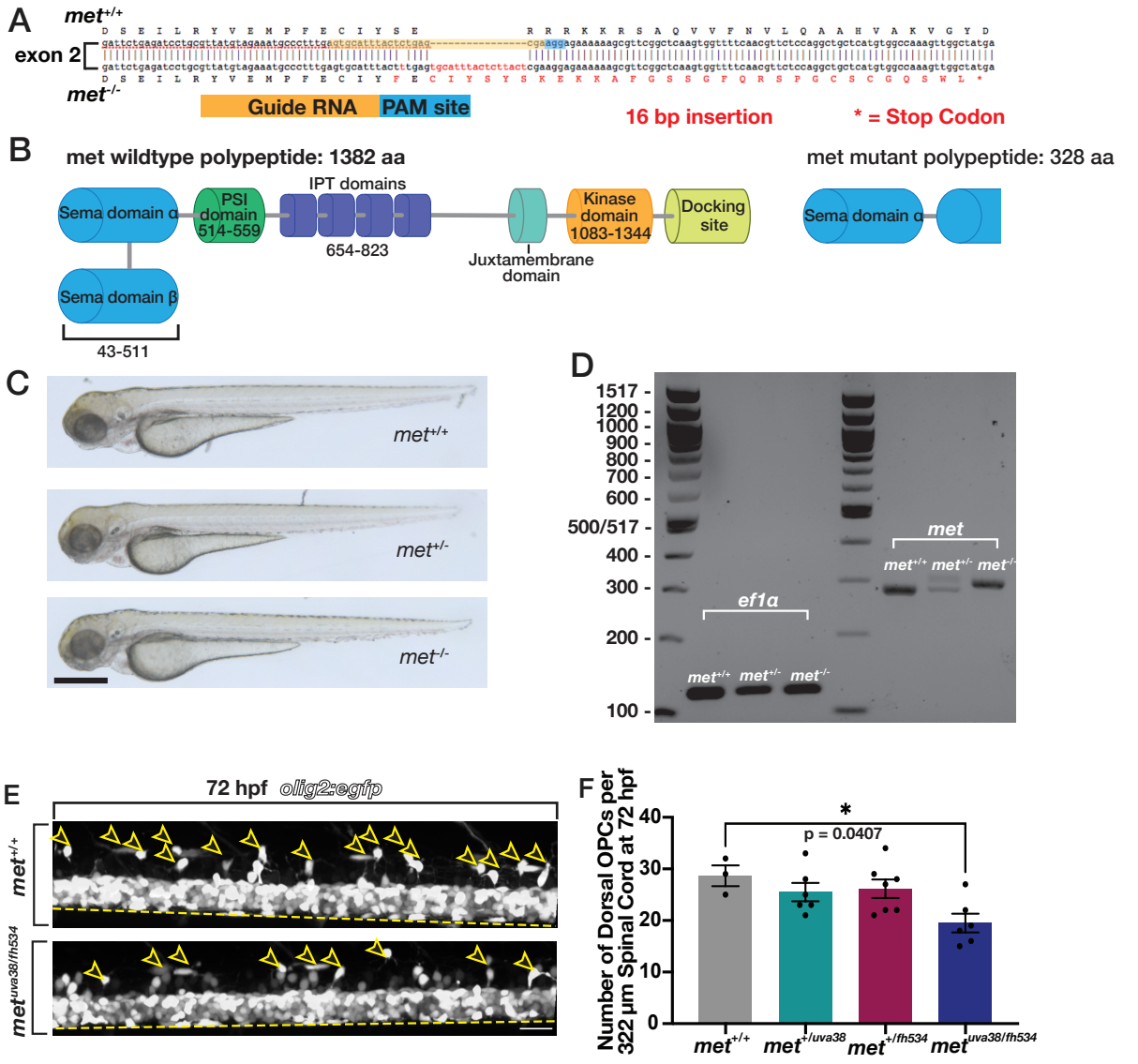


**Figure 3-6. Met mutants exhibit a 16 bp insertion and reduced dorsal OLCs.** (A) Diagram of *met* mutant created using CRISPR/Cas9 mutagenesis with gRNA target sequence (yellow) and PAM site (blue) resulting in a 16 base pair insertion causing a frameshift mutation and early stop codon (asterisk). (B) Diagram of wildtype Met protein and Met mutant polypeptide sequences. (C) Bright-field images *of met*$^{+/+}$, *met*$^{+/+}$, and *met*$^{-/-}$ siblings at 3 dpf reveal no developmental delay in *met*$^{-/-}$ larvae. (D) RT-PCR of mRNA transcripts extracted from 48 hpf *met*$^{+/+}$, *met*$^{+/-}$, and *met*$^{-/-}$ embryos demonstrating 16 bp insertion in *met*$^{+/-}$ and *met*$^{-/-}$ RNA transcripts. (E) Images of 72 hpf *olig2:egfp met*$^{+/+}$ and *met*$^{uva38/fh534}$ larvae spinal cords. Yellow open arrowheads denote dorsal OLCs. Dashed yellow line denotes ventral edge of the spinal cord. (F) Quantifications taken from spinal cord images of *met*$^{+/+}$ (n = 3), *met*$^{+/uva38}$ (n = 6), *met*$^{+/fh534}$ (n= 7), and *met*$^{uva38/fh534}$ (n = 6) larvae. Mean with SEM. Statistical test: 1-way ANOVA with Tukey's Multiple Comparison Test. Scale bars, 0.5 mm (A), 20 µm (C).

(Figure 3-6B). Importantly, these mutant larvae had an overall normal morphology and body length when compared to wildtype siblings (Figure 3-6C). To confirm the incorporation of a 16 base pair insertion, I isolated RNA from *met*$^{+/+}$, *met*$^{+/-}$, and *met*$^{-/-}$ larvae and performed RT-PCR. As expected, *met* heterozygous and homozygous larvae had a larger band compared to wildtype that was consistent with a 16 bp insertion (Figure 3-6D). Finally, to confirm that this mutation led to a loss of function mutation in *met,* we crossed a heterozygous *met*$^{uva38}$ adult with a *met*$^{fh534}$ heterozygous adult and imaged the spinal cord of 72 hpf *olig2:egfp* mutant larvae (Figure 3-6E). In these *met*$^{uva38/fh534}$ transheterozygous larvae, I observed a significant decrease in dorsal OPCs in when compared to wildtype siblings (Figure 3-6F).

I next used this new *met*$^{uva38}$ allele to assess the role of *met* in regulating developmental OPC migration. Using *in vivo,* time-lapse imaging in combination with our cell-tracking software in 55 hpf *olig2:egfp;met*$^{+/+}$, *met*$^{+/-}$, and *met*$^{-/-}$ larvae, I analyzed OPC migration (Wang, et al., 2018). This imaging of *olig2:egfp;met*$^{-/-}$ larvae revealed a significant decrease in the number of migrating OPCs compared to *met*$^{+/+}$ larvae ($p = 0.0137$) (Figure 3-7A and B). Interestingly, the decrease in OPC migration in the *met*$^{-/-}$ larvae primarily affected dorsally-migrating OPCs ($p = 0.0207$) (Figure 3-7C). There was also a decrease in dorsally migrating OPCs in *met*$^{+/-}$ larvae, which is likely due to the tightly regulated nature of Met signaling ($p = 0.0079$) (Figure 3-7C) (Zhang & Babic, 2015). In contrast, ventrally migrating OPCs in *met*$^{-/-}$ larvae were similar to *met*$^{+/+}$ and *met*$^{+/-}$ larvae, although there was a trend of reduced numbers of ventral migratory OPCs (Figure 3-7D). Finally, consistent with our Met inhibitor studies, OPCs showed no difference in average velocity of migration or distance traveled when *met* was perturbed (Figure 3-8). Taken together, these results demonstrate that *met* is required for dorsal OPC migration during developmental OPC tiling.

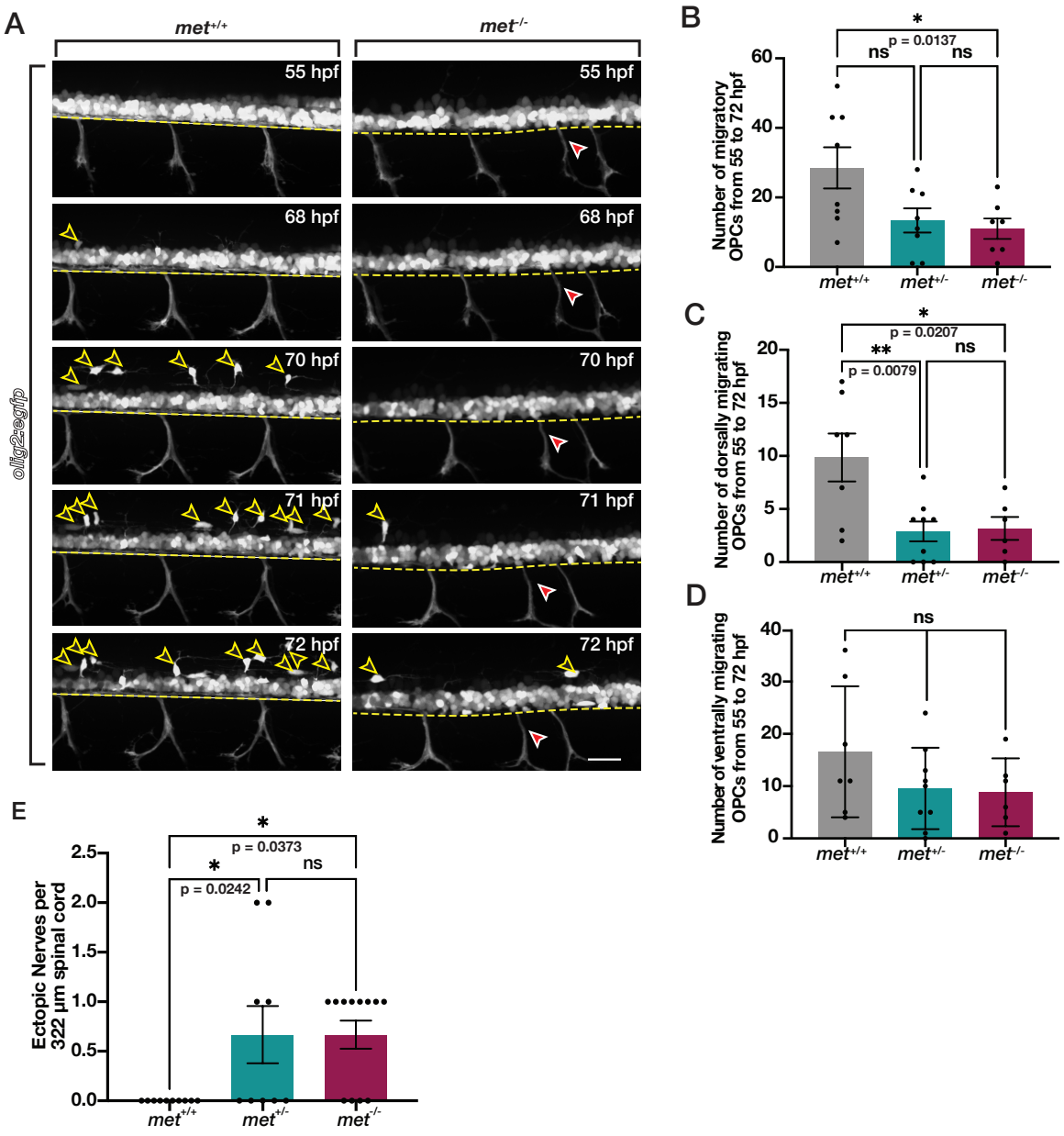


**Figure 3-7. Met is required for initiation of dorsal OPC migration.** (A) Images taken from 18 hour time-lapse imaging of 55 hpf *olig2:egfp* $met^{+/+}$, $met^{+/-}$, and $met^{-/-}$ larvae. Yellow open arrowheads denote dorsally migrating OPCs. White-outlined red arrowheads denote ectopic MN exit. Yellow dashed line denotes ventral edge of spinal cord. (B-D) Quantifications taken from time-lapse movies of 55 hpf *olig2:egfp* $met^{+/+}$ (n = 8), $met^{+/-}$ (n = 8), and $met^{-/-}$ (n = 6) larvae in (A). (E) Quantifications taken from lateral images of 55 hpf *olig2:egfp* $met^{+/+}$ (n = 11), $met^{+/-}$ (n = 9), and $met^{-/-}$ (n = 12) larvae. Mean with SEM. Statistical test: 1-way ANOVA with Tukey's Multiple Comparison Test was used for D-F. Scale bar, 20 µm.

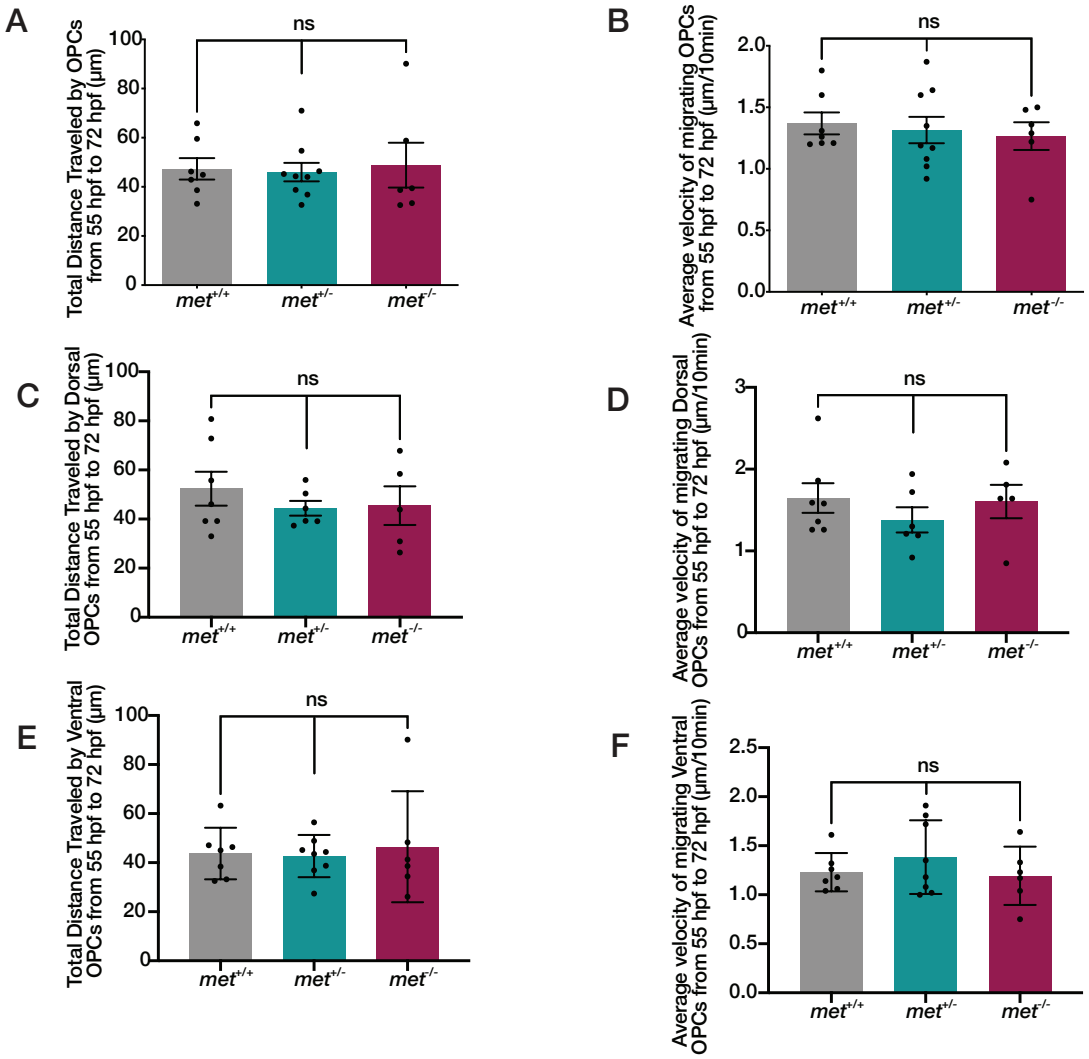


**Figure 3-8. Met mutants do not exhibit defects in OPC distance traveled or velocity.** (A-G) Quantifications taken from 18 hour time-lapse movies of 55 hpf *olig2:egfp met*$^{+/+}$ (n = 8), *met*$^{+/-}$ (n = 8), and *met*$^{-/-}$ (n = 6) larvae in (4C). Statistical test: 1-way ANOVA with Tukey's Multiple Comparison Test.

Interestingly, my new *met* mutant exhibited ectopic motor neurons (MNs) in both heterozygous and *met* mutant larvae (het, p = 0.0242; mutant, p = 0.0373) (Figure 3-7A and E). Previous studies investigating the role of Met and MNs show are wide range of potential roles for Met in MN development, however the overall consensus is that Met is required in a few subpopulations of MNs (Yamamoto, et al., 1997; Caton, et al., 2000; Tallafuss & Eisen, 2008). One study showed that different subsets of MNs, namely primary and secondary, respond differently to loss of Met, usually resulting in loss of

MNs or aberrant axon outgrowth and pathfinding (Tallafuss & Eisen, 2008). In contrast, Hgf is a chemoattractant for cranial MNs, and disruptions in Hgf and Met resulted in aberrant axon navigation (Caton, et al., 2000). Given this evidence, in combination with the ectopic nerves observed in my *met* mutant, I hypothesize that loss of *met* results in aberrant MN axon guidance resulting in ectopic MN exit. Utilizing MN-specific drivers and cell-specific knockout of *met* could uncover novel roles for Met in MN development and axon guidance. However, to stay within the scope of this project, I wanted to first more closely characterize the OPC phenotypes I observed in my *met* mutants.

To more closely examine the effect of *met* mutation on developmental OPC migration, I performed serial sectioning on 76 hpf *olig2:egfp;sox10:mrfp;met*$^{+/+}$, *met*$^{+/-}$, and *met*$^{/-}$ larvae. I then imaged transverse sections of the spinal cord and assessed the location and number of OLCs (Figure 3-9A). Similar to what I observed with the c-Met inhibitor, I observed a decrease in the overall number of OPCs in *met*$^{/-}$ larvae compared to wildtype siblings ($p = 0.0137$) (Figure 3-9B). Additionally, I observed a reduction in the number of OLCs in both the dorsal and ventral portions of the spinal cord in *met*$^{/-}$ larvae compared to their wildtype siblings (dorsal, $p = 0.0335$; ventral, $p = 0.0014$) (Figure 3-9C and D). This finding is slightly different than what I observed when looking at whole-mount, lateral views of the spinal cord in our *met* mutant larvae and larvae treated with MK2461. However, this difference is likely due to the fact that in lateral views, it is very difficult to visualize all ventral OLCs because of the expression of *olig2:egfp* in ventral spinal cord precursors and motor neurons. Therefore, my findings here with a careful analysis of OPC location in transverse sections is more accurate. Additionally, I observed an increase in the number of OLCs in the pMN domain in *met*$^{/-}$ larvae compared to wildtype siblings, which is consistent with what I observed in larvae treated with MK2461 ($p = 0.0013$) (Figure 3-9E). This data also fits with what I observed in time-lapse movies of *met* mutant larvae, where I observed OPCs in the

pMN domain of the spinal cord extending processes into the dorsal spinal cord that then failed to migrate dorsally. Similar to the inhibitor treatments, I observed no difference in the distribution of OPCs in the WM compared to the GW (Figure 3-9F). The increased number of OPCs in the pMN domain in *met*$^{-/-}$ larvae compared to wildtype siblings, and the OPC process extension behavior in our time-lapse imaging indicate that there is a reduction in the number of OPCs that are able to migrate out of the pMN domain. This data supports my hypothesis that OPCs require *met* for initial migration out of the pMN domain during development, while sparing OPC specification.

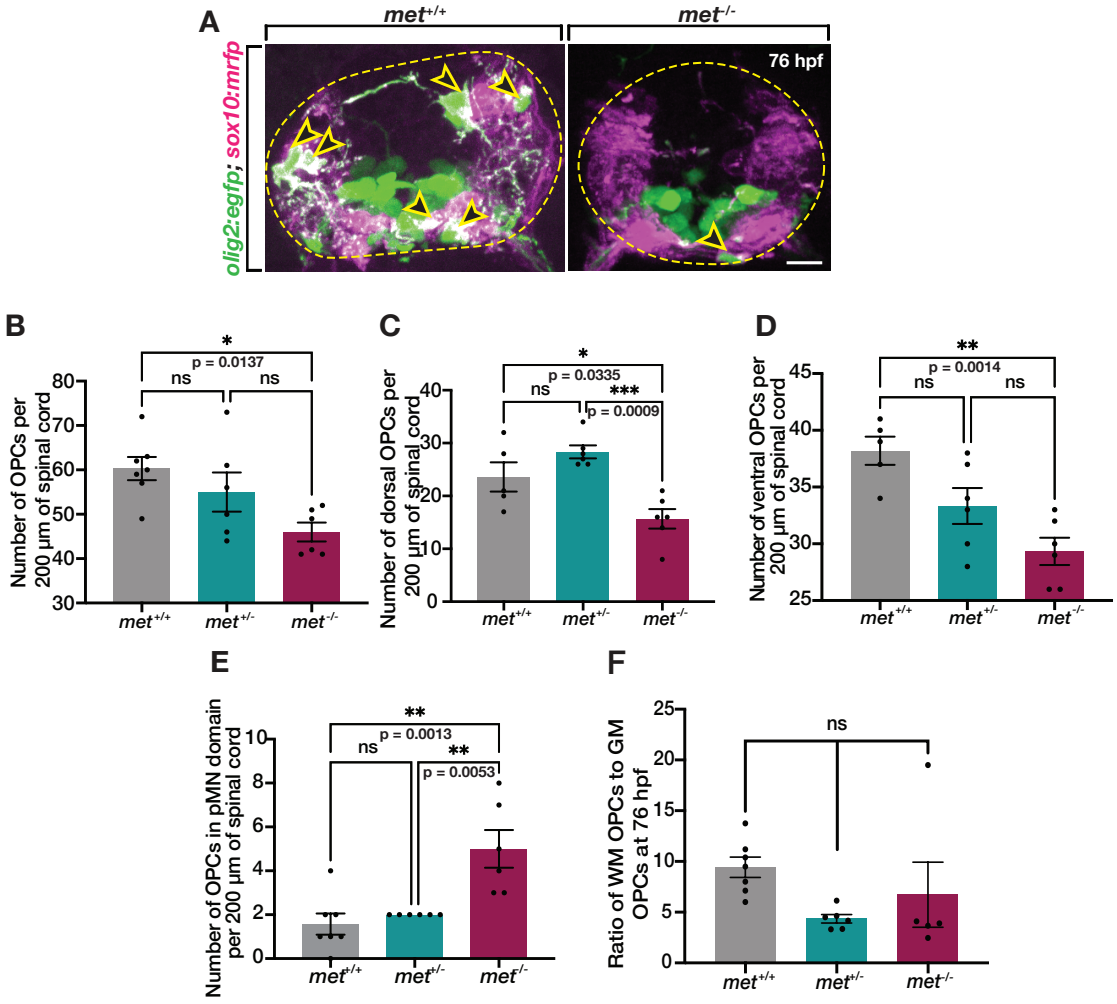


**Figure 3-9. *met* mutants exhibit reduced OPC numbers.** (A) Transverse sections of 76 hpf *olig2:egfp;sox10:mrfp met*$^{+/+}$ and *met*$^{-/-}$larvae. Yellow arrowheads denote *sox10*$^{+}$*/olig2*$^{+}$ OPCs. Dashed yellow circle denotes boundary of the spinal cord. (B-F) Quantifications of *olig2*$^{+}$*/sox10*$^{+}$ OLCs from serial

sections of 76 hpf *olig2:egfp;sox10:mrfp* $met^{+/+}$ (n = 7) , $met^{+/-}$ (n = 6), and $met^{-/-}$ (n = 6) larvae. Mean with SEM. Statistical test: 1-way ANOVA with Tukey's Multiple Comparison Test. Scale bar, 10 µm.

From these data, I hypothesize that the reduction in the number of OPCs in *met* $^{/-}$ larvae could be caused by either a reduction in OPC specification, which would lead to fewer OLCs in the spinal cord, or a reduction in OPC proliferation, which would result in wildtype numbers of OPCs during specification, but fewer OPCs during the migratory period. Met has been implicated in regulating cellular proliferation in a number of different cell types including hepatocytes, melanocytes, and other epithelial cell types (Tamagnone & Comoglio, 1997; Prat, et al., 1998; Viticchiè, et al., 2015). To investigate if the overall decrease of OPCs in *met*$^{/-}$ larvae is a consequence of reduced OPC specification, I did serial sectioning of 48 hpf *olig2:egfp;sox10:mrfp;*$met^{+/+}$, $met^{+/-}$, and *met*$^{/-}$ larvae (Figure 3-10). I chose 48 hpf because it is sufficiently after the window of

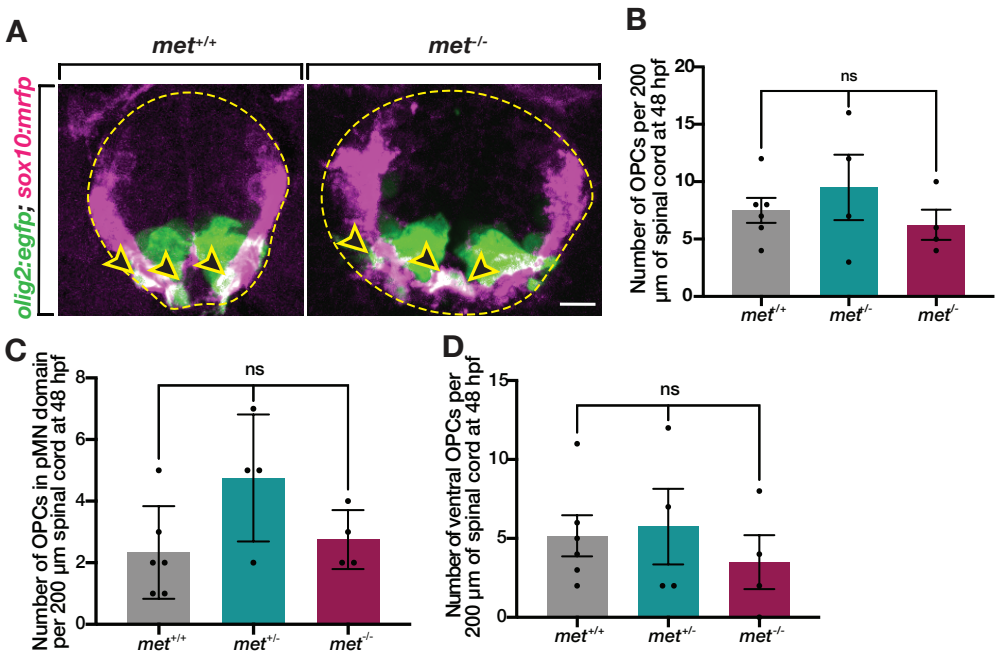


**Figure 3-10. *Met* mutants exhibit wildtype OPC specification.** (A) Transverse sections of 48 hpf *olig2:egfp;sox10:mrfp* $met^{+/+}$ and $met^{-/-}$ embryos. Open yellow arrowheads denote $sox10^{+}/olig2^{+}$ OPCs. Dashed yellow circle denotes boundary of spinal cord. (B-D) Quantifications of $olig2^{+}/sox10^{+}$ OPCs from serial sections of 48 hpf *olig2:egfp;sox10:mrfp* $met^{+/+}$ (n = 6) and $met^{+/-}$ (n = 4), and $met^{-/-}$ (n = 4) embryos. Mean with SEM. Statistical test: 1-way ANOVA with Tukey's Multiple Comparison Test. Scale bar, 10 µm.

OPC specification which begins at 36 hpf, but prior to the main migratory period of OPCs which begins at approximately 55 hpf (Kirby et al. 2006; Ravanelli et al. 2018). In these studies, I found that there was no difference in the number of OPCs in *met*$^{+/+}$, *met*$^{+/-}$, and *met*$^{/-}$ larvae at 48 hpf, which demonstrates that OPC specification is not affected by loss of *met* (Figure 3-10).

With OPC specification being unaffected in *met*$^{/-}$ larvae, I next hypothesized that the reduction in the number of OPCs in *met*$^{/-}$ larvae was caused by a decrease in Met-dependent OPC proliferation, which has previously been demonstrated (Ohya, et al., 2007; Gherardi, et al., 2012). To investigate OPC proliferation, I treated *olig2:egfp;sox10:mrfp;met*$^{+/+}$, *met*$^{+/-}$, and *met*$^{/-}$ larvae with EdU (5-ethynyl-2'-deoxyuridine) from 70 to 74 hpf in order to detect DNA synthesis in proliferative cells (Figure 3-11A). I then imaged lateral spinal cords of EdU-treated larvae and quantified *olig2*$^{+}$/*sox10*$^{+}$/EdU$^{+}$ OPCs (Figure 3-11B). I observed that *met*$^{/-}$ larvae had fewer EdU$^{+}$ OLCs compared to wildtype and heterozygous siblings at 74 hpf (wt, p = 0.0246; heterozygous, p = 0.0249) (Figure 3-11C). These results demonstrate that the reduction in OLCs in *met*$^{/-}$ larvae is due to a decrease in proliferation in OPCs and that Met may also play a role in regulating OPC proliferation during development.

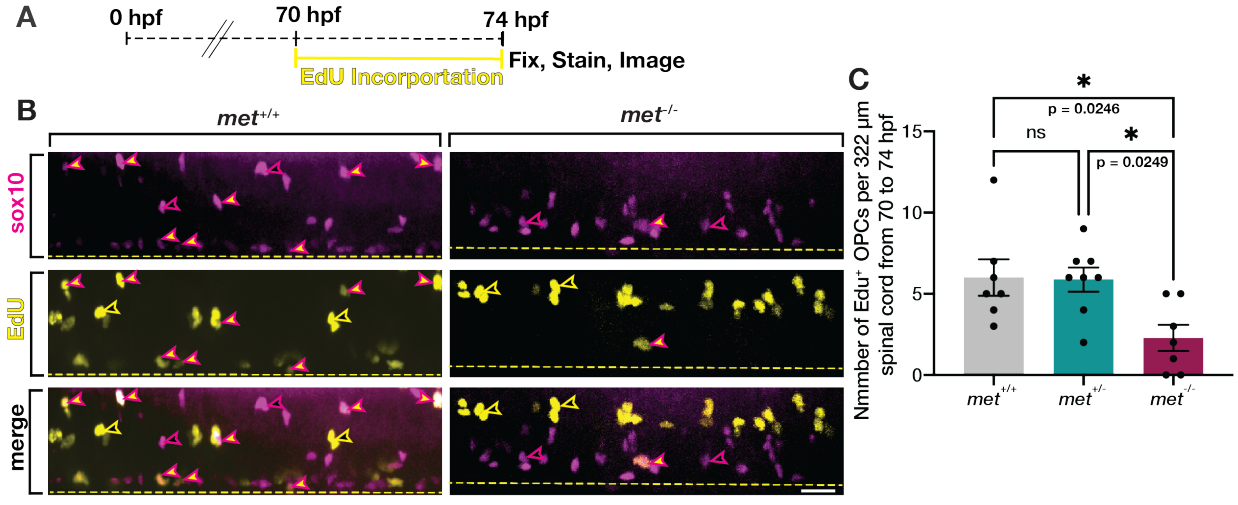


**Figure 3-11. *Met* mutants exhibit reduced OPC proliferation.** (A) EdU treatment paradigm. (B) Spinal cord images of 74 hpf *olig2:egfp;sox10:mrfp met*$^{+/+}$ and *met*$^{-/-}$ zebrafish larvae. Magenta-outlined yellow

arrowheads denote *sox10*$^{+}$/*olig2*$^{+}$/EdU$^{+}$ OPCs. Magenta open arrowheads denote *sox10*$^{+}$/*olig2*$^{+}$/EdU$^{-}$ OLCs. Yellow open arrowheads denote *sox10*$^{-}$/*olig2*$^{-}$/EdU$^{+}$ cells. Yellow dashed line denotes ventral edge of the spinal cord. (C) Quantifications of *sox10*$^{+}$/*olig2*$^{+}$/EdU$^{+}$ OLCs from spinal cord images of 76 hpf *olig2:egfp;sox10:mrfp* EdU labeled *met*$^{+/+}$ (n = 7) , *met*$^{+/-}$ (n = 8), and *met*$^{-/-}$ (n = 7) larvae. Mean with SEM. Statistical test: 1-way ANOVA with Tukey's Multiple Comparison Test. Scale bars, 20 μm.

## Met knock-down in pre-migratory OPCs reduces migration out of the ventral spinal cord

During development, Met is expressed in a number of developing CNS neural populations, including motor neurons (Latimer & Jessen, 2008). Because normal neuronal developmental influences OPC development (Ravanelli et al. 2018), I wanted to ensure that the phenotypes I observed in our inhibitor-treated and whole animal *met* mutant studies were not due to non-cell autonomous effects on OPCs. Therefore, I created cell lineage specific Met dominant negative constructs to specifically perturb Met signaling in OLCs.

To do this, I used site-directed mutagenesis to selectively mutate three critical tyrosines in the docking domain of the c-Met receptor (Figure 3-12A), which, following Met dimerization, are trans-phosphorylated allowing for adaptor protein binding and downstream signaling (Soriano, et al., 1995; Birchmeier & Gherardi, 1998; Viticchiè, et al., 2015) (Figure 3-12B). Previously published dominant negative met (DNmet) constructs containing phenylalanine substitutions in the three docking site tyrosines of c-Met were successfully used in *in vitro* cell culture and zebrafish larvae for cell-specific reduction of Met signaling (Bardelli, et al., 1999; Firon, et al., 2000; Giordano, et al., 2002; Latimer & Jessen, 2008). The mutation of these tyrosines into phenylalanines physically prevents autophosphorylation of the docking site, thus preventing adaptor protein binding and downstream signaling (Ponzetto, et al., 1996; Bardelli, et al., 1999; Firon, et al., 2000). I employed the same approach of creating point mutations that result in amino acid substitution of tyrosine to phenylalanine for the same critical

tyrosines in the docking domain of the c-Met receptor as these previously published DNmet constructs (Firon, et al., 2000; Giordano, et al., 2002; Latimer & Jessen, 2008). I confirmed successful mutation using Sanger sequencing, then drove our DNmet construct using either a *sox10* or *olig1* promoter (Figure 3-12D). The *sox10:DNmet* construct reduces Met signaling in glial cells and OPCs upon their specification beginning around 36 hpf (Dawson et al. 2000; Ravanelli et al. 2018) (Figure 3-12C). The *olig1:DNmet* construct reduces Met signaling in OLCs at approximately 60 hpf, during their migratory phase (Auer et al. 2018) (Figure 3-12C). I additionally included an *IRES:GFP* reporter to more easily genotype and identify animals that contain the dominant negative constructs (Figure 3-12D). Taken together, I can use these constructs to temporally control Met signaling in OLCs by modulating it in either pre-migratory OPCs using *sox10:DNmet* or migratory OLCs using *olig1:DNmet*.

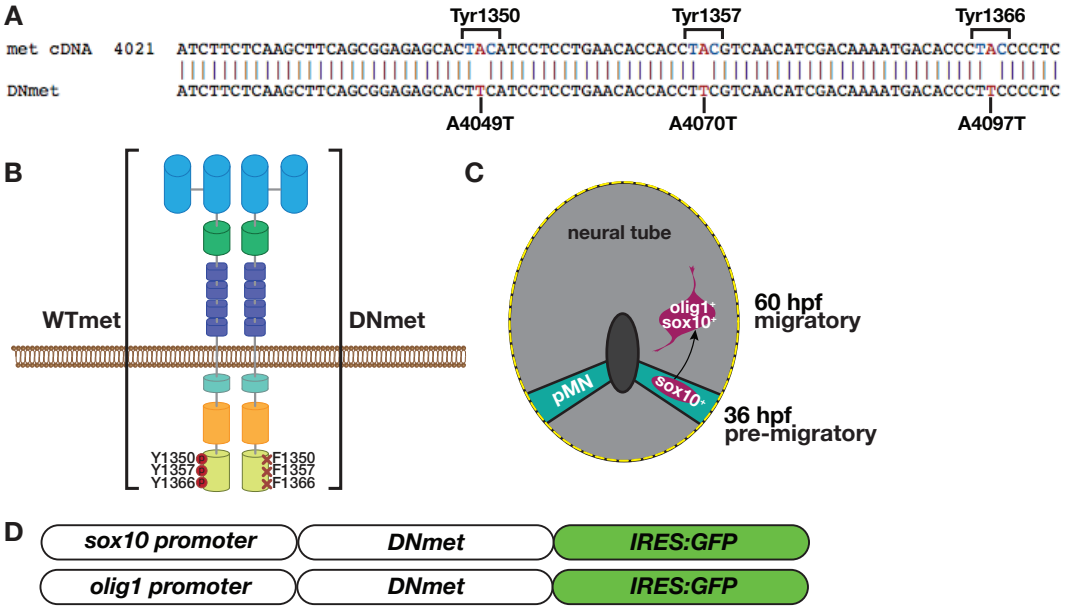


**Figure 3-12. Cell-specific knock-down of Met signaling.** (A) Schematic of Met receptor showing site-specific mutations converting adenines (A) to thymines (T) resulting in amino acid changes of tyrosines (Y) to phenylalanines (F). (B) Diagram of amino acid substitutions in docking site tyrosines created using site-directed mutagenesis. (C) Diagram of developing neural tube showing *sox10* turns on in pre-migratory OPCs around 36 hpf and *olig1* turns on in migratory OPCs around 60 hpf. (D) Schematic of DNmet

constructs showing *DNmet* is driven by either a *sox10* or *olig1* promoter and includes *IRES:GFP* coding sequence.

To investigate the effect of OPC-specific reduction of Met signaling, I used sox10 antibody labeling to assess the position of OLCs in the spinal cord in *sox10:DNmet* and *olig1:DNmet* embryos and larvae (Figure 3-13A). At 55 hpf, I observed that the number of OPCs in both *sox10:DNmet* and *olig1:DNmet* larvae were unchanged compared to wildtype siblings (Figure 3-13B), supporting my conclusion that Met is not required for OPC specification. However, I observed decreased numbers of dorsal OPCs in *sox10:DNmet* larvae when compared to wildtype siblings at this stage ($p = 0.0103$) (Figure 3-13C). In contrast, while the number of ventral OPCs was unchanged compared to wildtype and *olig1:DNmet* larvae (Figure 3-13D), the *sox10:DNmet* larvae exhibited a significant increase in the number of OPCs in the pMN domain compared to both wildtype ($p = 0.0063$) and *olig1:DNmet* ($p < 0.0001$) larvae at 55 hpf (Figure 3-13E). These results demonstrate a significant reduction in dorsal migration of OPCs out of the pMN domain when Met signaling is reduced in pre-migratory OPCs using the *sox10:DNmet* construct. Additionally, while the overall positioning of the OPCs in the spinal cord among the three groups at 55 hpf demonstrated a large population of ventral OPCs, *sox10:DNmet* larvae exhibited an expanded population of pMN domain OPCs that was significantly different from both wildtype ($p < 0.0001$) and *olig1:DNmet* larvae ($p < 0.0001$) (Figure 3-13F and G). These results demonstrate that inhibition of Met signaling in pre-migratory OPCs causes a significant shift in the distribution of the position of OPCs toward the pMN domain at 55 hpf, indicating that OPCs require Met signaling to migrate dorsally during development.

I wanted to further examine the effect of reducing Met signaling in OLCs by looking at OLC positioning in the spinal cord toward the end of the migratory period at 72 hpf. I used sox10 antibody labeling to identify OLCs in the spinal cord and found that, at 72 hpf, the number of OLCs remained unchanged compared to wildtype in both

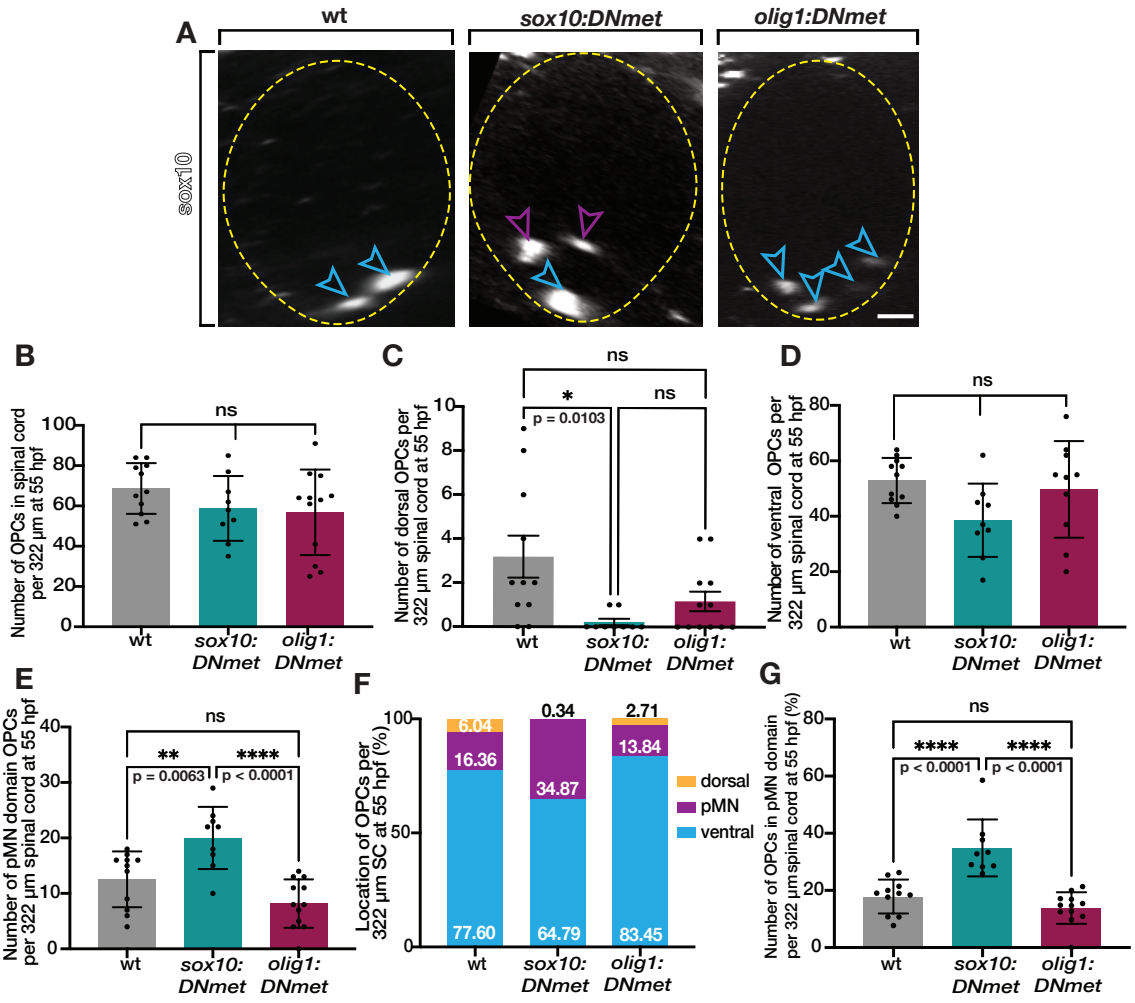


**Figure 3-13. *Sox10:DNmet* reduces OPC migration at 55 hpf.** (A) Transverse sections of sox10 antibody labeled 55 hpf wildtype, *sox10:DNmet*, and *olig1:DNmet* larvae. Blue open arrowheads denote ventral OPCs. Purple open arrowheads denote pMN domain OPCs. Yellow dashed circle denotes spinal cord boundary. (B-G) Quantifications taken from images of 55 hpf sox10 antibody labeled wildtype (n = 10), *sox10DN:met* (n = 8), and *olig1:DNmet* (n = 12) larvae spinal cords. Mean with SEM. Statistical test: 1-way ANOVA with Tukeys's Multiple Comparison Test. Scale bar, 20 µm.

the *sox10:DNmet* and *olig1:DNmet* larvae (Figure 3-14A and B). Interestingly, at 72 hpf the number of dorsal OLCs was reduced in *sox10:DNmet* larvae compared to both wildtype (p = 0.0042) and *olig1:DNmet* (p = 0.0461) larvae (Figure 3-14C). Additionally, ventral OLCs were reduced in *sox10:DNmet* larvae compared to wildtype (p = 0.0286) (Figure 3-14D). Concordantly, the number of pMN domain OLCs in *sox10:DNmet* was

significantly increased compared to both wildtype ($p < 0.0001$) and *olig1:DNmet* ($p < 0.0001$) larvae (Figure 3-14E). The significantly increased percentage of OLCs in the pMN domain in *sox10:DNmet* larvae resulted in a reduced percentage of both dorsal and ventral OLCs in *sox10:DNmet* larvae compared to both wildtype and *olig1:DNmet* larvae at this stage (Figure 3-14F and G). Additionally, *olig1:DNmet* larvae had a slightly increased percentage of pMN domain OLCs when compared to wildtype ($p = 0.0147$), though significantly less than *sox10:DNmet* ($p < 0.0001$), indicating that reducing Met signaling later in developmental can also affect OLC positioning (Figure 3-14G).

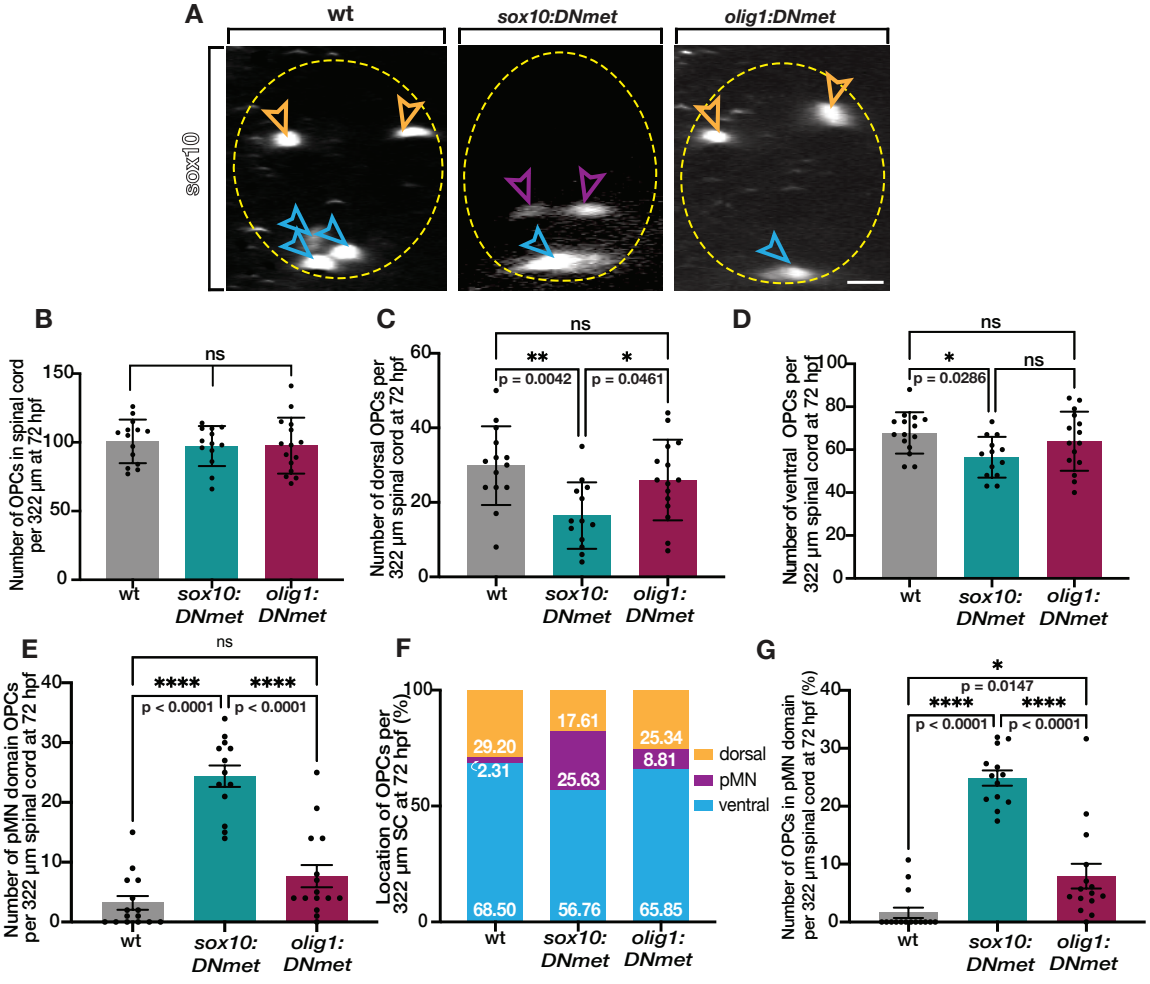


**Figure 3-14.** Met knock-down migration defects in pre-migratory OPCs persist to 72 hpf. (A) Transverse sections of sox10 antibody labeled 72 hpf wildtype, *sox10:DNmet*, and *olig1:DNmet* zebrafish larvae. Orange open arrowheads denote dorsal OLCs. Purple open arrowheads denote pMN domain OLCs. Blue

open arrowheads denote ventral OLCs. Yellow dashed circle denotes spinal cord boundary. (B-G) Quantifications taken from images of 72 hpf sox10 antibody labeled wildtype (n = 14), *sox10DN:met* (n = 13), and *olig1:DNmet* (n = 15) spinal cords. Mean with SEM. Statistical test: 1-way ANOVA with Tukey's Multiple Comparison Test. Scale bar, 20 μm.

Taken together, these data demonstrate that reducing Met signaling specifically in pre-migratory OPCs causes a reduction in dorsal OPC migration following specification. Additionally, this reduction in migration is not observed when Met is knocked down in OLCs that are already in the migratory window. Therefore, Met acts cell-autonomously to induce OPC migration, following specification, during developmental OPC tiling.

**OPCs increase proliferation in response to reduced numbers in *met* mutants**

OPCs are a robust population of cells that are able to sense a reduction in density and respond by upregulating proliferation in the remaining OPCs (Kirby, et al., 2006; Hughes, et al., 2013; Birey & Aguirre, 2015). In order to determine if OPCs in *met* mutants respond in a similar way, I conducted 24 hour *in vivo* time-lapse imaging in 76 hpf *olig2:egf;met*$^{+/+}$, *met*$^{+/-}$, and *met*$^{/-}$ larvae (Figure 3-15A). Using our cell-tracking software, I quantified the numbers of OPCs that migrated from 3 to 4 dpf. Interestingly, I found that there is no significant difference between the numbers of OPCs that migrate from 3 to 4 dpf in *met*$^{+/+}$, *met*$^{+/-}$, and *met*$^{/-}$ larvae (Figure 3-15B). Additionally, there is no difference in the number of dorsally or ventrally migrating OPCs (Figure 3-15C and D). These results demonstrate that by 4 dpf, the number of OPCs in *met*$^{/-}$ larvae have recovered to wildtype numbers of OPCs. It is possible that the recovery of OPCs could be due to a delay in OPC migration out of the pMN domain, however, there was an increase in the number of cell divisions in *met*$^{/-}$ larvae compared to heterozygous siblings ($p = 0.0332$) (Figure 3-15E). These results indicate that OPCs are responding to the reduction in the number of OPCs by upregulating proliferation.

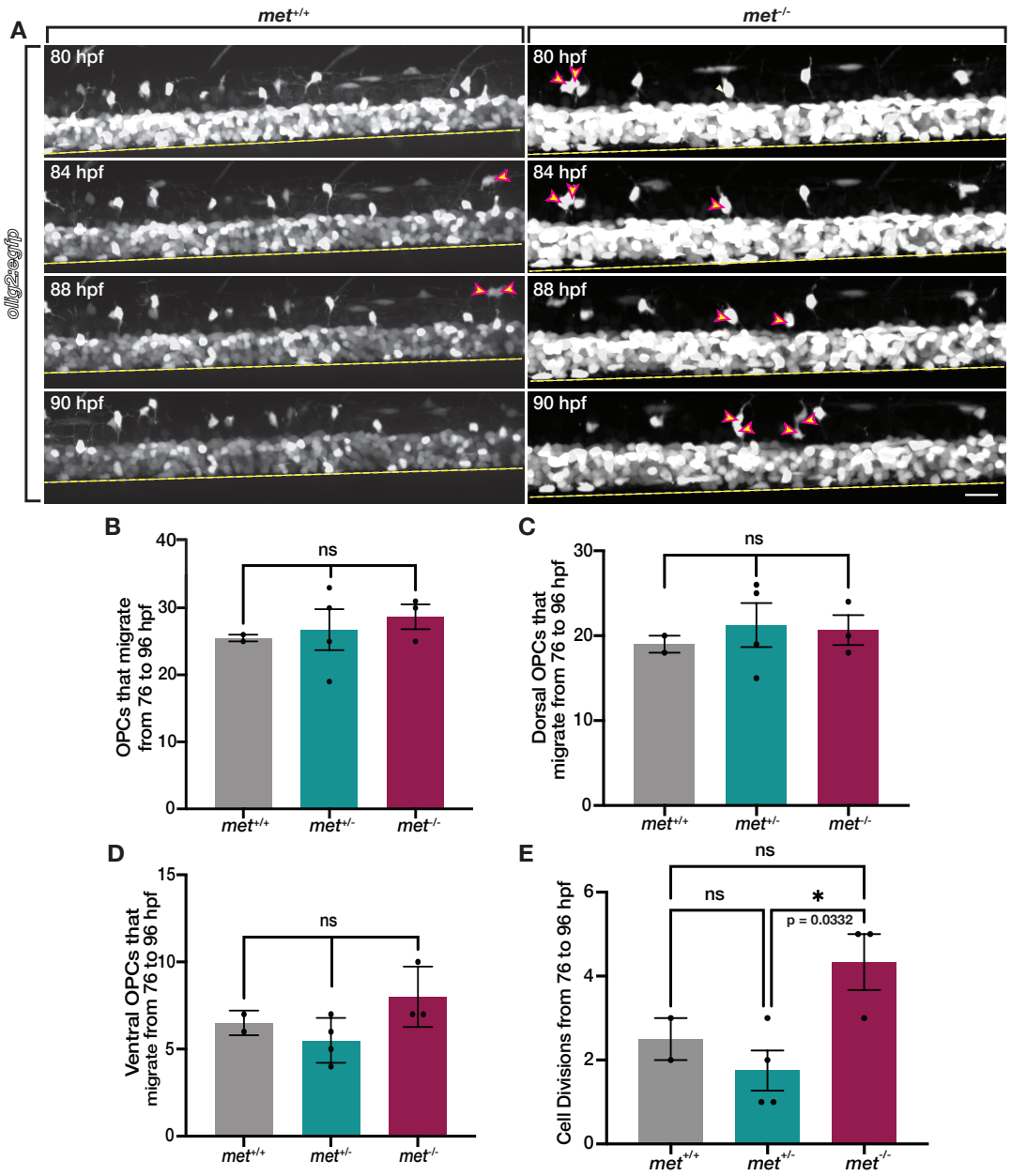


**Figure 3-15. OPC migration defects in *met*$^{-/-}$ larvae recover by 4 dpf.** (A) Images taken from 24 hour time-lapse imaging of 80 hpf *olig2:egfp* *met*$^{+/+}$ and *met*$^{-/-}$ larvae. Yellow-filled pink arrowheads denote dividing cells. Yellow dashed line denotes ventral edge of the spinal cord. (B-E) Quantifications taken from 24 hour time-lapse images of 80 hpf *olig2:EGFP* *met*$^{+/+}$ (n = 2), *met*$^{+/-}$ (n = 4), and *met*$^{-/-}$ (n = 3) larvae. Mean with SEM. Statistical test: 1-way ANOVA with Tukey's Multiple Comparison Test was used for D-F. Scale bar, 20 μm.

To more directly assess OPC proliferation, I treated *olig2:egfp;sox10:mrfp;met*$^{+/+}$, *met*$^{+/-}$, and *met*$^{/-}$ larvae with EdU from 96 to 102 hpf to detect DNA synthesis in proliferative cells (Figure 3-16A). I then imaged lateral spinal cords of EdU-treated

larvae and quantified *olig2*$^{+}$/*sox10*$^{+}$/EdU$^{+}$ OLCs (Figure 3-16B). I observed a significant increase in the number of EdU$^{+}$ OLCs in 4 dpf *met*$^{-/-}$ larvae compared to wildtype larvae ($p = 0.0244$) (Figure 3-16C). This active response to the reduction in OPC numbers of upregulating OPC proliferation in *met* mutants supports previous data demonstrating the robust ability of OPCs to maintain proper density and tiling (Kirby, et al., 2006; Hughes, et al., 2013; Birey & Aguirre, 2015). Additionally, it indicates that there is a population of OPCs that migrate and proliferate independently of Met signaling and are therefore able to respond to *met* mutant OPC tiling defects. Further investigation into gene expression differences between OPCs that exhibit Met-dependent tiling and OPCs that exhibit Met-independent tiling would allow for identification of which OPCs respond to the reduction in OPC numbers.

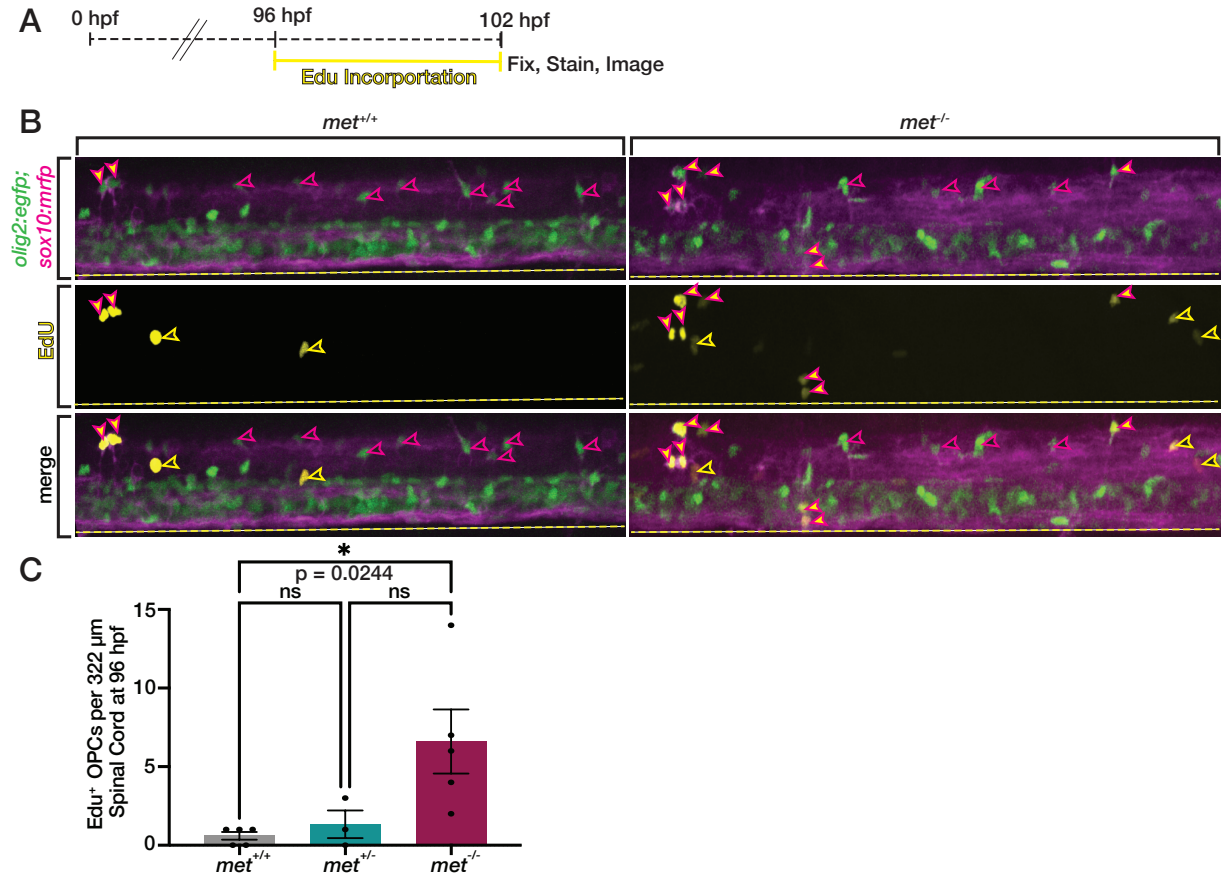


**Figure 3-16. OPCs respond to migration defects in *met* mutants by increasing proliferation.** (A) EdU treatment paradigm. (B) Spinal cord images of 102 hpf *olig2:egfp;sox10:mrfp* *met*$^{+/+}$ and *met*$^{-/-}$ larvae.

Magenta-outlined yellow arrowheads denote *sox10*$^{+}$/*olig2*$^{+}$/EdU$^{+}$ OPCs. Magenta open arrowheads denote *sox10*$^{+}$/*olig2*$^{+}$/EdU$^{-}$ OLCs. Yellow open arrowheads denote *sox10*$^{-}$/*olig2*$^{-}$/EdU$^{+}$ cells. Yellow dashed line denotes ventral edge of the spinal cord. (C) Quantifications of *sox10*$^{+}$/*olig2*$^{+}$/EdU$^{+}$ OLCs from spinal cord images of 102 hpf *olig2:egfp;sox10:mrfp* EdU labeled *met*$^{+/+}$ (n = 7) , *met*$^{+/-}$ (n = 8), and *met*$^{-/-}$ (n = 7) larvae. Mean with SEM. Statistical test: 1-way ANOVA with Tukey's Multiple Comparison Test.

Finally, after observing that OPCs respond to reduced OPC numbers by proliferating in *met* mutants, I wanted to investigate any other potential consequences of altering OPC tiling using *met* mutant transgenic larvae. One potential consequence of altered tiling could be an altered ability for OPCs to differentiate into oligodendrocytes and initiate myelination, which are the developmental processes that immediately follow OPC tiling. To assess initiation of myelination, I used an RNA probe specific to *myelin basic protein a (mbpa)* in an *in situ* hybridization experiment conducted on 5 dpf wildtype, *met*$^{-/-}$, *sox10:DNmet,* and *olig1:DNmet* larvae. *Mbpa* is expressed by oligodendrocytes beginning around 4 dpf just prior to initiating myelination (Dubois-Dalcq, et al., 1986; Li, et al., 2007; Almeida, et al., 2011). Following *mbpa in situ* hybridization, I sectioned and imaged transverse sections of 5 dpf wildtype, *met*$^{-/-}$, *sox10:DNmet,* and *olig1:DNmet* larvae and found robust *mbpa* expression in the white matter of all larvae assessed that was not visibly different from wildtype (Figure 3-17). Robust *mbpa* expression indicates that OPCs in Met loss-of-function transgenic larvae are capable of differentiating into oligodendrocytes and initiating myelination. More work will need to be done to ensure that myelination is wildtype in Met loss-of-function zebrafish. However, evidence that *met*$^{-/-}$ zebrafish can

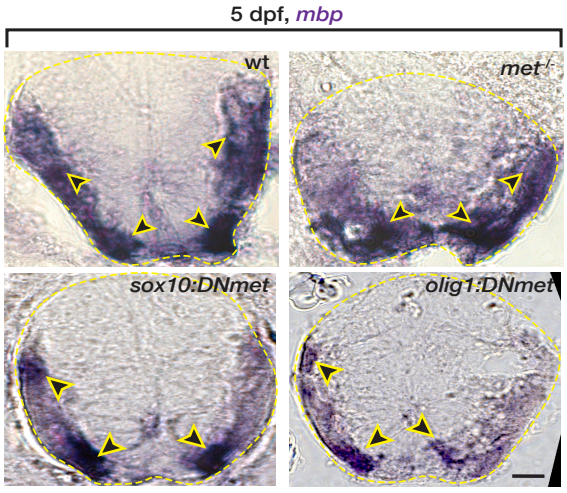


**Figure 3-17.** Loss of met signaling does not affect myelination. Transverse sections of *in situ* hybridizations showing *mbpa* expression in the spinal cord of 5 dpf wildtype, *met*$^{-/-}$, *sox10:DNmet*, and *olig1:DNmet* larvae. Scale bar = 10 µm.

be reared to adulthood without motor defects indicates that myelination in those mutants is sufficient for normal development processes (Nord, et al., 2019).

**Hepatocyte growth factor signaling is required for OPC tiling**

Because Hgf is the ligand for Met signaling, I wanted to investigate whether there would be a reduction in dorsal OLC numbers in *hgfa* mutants, as well (Isabella, et al., 2020). To do this, I used sox10 antibody labeling on 72 hpf *hgfa*$^{+/+}$, *hgfa*$^{+/-}$, *hgfa*$^{-/-}$ larvae and imaged transverse sections of the spinal cord to quantify the number of sox10$^{+}$ OLCs (Figure 3-18). I hypothesized that I would see a very similar change in OPC migration to what I observed in *met* mutant larvae. As expected, I observed a decrease in the overall number of OLCs in *hgfa*$^{-/-}$ larvae compared to wildtype siblings ($p = 0.0008$) (Figure 3-18B). Furthermore, I found that there was a significant decrease in the number of dorsal OLCs in *hgfa*$^{-/-}$ larvae compared to wildtype siblings ($p < 0.0001$), though the number of ventral OLCs in *hgfa*$^{-/-}$ larvae was not significantly different compared to wildtype siblings (Figure 3-18C and D). Finally, the number of OLCs in the pMN domain in *hgfa*$^{-/-}$ larvae was increased compared to wildtype and heterozygous siblings (wt, $p = 0.0004$; het, $p = 0.0200$) (Figure 3-18E). These data are all consistent with what I observed in *met* mutant larvae and further support that the Met signaling pathway is required for developmental OPC migration.

After verifying that *hgfa* mutants exhibited similar tiling defects as *met* mutants, I next wanted to identify the source of Hgf in the developing zebrafish spinal cord. RNA-sequencing experiments reveal that Hgf is highly expressed in mouse and human astrocytes and not highly expressed by other glial or neuronal cell types (Zhang, et al., 2016; Lake, et al., 2016). Until very recently, it was believed that zebrafish lack astrocytes and that radial glia instead perform many of the same functions as astrocytes (Lyons & Talbot, 2014). Emerging evidence supports the presence and function of astrocytes in zebrafish (Chen, et al., 2020), however, numerous papers also demonstrate that radial

glia perform many similar functions to astrocytes, such as neuronal maintenance, spinal cord injury response, and blood-brain-barrier maintenance (Corbo, et al., 2012; Becker & Becker, 2014; Lyons & Talbot, 2014; Than-Trong & Bally-Cuif, 2015).

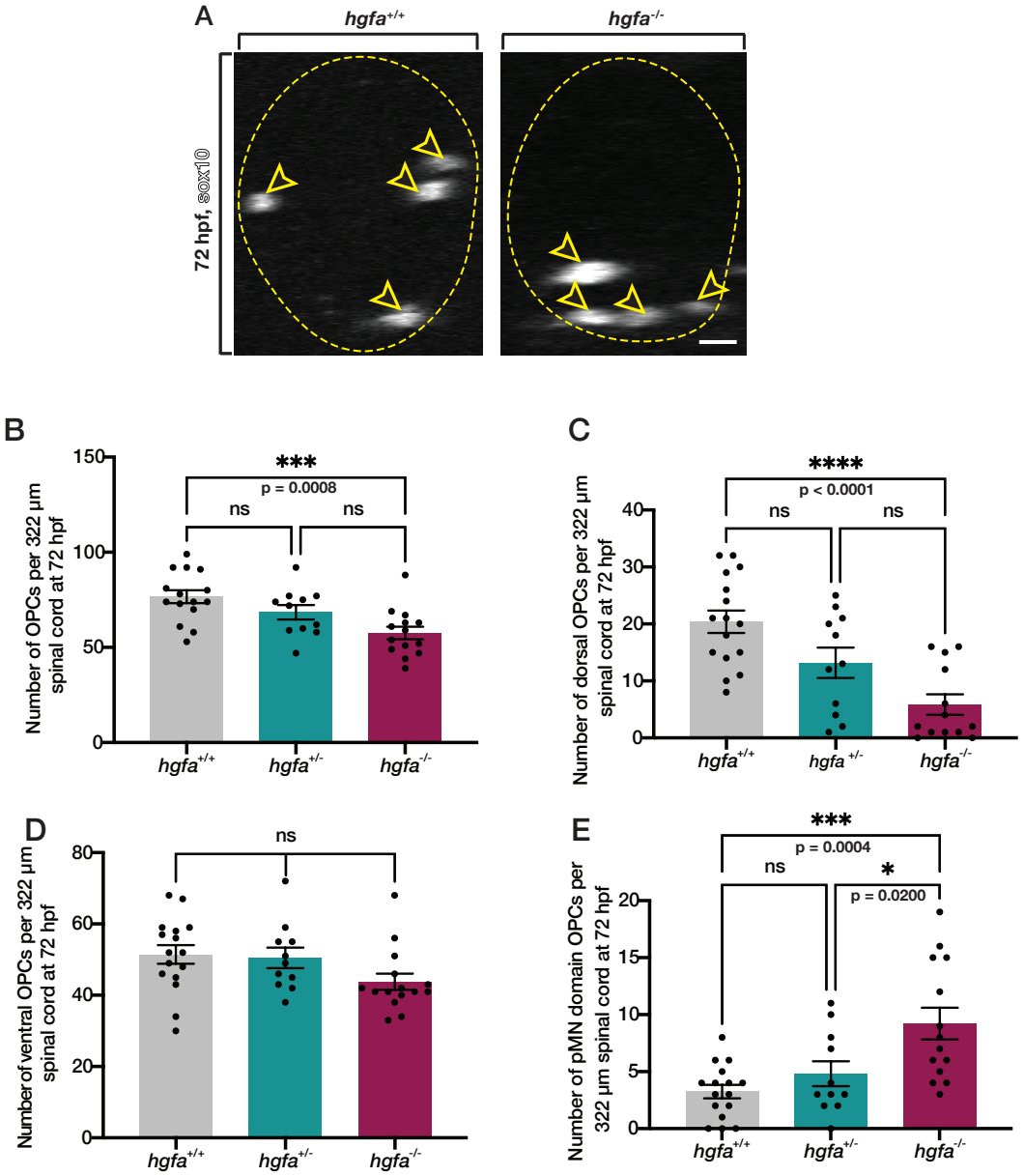


**Figure 3-18. *hgfa* mutants exhibit reduced OPC numbers.** (A) Transverse sections of sox10 antibody labeled 72 hpf wildtype, *hgfa*$^{+/+}$, and *hgfa*$^{-/-}$ larvae. Yellow open arrowheads denote sox10$^{+}$ OLCs. Dashed yellow circle denotes boundary of spinal cord. (B-E) Quantifications taken from images of 72 hpf sox10 antibody labeled *hgfa*$^{+/+}$ (n = 14), *hgfa*$^{+/-}$ (n = 11), and *hgfa*$^{-/-}$(n = 14) larval spinal cords. Mean with SEM. Statistical test: 1-way ANOVA with Tukey's Multiple Comparison Test. Scale bar, 20 µm.

To determine if radial glia are the source of Hgf in zebrafish development, I utilized a mutant our lab discovered in an ENU mutagenesis screen called *failure-to-launch (ftl)*. ENU, also known as N-ethyl-N-nitrosourea, is a potent mutagen that is utilized in genetic screens to induce random point mutations in adult male zebrafish whose progeny are then screened for phenotypes of interest (de Bruijn, et al., 2009). One of the phenotypes observed in time-lapse imaging of 55 hpf *ftl*$^{+/+}$ and *ftl*$^{/-}$ larvae is the reduction in dorsal OPC migration in *ftl* mutants compared to their wild-type siblings (Figure 3-19A). Further characterization of the *ftl* mutant involved using a Zrf1 antibody to label GFAP$^{+}$ (glial fibrillary acidic protein) radial glial cell processes. Zrf1 labeling in 72 hpf *ftl*$^{+/+}$ and *ftl*$^{/-}$ larvae revealed that there were fewer radial glial cell processes in *ftl* mutants compared to their wild-type siblings (Figure 3-19B). A TUNEL (Terminal deoxynucleotidyl transferase dUTP nick end labeling) assay was performed to label double-strand DNA breaks that occur during apoptosis in 48 hpf *ftl*$^{+/+}$ and *ftl*$^{/-}$ larvae, which is prior to the observed OPC migration and radial glial defects in *ftl* mutants. TUNEL labeling revealed an increased number of apoptotic cells along the center line of the spinal cord corresponding to the location of radial glial cell bodies (Barry, et al., 2013) (Figure 3-19C). Additionally, genomic mapping in *ftl* mutants revealed that it is on a different chromosome from *met* and *hgfa*. These results led us to conclude that the *ftl* mutation encodes for a gene that is necessary for radial glia survival and that radial glia potentially express or secrete a protein that influences OPC migration.

Because the OPC migration phenotype in *ftl* mutants phenocopies the OPC migration phenotype observed in both *met* and *hgfa* mutants and radial glia could be similar to astrocytes in their expression of Hgf, I wanted to further characterize the Met signaling pathway in *ftl* mutants. To do this, I conducted *hgfa in situ* hybridization in 55 hpf *ftl*$^{+/+}$ and *ftl*$^{/-}$ larvae and observed wildtype *hgfa* staining in the muscle in both *ftl*$^{+/+}$

and *ftl*$^{-/-}$ larvae (Figure 3-19D). However, *ftl*$^{-/-}$ larvae exhibited an absence of *hgfa* in the CNS compared to *ftl*$^{+/+}$ larvae (Figure 3-19D). These results demonstrate that

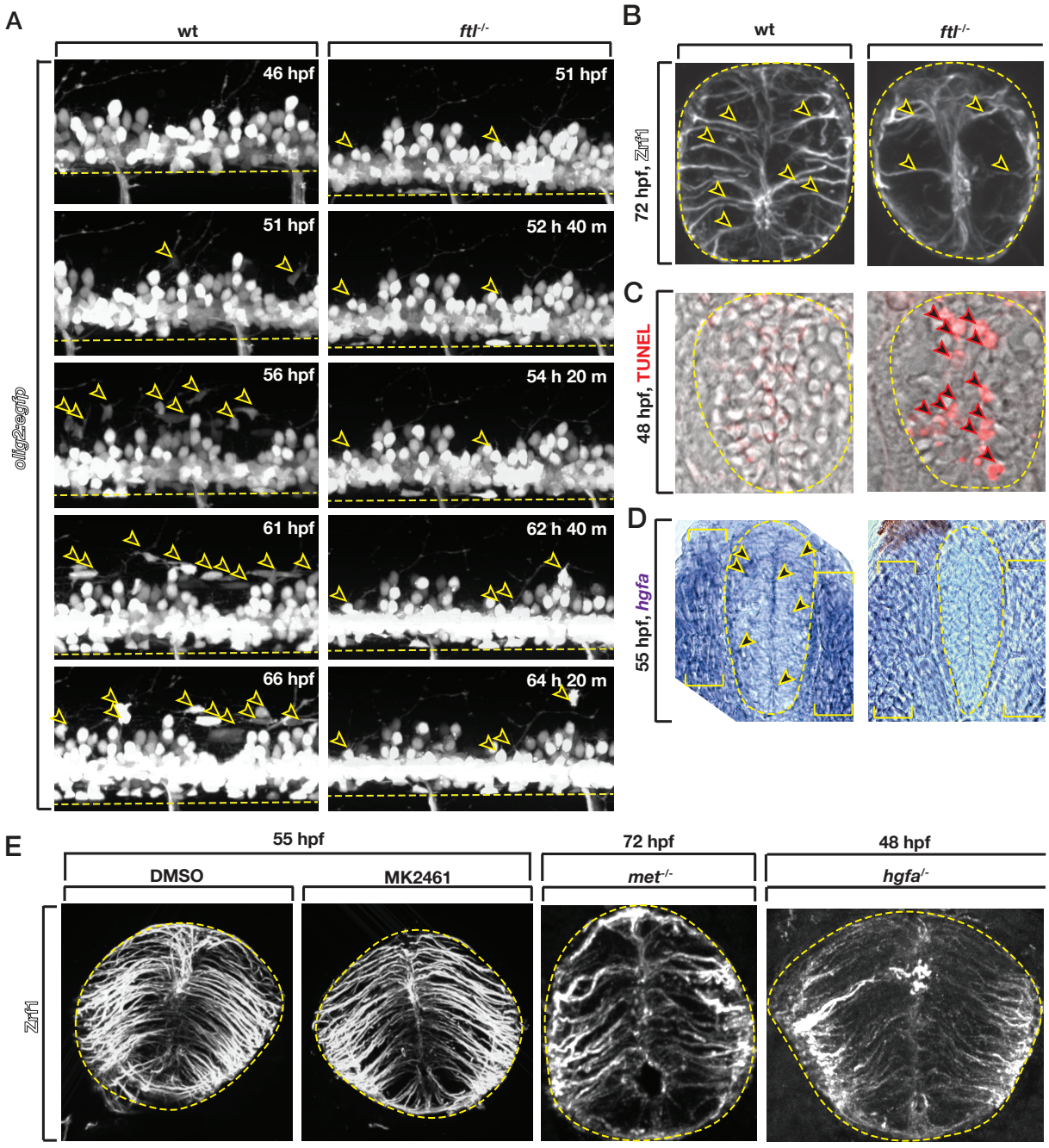


**Figure 3-19.** Radial glial cell death causes reduced *hgfa* expression in the spinal cord. (A) Images taken from 24 hour time-lapse imaging of 46 hpf *olig2:egfp* wt and *ftl*$^{-/-}$ larvae. Yellow open arrowheads denote dorsal OPCs. Yellow-dashed line denotes ventral edge of the spinal cord. (B) Transverse sections of Zrf1 antibody labeled 72 hpf wt and *ftl*$^{-/-}$ larvae. Yellow open arrowheads denote radial glia processes. (C) Transverse sections of TUNEL-stained 48 hpf wt and *ftl*$^{-/-}$ larvae. Red outlined arrow heads denote apoptotic

cells. (D) Transverse sections of *hgfa in situ* hybridization in 55 hpf wt and *ftl*$^{-/-}$ larvae. Yellow brackets denote wildtype *hgfa* expression in the muscle. Yellow arrowheads denote *hgfa* expression in the CNS. (E) Transverse sections of Zrf1 antibody labeled 55 hpf 1% DMSO and 10 µM MK2451 in 1% DMSO treated larvae, 72 hpf *met*$^{-/-}$ larvae, and 48 hpf *hgfa*$^{-/-}$ larvae. Yellow-dashed circle denotes spinal cord boundary. Experiments and images (A-C) were conducted by Andrew Latimer, PhD.

loss of radial glia reduces *hgfa* signaling in the spinal cord and supports my hypothesis that zebrafish radial glia secrete Hgfa. Additionally, I conducted Zrf1 antibody labeling on MK2461-treated, *met*$^{-/-}$, and *hgfa*$^{-/-}$ larvae and observed no difference in radial glial processes compared to DMSO-treated and wildtype larvae, demonstrating that the OPC migration defects in loss of Met signaling mutants is not caused by radial glial defects like those observed in *ftl* (Figure 3-19E). Finally, in order to directly assess the source of Hgfa, I used an HGF antibody in combination with a Zrf1 antibody in 48 hpf larvae. I then imaged transverse sections of the spinal cord and observed colocalization in the center-line and distal portions of the radial glia cell processes (Figure 3-20). Based on these findings, I propose that radial glia are the source of Hgfa in the developing zebrafish spinal cord.

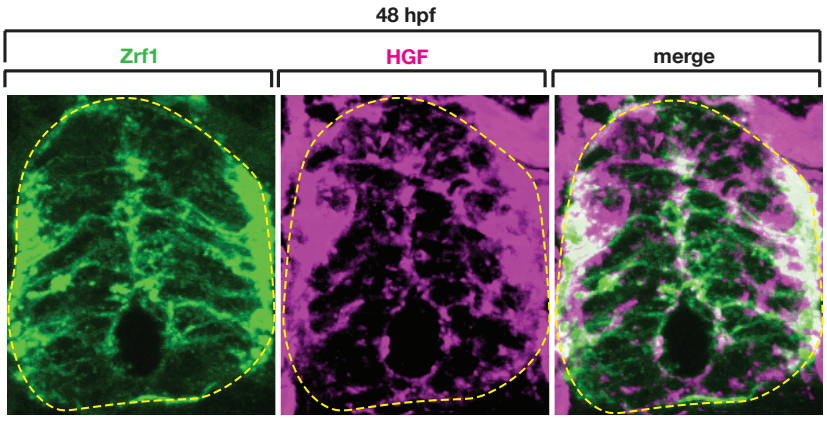


**Figure 3-20. Radial glia express Hgf.** Transverse section of Zrf1 and HGF antibody labeled 48 hpf larva.

## Discussion

OPC tiling is a complex process involving numerous signaling molecules that regulate various cellular processes including migration, proliferation, and contact-mediated repulsion. In this study, I conducted the first *in vivo* investigation into the role of the Met signaling pathway in OPC tiling, primarily focused on its effects on OPC migration and proliferation. Previous studies involving the Met signaling pathway and OPC tiling utilized *in vitro* cell cultures of primary rat and mouse OPCs and pharmacological techniques to observe the effect of Hgf on OPC chemotaxis and cell division (Yan & Rivkees, 2002; Lalive, et al., 2005; Ohya, et al., 2007). To investigate the role of the Met signaling pathway in OPC tiling, I used zebrafish as a vertebrate model in combination with CRISPR/Cas9 mutagenesis, site-directed mutagenesis, and pharmacological interventions. I demonstrated that Met is expressed by OPCs and that loss of Met in either whole animal knock-out or cell-specific knock-down results in decreased OPC migration and proliferation. Furthermore, I demonstrate that whole animal knock-out of *hgfa* results in the same OPC migration phenotype observed in the Met studies. Finally, utilizing a zebrafish mutant that exhibits radial glial cell death and phenocopies the OPC migration defects observed in loss of Met signaling mutants, I demonstrated that radial glial cell death results in reduced *hgfa* expression in the spinal cord. Overall, I demonstrated that

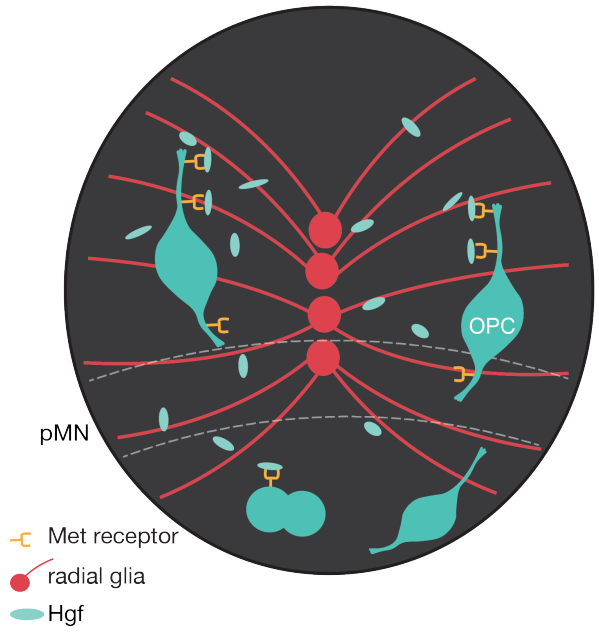


**Figure 3-21. The Met signaling pathway in the zebrafish spinal cord.** This diagram demonstrates a model for Met signaling in the zebrafish spinal cord, where radial glia (red) secrete Hgfa (blue), which binds to Met receptors (orange) on OPCs to induce dorsal OPC migration and OPC proliferation.

following specification, OPCs express Met and respond to Hgfa that is secreted from radial glia in order to initiate OPC migration and proliferation during developmental tiling (Figure 3-21). This comprehensive work characterizing the role of Met signaling in OPC tiling and the potential source of Hgf lays a foundation to explore more nuanced influences of Met signaling in OPCs and how this signaling is regulated to allow for differentiation and injury-response.

**Heterogeneous express of met signaling in OPCs**

Our Met expression analysis in Figure 3-4 revealed a small population of pre-migratory and migratory OPCs that did not express Met. Additionally, in loss of Met signaling mutants, I observed OPCs that were able to migrate dorsally. Based on these results it is likely that there is a population of OPCs that are capable of migrating in a Met-independent manner. There are of a number of molecules that have been shown to influence OPC chemotaxis and it is possible that different populations of OPCs utilize different mechanisms to initiate migration. A number of recent studies that utilized gene expression analysis experiments, such as RNA-seq, sought to gain more insight into the question of whether there are different subpopulations (Kitada and Rowitch 2006; Dimou and Simons 2017; Horiuchi et al. 2017; Marisca et al. 2020). A common theme of these studies is identifying markers for OPCs located in different regions of the CNS, such as gray matter vs white matter or brain vs spinal cord. However, my data suggests that OPCs within the same region of the spinal cord may also express different genes and utilize different tiling mechanisms. Furthermore, the observed proliferative response of OPCs to the initial lack of migration in *met* mutants should be further investigated to determine if OPCs that lack *met* expression in wildtype OPC development are responding to the lack of OPC migration in *met* mutants by upregulating proliferation. To do this, an analysis of the genetic differences between $Met^+$ and $Met^-$ OPCs would need to be done to identify markers unique to $Met^-$ OPCs.

These markers could then be used to label the Met$^-$ population and observe how they respond in a *met*$^{-/-}$ background. Being able to identify Met$^-$ OPCs would be incredibly useful to gain more insight into whether there are different subpopulations of OPCs and to investigate other mechanisms that OPCs use to migrate and proliferate during developmental tiling.

**Met signaling regulation in OPCs during development and injury response**

Another aspect of Met signaling and OPC tiling is that Met signaling must be down-regulated in order for OPCs to differentiate into myelinating oligodendrocytes (Ohya, et al., 2007). Met signaling can be modulated by either down-regulating the expression of the Met receptor and/or its ability to signal or by reducing the presence of the ligand Hgf. Because Hgf is a secreted signaling molecule that is utilized by many different cell types during CNS development, understanding the ways in which OPCs downregulate Met signaling would better elucidate how Met signaling is regulated in OPCs specifically. One study using rat OPCs in culture demonstrated that the gene *CD82* is highly upregulated in OPCs and that CD82 directly inhibits Hgf-induced chemotaxis of OPCs (Mela & Goldman, 2013). RNA seq experiments our lab conducted in 2017 revealed that OPCs at 72 hpf uniquely express both zebrafish orthologs of *CD82, cd82a* and *cd82b*. Further investigation in to the expression patterns of *cd82a* and *cd82b* to confirm the RNA-seq results would be the first step to investigating if OPCs in zebrafish are downregulating Met signaling in the same way as rat and mouse OPCs. Once expression is confirmed, CRISPR/Cas9 mutagenesis could be used to investigate the consequences of loss of *cd82a* and *b* on OPC tiling. If *cd82a* and *b* downregulate Met signaling in OPCs during development, then I would expect reduced OPC differentiation and reduced myelination in the CNS. These cursory experiments would demonstrate the influence of *cd82a* and *b* on developmental OPC tiling and provide some insight into the regulation of Met signaling.

Investigating the regulation of Met signaling in OPC tiling during development will also be invaluable in understanding how OPCs respond to CNS injury and disease. Previous studies using the disease model for multiple sclerosis in mice, experimental autoimmune encephalomyelitis (EAE), demonstrated that macrophages and microglia release HGF and OPCs upregulate Met signaling and chemotaxis in response to demyelinated lesions (Lalive, et al., 2005; Moransard, et al., 2009). It is possible that *cd82* also plays a role in selectively up or downregulating OPC migration in both development and disease contexts. Beyond these studies, little is known about how OPCs respond to injury and initiate migration and it is possible that OPCs utilize the same migration mechanisms in both development and injury-response. With so much still unknown about how OPC behaviors are molecularly-mediated, this work demonstrates the critical role that Met signaling plays in regulating initial OPC migration during development. Future work will need to be done to identify how Met signaling is regulated in OPCs and what role, if any, Met plays in other OPC processes, such as adult tiling and injury-response.

# Chapter IV

# Novel Mediators of Oligodendrocyte Progenitor Cell Tiling


## Abstract

Developmental oligodendrocyte progenitor cell (OPC) tiling is a process where OPCs disperse and become evenly tiled throughout the central nervous system (CNS). This process is comprised of migration, proliferation, and contact-mediated repulsion (CMR). In this study, I identify novel mediators of OPC proliferation and CMR by investigating candidate genes proposed to mediate OPC development in the developing mouse spinal cord. Using zebrafish as a vertebrate model, I demonstrate that *netrin-1* (*ntn1*), a proposed mediator of OPC migration, also mediates OPC proliferation. I then show that *lingo1a* mutants exhibit tiling defects that implicate Lingo1 as a mediator of CMR between OPCs. These findings provide insight into how these critical tiling processes are molecularly mediated, which is necessary for a comprehensive understanding of OPC development.


## Introduction

OPC tiling has primarily been studied by focusing on either describing tiling phenomenologically or identifying chemotactic molecules that influence OPC migration (Sugimoto, et al., 2001; De Castro & Bribián, 2005; Kirby, et al., 2006; Binamé, et al., 2013). Based on these studies, it is clear that OPCs dynamically remodel their cell processes and undergo a robust proliferative period following their initial migration, however, only a handful a potential mediators of process remodeling and OPC proliferation have been identified (Yan & Rivkees, 2002; Li, et al., 2018; Dobrowolski, et al., 2020; Lorenzati, et al., 2021). Many of these studies utilize the markers *sox10* and *olig2* to selectively label OPCs, however, unique markers specific to OPCs would greatly improve investigations into OPC development. In this chapter, I

demonstrate novel markers that are uniquely expressed by OPCs that could be used to selectively label OPCs.

These unique markers would be impactful when studying OPC process remodeling, which can be particularly difficult to discern in an *olig2:egfp* larvae that labels all motor neurons in addition to OPCs. In this chapter, I describe my investigation into OPC process remodeling that utilized a glutamate transport inhibitor. A number of studies have investigated the contribution of neuronal activity and neurotransmitter signaling on OLC development (Gudz, et al., 2006; Gibson, et al., 2014; Linneberg, et al., 2015; Fannon, et al., 2015; Zhu, et al., 2016). However, only a handful of studies have demonstrated that neurotransmitter signaling through receptors on OPCs influences OPC migration and positioning (Gudz et al. 2006; Piller et al. 2021). A paper recently published by our lab demonstrates that glutamate signaling acts cell-autonomously in OPCs to induce dorsal OPC migration (Piller et al. 2021). This study in combination with my investigation into glutamate transport in regulating OPC processes demonstrates the need for further investigation into how neuronal activity influences earlier developmental tiling processes of migration and process remodeling.

During OPC migration, OPCs exhibit robust proliferation. The majority of the mediators proposed to influence OPC proliferation were identified in tandem to their role as mediators of OPC migration (Figure 1-3). For example, Netrin-1 (Ntn1) is a secreted signaling protein initially identified as a chemorepellent molecule that causes OPCs to retract their processes and reverse their direction of migration (Spassky, et al., 2002; Jarjour, et al., 2003; Tsai, 2006; Rajasekharan, et al., 2010). Additionally, it was proposed that Ntn1 expression in the floor plate of the spinal cord results in OPCs being repelled out of the ventral spinal cord resulting in OPC dispersal (Tsai, 2006). My investigation of OPC tiling, however, demonstrates a large population of OPCs in the ventral spinal cord making this an unlikely model for mediating dispersal of all OPCs (Figure 3-5B, 3-9A, 3-10A). In this chapter, I describe my investigations into Netrin-1

signaling in OPC tiling and show that Netrin-1 promotes OPC proliferation and OPC migration following cell division.

## Proposed mediators of OPC contact-mediated repulsion

Contact-mediated repulsion (CMR) is the least investigated process of OPC tiling. CMR is observed in OPCs from the moment they are specified. As OPCs dynamically remodel their processes and begin migration, OPC processes probe the surrounding environment for chemotactic signals. If one OPC process contacts another OPC process, either on itself or on a neighboring OPC, the process will contract and, in the case of two neighboring OPCs contacting each other, the OPCs will then change their migratory direction to migrate away from each other (Figure 4-1). These observations suggest that transmembrane receptors capable of bi-directional signaling in both cells are mediating the retraction of OPC processes (Ross, et al., 2016). Canonical bi-directional signaling candidates include Eph-Ephrin signaling, Dscams, and Lingo1 (Zimmer, et al., 2003; Noren & Pasquale, 2004; Millard, et al., 2007; Mayor & Carmona-Fontaine, 2010).

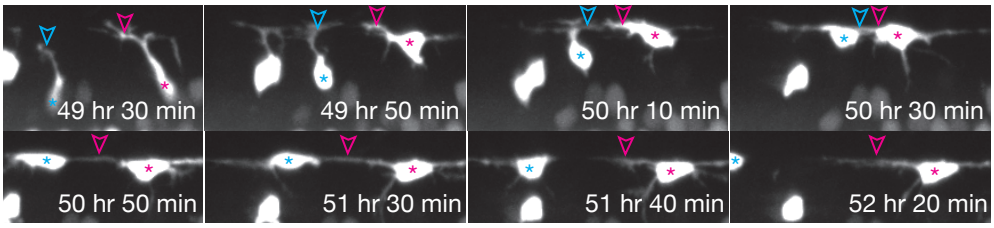


**Figure 4-1. Oligodendrocyte progenitor cells exhibit contact-mediated repulsion.** Images taken from 24 hour time-lapse imaging of 48 hpf *olig2:egfp* larva. Asterisks denote OPC cell bodies. Arrowheads denote cell processes.

In our 2017 RNA-seq experiment, we identified that OPCs express a number of each of these canonical CMR mediators (Figure 4-2). Ephrins are membrane-bound proteins that interact with membrane-bound Eph receptors, often resulting in repulsion of the Ephrin- and Eph-expressing cells (Zimmer, et al., 2003; Egea & Klein, 2007).

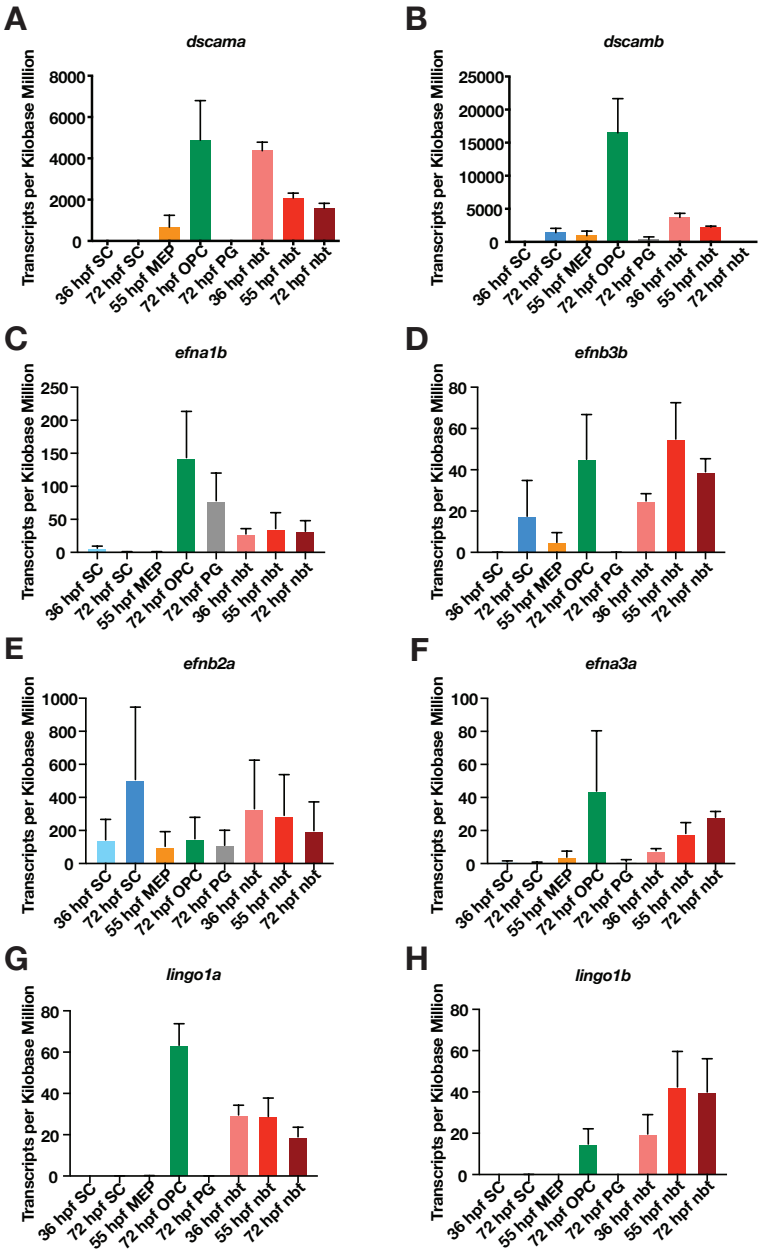


**Figure 4-2. OPCs express canonical mediators of CMR.** (A – H) Quantifications taken from RNA-sequencing experiments that isolated and quantified RNA from 36 and 72 hpf Schwann cells (SC), 55 hpf Motor Exit Point Glia (MEP), 72 hpf oligodendrocyte lineage cells (OPC), and 36, 55, and 72 hpf neurons expressing Neural beta-tubulin (nbt).

Eph-Ephrin signaling has been extensively studied in mediating neuronal migration and axon guidance resulting in segmentation of different neuronal populations (Rodger, et al., 2012; Villar-Cerviño, et al., 2013). One study also demonstrated that Eph-Ephrin

interactions between Eph-expressing axons and Ephrin-expressing OPCs mediates axonophilic migration of OPCs along axons of retinal ganglion cells (Prestoz, et al., 2004). Based on these studies, my undergraduate research assistant, Leah Hogenmiller, acquired an *ephrinb2a* zebrafish mutant and investigated if loss of *ephrinb2a* resulted in OPC tiling defects. Using low-magnification imaging, she observed no difference in the number of dorsally migrated OPCs or spacing between OPCs in *ephrinb2a* mutants compared to wildtype siblings (data not shown). Therefore, we concluded that *ephrinb2a* does not contribute to OPC tiling and I sought to investigate other candidates of CMR between OPCs.

Another family of membrane-bound signaling molecules is the Dscam family of immunoglobulin surface molecules (Hattori, et al., 2008). Dscams (Down syndrome cell adhesion molecules) are capable of heterotypic and homotypic binding to produce either adhesion or repulsion. They are most extensively studied in the developing retina in mediating self-recognition and self-avoidance of developing retinal neurons (Hattori, et al., 2008; Ly, et al., 2008; Fuerst, et al., 2008). In a recent paper, RNA-sequencing of human OPCs revealed high expression *DSCAM*, however, knock-down of *DSCAM* using short hairpin RNA (shRNA) directed at *DSCAM* did not affect OPC migration or CMR (Huang, et al., 2020). In this chapter, I demonstrate that *dscama* mutants also do not affect CMR between developing OPCs in zebrafish larvae. However, I observed that there are OPCs in the peripheral nervous system in *dscama* mutants indicating that *dscama* may be required in mediating CMR between OPCs and other glial or neuronal cell types.

Finally in this chapter, I investigate the contribution of *lingo1a* to OPC CMR. Lingo-1 (Leucine rich repeat and Immunoglobulin-like domain-containing Nogo receptor-interacting protein 1) is a transmembrane protein that is capable of self-interacting. It is most extensively studied for its role in inhibiting oligodendrocyte myelination (Yin & Hu, 2014; Zhang, et al., 2015). Additionally, a Lingo-1 antagonist

was shown to cause increased myelination following injury (Ruggieri et al. 2017). One study, however, more directly assessed the effect of Lingo-1 on OPC development (Jepson, et al., 2012). This study found that when extracellular Lingo-1 fragments were applied to an OPC cell culture, OPC maturation was inhibited (Jepson, et al., 2012). The authors hypothesized that Lingo-1 proteins on axons and OPCs self-interact to inhibit myelination. However, they also showed that Lingo1 caused downstream activation of RhoA, an essential effector of OPC migration, implicating a role for Lingo1 in stimulating OPC migration, potentially following CMR (Jepson, et al., 2012). Based on these investigations into Lingo1 and its role in inhibiting myelination, a Lingo1 antagonist entered phase 3 clinical trials as a treatment to inhibit Lingo1 expressed on axons to promote remyelination in multiple sclerosis patients (Ciccione 2016). However, this clinical trial failed to increase remyelination in these patients, suggesting that the role of Lingo1 in OPC development is not via a straightforward axon-glial interaction. My investigation into a *lingo1a* mutant revealed increased numbers of OPCs and altered spacing between OPCs, which indicates that *lingo1a* is involved in regulating OPC tiling and may mediate CMR.

Taken together, my preliminary investigations into mediators of the OPC tiling processes of proliferation and CMR reveal a number of novel pathways that influence OPC development. Further investigations into the regulation of each of the pathways will provide more insight into the complex emergent process of OPC tiling.

## Results

### Identifying oligodendrocyte progenitor cells

In order to study OPCs, reliable markers of OPCs must be identified to isolate their behaviors from other glial and neuronal cell types in the developing spinal cord. Sox10 and olig2 are reliable markers of OPCs and oligodendrocyte lineage cells (OLCs), which can make it difficult to distinguish an OPC from an oligodendrocyte without

further examination of morphological features, such as number of cellular processes or migratory ability (Kamen, et al., 2021). An RNA-seq investigation conducted by Dr. Andrew Latimer, a research scientist in the Kucenas lab, revealed new genes that were uniquely expressed in OLCs at 72 hpf. To confirm these RNA-seq findings, I generated RNA probes specific to the uniquely expressed genes that I then used for *in situ* hybridization experiments to reveal the location of gene expression. I investigated the

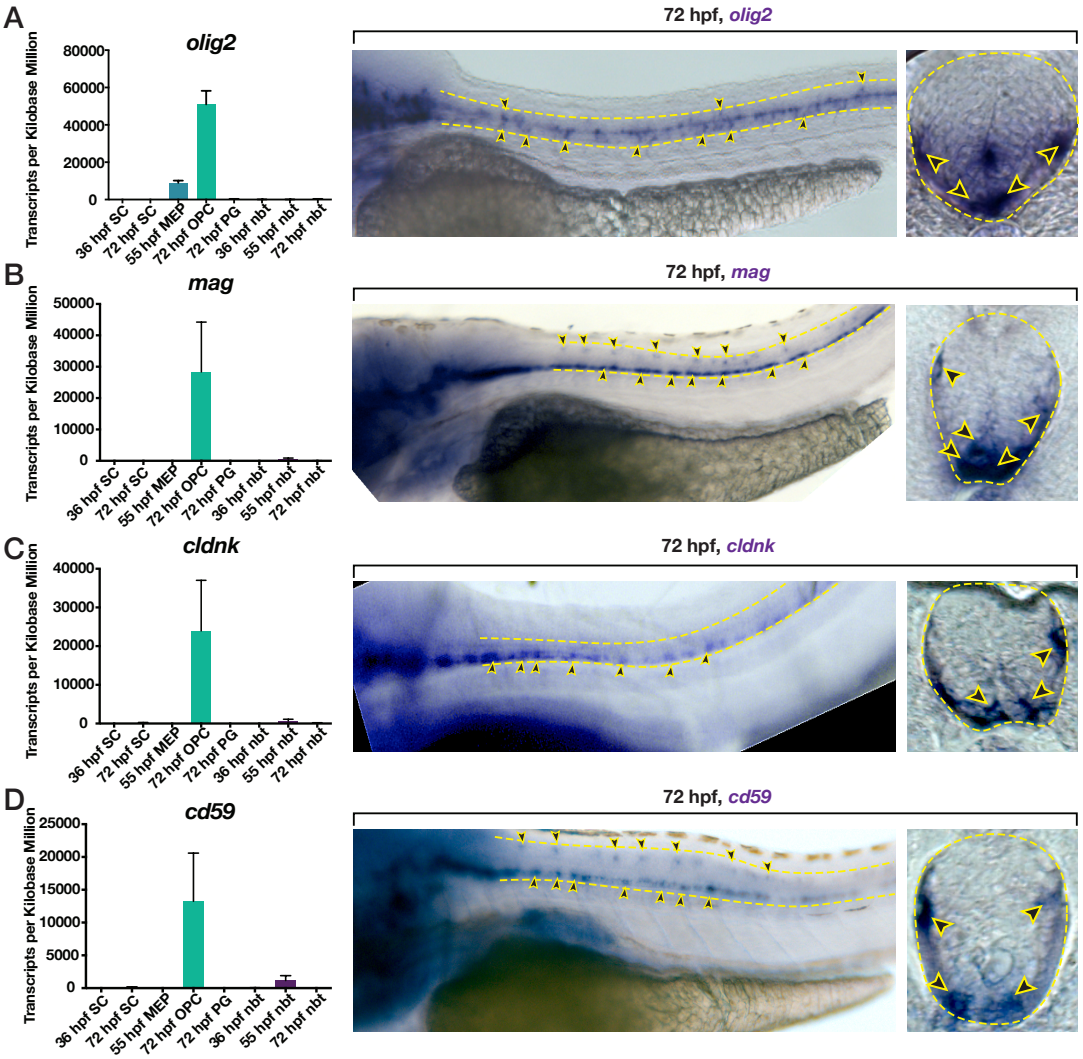


**Figure 4-3. Identifying OPC-specific markers.** RNA expression levels and *in situ* hybridizations in 72 hpf larvae showing lateral and transverse-section views of the spinal cord for (A) *olig2,* (B) *mag,* (C) *cldnk,* and (D) *cd59*. Arrowheads denote OPCs. Yellow dashed lines denote extent of spinal cord in lateral views. Yellow dashed circle denotes extent of spinal cord in transverse-section views.

expression of *mag* (*myelin associated glycoprotein*), *cldnk* (*claudin k*), and *cd59* and compared their expression to *olig2* as a control. I found robust, unique OLC expression by each of the genes investigated (Figure 4-3). Further characterization of the expression pattern of each of these genes throughout development is needed to determine if these genes are unique to OPCs or are general markers of OLCs. However, new transgenic lines that label OLCs from OPC specification throughout development would greatly improve the ability to observe OPC tiling behaviors.

**Glutamate transport inhibition alters OPC process morphology**

OPCs extend elaborate cellular processes that are supported by a complex microtubule rich cytoskeleton (Richter-Landsberg, 2008). These processes actively remodel during migration and CMR and are required for proper spacing and differentiation into oligodendrocytes (Richter-Landsberg, 2008; Thomason, et al., 2020). The majority of work investigating OLC cytoskeletal structures is focused on the cytoskeletal rearrangements that take place during process elaboration and myelination in oligodendrocytes. However, a few studies have shown that downstream signaling effectors such as JNK1 (c-Jun N-terminal kinase 1), RhoA (ras homolog family member A), and MAPK (mitogen activated protein kinase) are required for OPCs to exhibit complex branching structures and loss of these effectors results in less-ramified cell morphology and reduced territory occupancy in tiled adult OPCs (Rajasekharan, et al., 2009, 2010; Cullen, et al., 2021; Lorenzati, et al., 2021). Recent studies, including two from our lab, have that shown OPC developmental behaviors, such as dorsal OPC migration and OPC exit from the spinal cord, are influenced by neurotransmitter signaling through glutamate receptors expressed by OPCs (Gudz et al. 2006; Fannon et al. 2015; Fontenas et al. 2019; Piller et al. 2021). Neurotransmitter signaling has also been shown to influence dendritic remodeling and morphology in developing axons (Wong, et al., 2000; Wong & Wong, 2001).

In collaboration with the Fuss lab at Virginia Commonwealth University, Leah Hogenmiller, and I investigated the effect of inhibiting glutamate transport using the drug TBOA (DL-threo-β-benzylozyaspartic acid) on OPC morphology during OPC migration. We treated 24 hpf *sox10:mrfp* larvae, where *sox10* regulatory sequences drive membrane-RFP in glial cells, with DMSO, 0.2 mM, or 0.4 mM TBOA. We then used time-lapse imaging of 55 hpf DMSO- and TBOA-treated larvae to observe morphological changes in OPC cell processes during initial OPC migration. We found

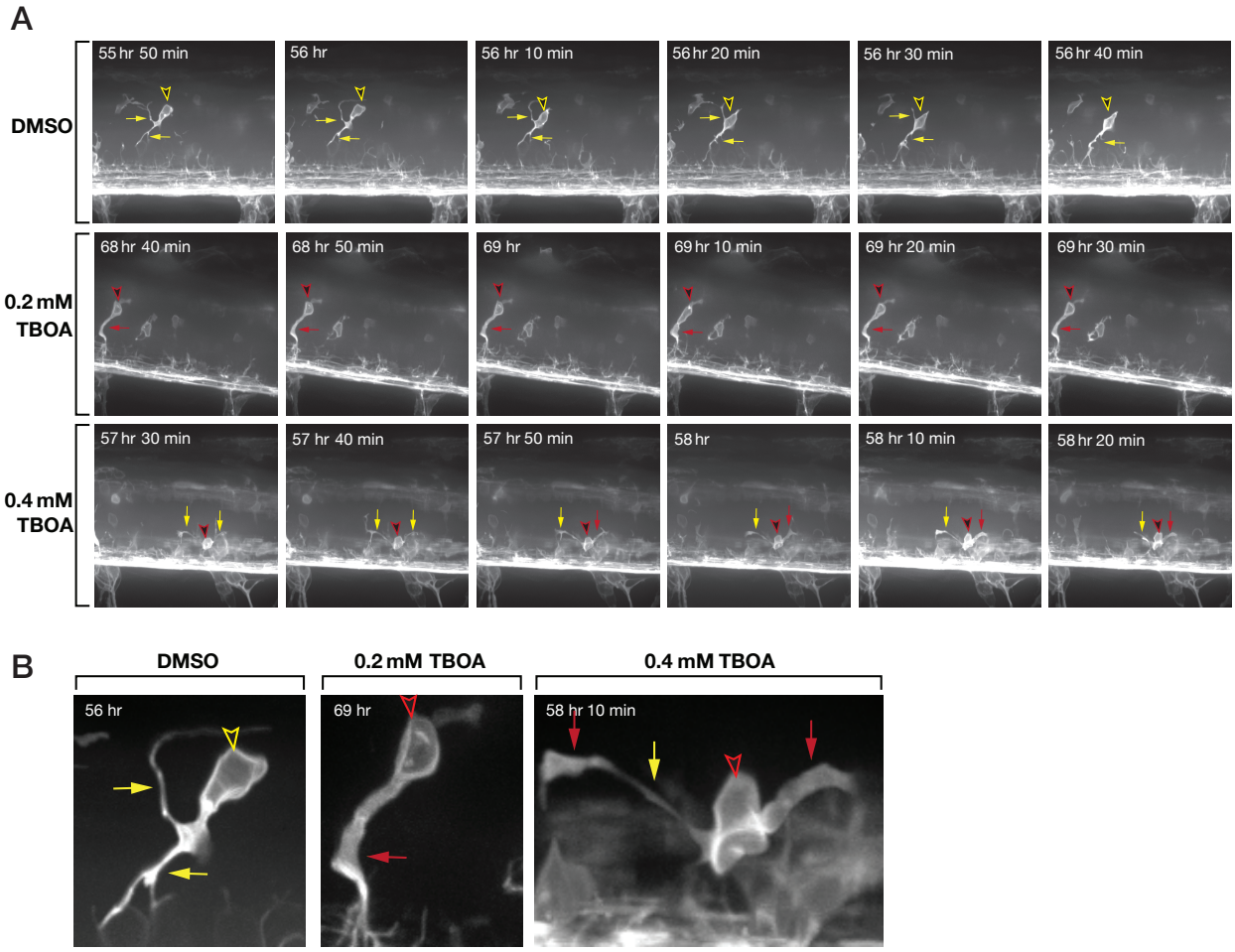


**Figure 4-4. Inhibiting glutamate transporters alters OPC process morphology.** (A) Images taken from 18 hr time-lapses of *sox10:mrfp* larvae treated with 1% DMSO, 0.2 mM TBOA in 1% DMSO, or 0.4 mM TBOA in 1% DMSO beginning at 55 hpf. (B) Close up images of OPCs taken from the time-lapse images in (A). Yellow-outlined arrowheads denote DMSO-treated OPCs. Red-outlined arrowheads denote TBOA-treated OPCs. Yellow arrows denote wild-type OPC process morphology. Red arrows denote altered OPC process morphology.

that TBOA treatment resulted in altered OPC process morphology where the processes appear wider and less dynamic when compared to DMSO controls (Figure 4-4). More work needs to be done to investigate the functional consequences of this altered cell morphology. However, given that cytoskeleton function is an integral part of myelination, I hypothesize that altered process morphology would result in reduced migration and defects in myelination (Zuchero, et al., 2015; Brown & Verden, 2017). This preliminary investigation showing that OPC process morphology can be perturbed when glutamate transport is inhibited demonstrates the need for more thorough investigation into how OPC process morphology is regulated during developmental tiling.

**Netrin-1 promotes oligodendrocyte progenitor cell proliferation**

Proliferation is an integral part of OPC tiling because it regulates the number of OPCs available to disperse throughout the CNS and mature into myelinating oligodendrocytes. Few mediators of OPC proliferation have been proposed and many were identified for their contributions to OPC migration. The majority of studies into the contribution of *ntn1* to OPC development revealed a chemorepellent effect of Ntn1 on migrating OPCs (Jarjour, et al., 2003). Additionally, mouse *Ntn1* mutants exhibited a reduced number of OPCs and reduced OPC migration in the spinal cord (Tsai, 2006). Based on these findings, I investigated the role of *Ntn1* in OPC development by knocking-down the zebrafish *Ntn1* orthologs, *ntn1a* and *ntn1b,* which are highly similar to both mouse and human *Ntn1*. To knock-down *ntn1a* and *b,* I utilized morpholinos (MOs), which are antisense oligonucleotides that bind to and functionally block translation of target mRNAs. I injected one-cell *olig2:egfp* embryos with 0.6 mM *ntn1a* MO, 0.6 mM *ntn1b* MO, or a combination of 0.4 mM *ntn1a* and 0.4 mM *ntn1b* MOs to knock-down *ntn1a, ntn1b,* or both, respectively. I then conducted 24-hour *in vivo* time-lapse imaging of 48 hpf uninjected, 0.6 mM *ntn1a* MO injected, 0.6 mM *ntn1b* MO

injected, and 0.4 mM *ntn1a* and 0.4 mM *ntn1b* MO injected embryos (Figure 4-5A). Time-lapse imaging revealed no difference in the number of OPCs that migrate from 48 to 72 hpf in MO injected larvae compared to uninjected controls (data not shown). However, there was a significant decrease in the number of OPC cell divisions observed in all *ntn1a* and *b* MO injected larvae compared to uninjected controls ($p < 0.0001$) (Figure 4-5B). Interestingly, I also noticed altered OPC migration phenotypes following cell division, where daughter cells did not rapidly migrate away from each other following division in *ntn1a* and *b* injected larvae compared to uninjected controls (Figure 4-5A). These results demonstrate that *ntn1* is required for OPC proliferation and potentially has a role in mediating migration following proliferation.

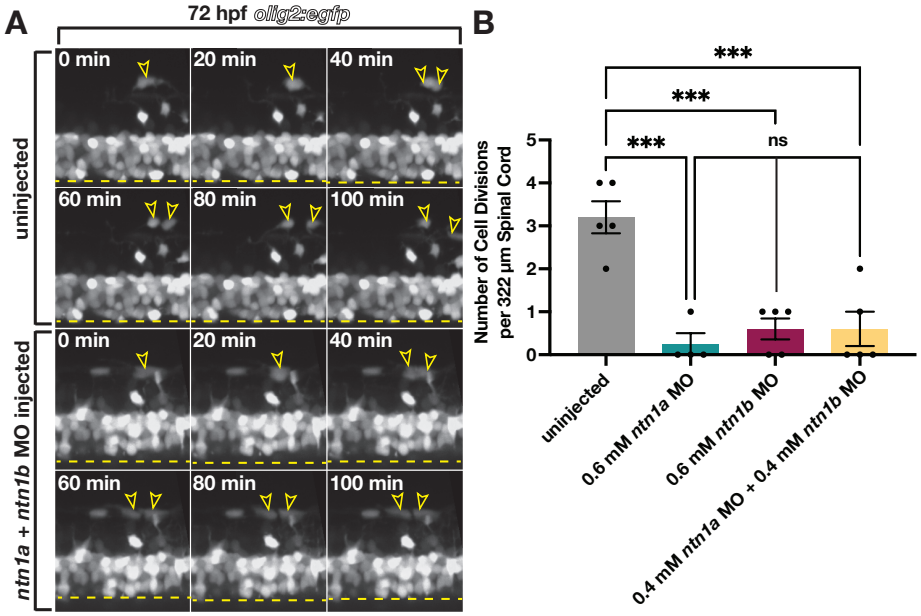


**Figure 4-5. *Ntn1* knock-down reduces OPC proliferation.** (A) Images taken from 24 hpf time-lapse imaging of 72 hpf *olig2:egfp* uninjected and a 0.4 mM *ntn1a* MO and 0.4 mM *ntn1b* MO mixture injected larvae. Arrowheads denote OPCs that divided. (B) Quantifications taken from time-lapse imaging of 72 hpf *olig2:egfp* uninjected (n = 5), 0.6 mM *ntn1a* MO (n = 3), 0.6 mM *ntn1b* MO (n = 5) and a 0.4 mM *ntn1a* MO and 0.4 mM *ntn1b* MO mix (n = 5) injected larvae. Mean with SEM. Statistical test: 1-way ANOVA with Tukey's Multiple Comparison Test.

After demonstrating that *ntn1* influences OPC proliferation, I sought to determine if *ntn1a* and *b* act cell-autonomously to mediate OPC proliferation by

investigating where *ntn1a* and *b* are expressed. To determine expression, I designed RNA-probes specific to *ntn1a* and *b* to be used *in situ* hybridization experiments on 55 hpf larvae. I used an RNA-probe specific to *olig2* as a control. Intriguingly, I found differential expression of *ntn1a* and *b*, with *ntn1a* being predominantly expressed in the pMN domain similar to *olig2* and *ntn1b* expressed in the ventral floor plate, similarly to previously published investigations into *Ntn1* expression (Tsai, 2006) (Figure 4-6A). I next wanted to investigate *ntn1a* and *b* expression at 72 hpf using a fluorescent *in situ* hybridization protocol called hybridization chain reaction using commercially designed probes for *ntn1a* and *b* in *olig2:egfp* larvae. I found that by 72 hpf, *ntn1a* and *b* expression was restricted specifically to dorsal OPCs (Figured 4-6B). The 55 hpf *in situ* results suggests that *ntn1a* and *b* could be serving different functions at the beginning of the OPC migratory period. One possibility is that *ntn1b* is acting similarly to *Ntn1* in mouse studies by repelling a population of OPCs out of the pMN domain, while *ntn1a* is expressed in OPCs to facilitate OPC proliferation. By 72 hpf, OPCs express both *ntn1a*

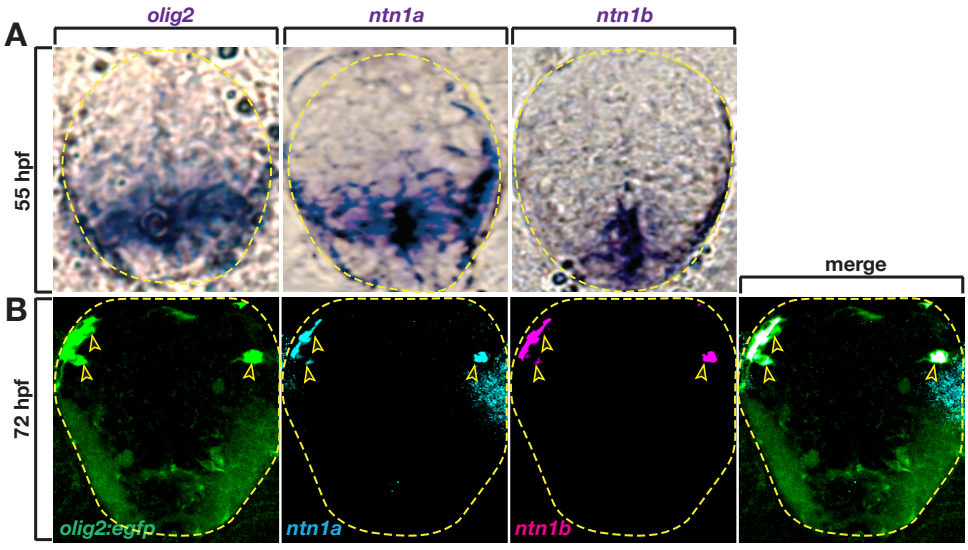


**Figure 4-6. *Ntn1* expression in the developing zebrafish spinal cord.** (A) Transverse sections of *in situ* hybridization in 55 hpf wild-type larvae showing *olig2, ntn1a,* and *ntn1b* expression. (B) Transverse sections of fluorescent hybridization chain reaction *in situ* hybridization for *ntn1* and *ntn1b* on 72 hpf *olig2:egfp* larvae. Yellow open arrowheads denote dorsal OPCs. Dashed yellow circle denotes boundary of spinal cord.

and *b* suggesting that both signals are utilized for proliferation and possibly migration following proliferation. Taken together, these results indicate the *ntn1a* and *b* act cell-autonomously to mediate OPC proliferation during tiling.

### *Dscama* is not required for homotypic OPC contact-mediated repulsion

To identify mediators of CMR between OPCs, I investigated canonical mediators of CMR in other cell types that were expressed by OPCs. I found that *Dscam* was highly expressed in mouse OPCs and the zebrafish orthologs, *dscama* and *b*, were highly expressed in zebrafish OPCs in our RNA-seq experiments (Zeisel, et al., 2015) (Figure 4-2A-B). Based on this unique expression of *dscam* in OPCs, I investigated *dscama* as a mediator of OPC CMR using CRISPR/Cas9 mutagenesis (Hwang, et al., 2013; Hruscha, et al., 2013). Using CHOPCHOP, I made a gRNA specific to the coding region of *dscama* (Labun, et al., 2019). Using this synthesized gRNA, I injected one-cell *olig2:egfp;sox10:tagrfp* embryos with the gRNA for *dscama* and Cas9 protein and grew potential founders to adulthood. I then outcrossed putative founders, screened for frameshift mutations in their offspring, and identified a founder with a mutation that resulted in a 5 base pair deletion. I used *in vivo* time-lapse imaging in 72 hpf *olig2:egfp;sox10:tagrfp; dscama*$^{+/+}$, *dscama*$^{+/\perp 5bp}$, and *dscama*$^{\perp 5bp/\perp 5bp}$ larvae (Figure 4-7A). I observed no difference in migratory behavior, spacing between neighboring OPCs, or the number of dorsal OPCs in *dscama*$^{\perp 5bp/\perp 5bp}$ compared to *dscama*$^{+/+}$ and *dscama*$^{+/\perp 5bp}$ larvae (Figure 4-7B).

One intriguing phenotype I observed in the *dscama*$^{\perp 5bp/\perp 5bp}$ larvae is the presence of OPCs in the peripheral nervous system (PNS) (Figure 4-7A and C). OPCs are an obligate CNS glial cell type that are almost never observed in the periphery. In a 2014 paper, our lab demonstrated that contact-mediated inhibition between OPCs and motor exit point (MEP) glia restricts OPCs to the spinal cord (Smith, et al., 2014). Additionally, our RNA-seq results demonstrate that MEP glia also express *dscama* and *dscamb* (Figure

4-2A-B). The presence of peripheral OPCs in our *dscama* mutants indicates that *dscama* mediates the contact-inhibition between OPCs and MEP glia that restricts OPCs to the CNS. This exciting preliminary finding lays the groundwork for understanding the function of *dscam* expression in OPCs and how the CNS and PNS maintain segregated populations of glial cells.

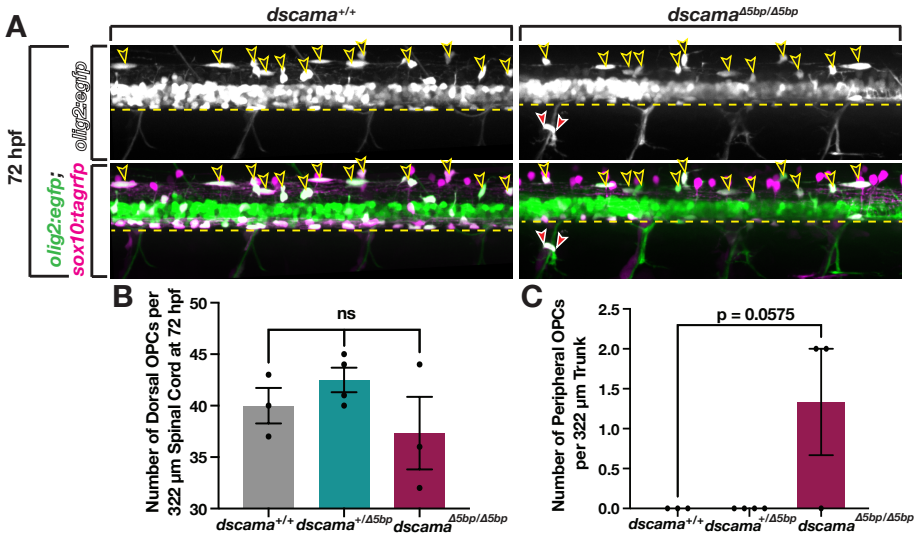


**Figure 4-7. *dscama* is dispensable for OPC contact-mediated repulsion.** (A) Lateral images of 72 hpf *olig2:egfp;sox10:tagrfp dscama*$^{+/+}$ and *dscama*$^{\Delta 5bp/\Delta 5bp}$ larvae. Yellow open arrowheads denote dorsal OPCs. White-outlined red arrowheads denote peripheral OPCs. Yellow dashed line denotes ventral edge of the spinal cord. (B) Quantifications taken from lateral images of 72 hpf *olig2:egfp;sox10:tagrfp dscama*$^{+/+}$ (n = 3), *dscama*$^{+/\Delta 5bp}$ (n = 4) and *dscama*$^{\Delta 5bp/\Delta 5bp}$ (n = 3) larvae. Mean with SEM. Statistical test: 1-way ANOVA with Tukey's Multiple Comparison Test.

## *Lingo1a* is a novel mediator of contact-mediated repulsion during OPC tiling

While Lingo1 has not been previously shown to mediate CMR, it is a transmembrane receptor capable of bidirectional self-signaling and is implicated in mediating OPC development and migration (Jepson, et al., 2012; Yin & Hu, 2014; Y. Zhang, et al., 2015). Therefore, I wanted to investigate if Lingo1 contributes to OPC development, and more specifically to CMR, by utilizing a zebrafish mutant for the *Lingo1* zebrafish ortholog, *lingo1a*. This *lingo1a* mutant was created by Dr. Laura

Fontenas, a post-doc in the Kucenas lab, by using CRISPR/Cas9 mutagenesis to generate a 14 base pair deletion resulting in an early stop codon. I then conducted *in vivo* time-lapse imaging in 72 hpf *olig2:egfp;lingo1a*$^{+/+}$, *lingo1a*$^{+/-}$, and *lingo1a*$^{-/-}$ larvae (Figure 4-8A). I found that at 72 hpf *lingo1a*$^{-/-}$ larvae had an increased number of OPCs in the

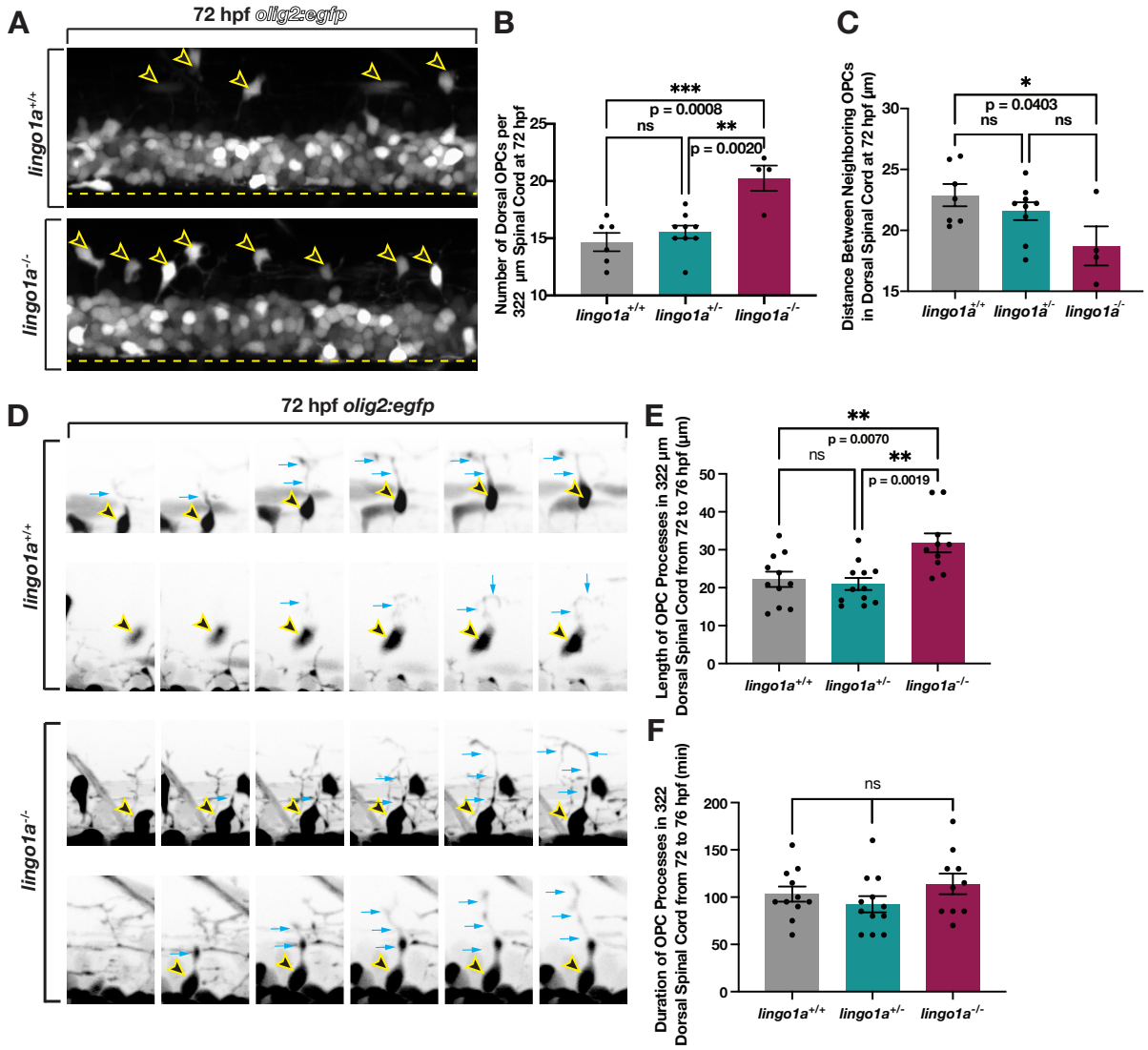


**Figure 4-8. *lingo1a* mutants exhibit increased OPCs and process length.** (A) Lateral images of 72 hpf *olig2:egfp lingo1a*$^{+/+}$ and *lingo1a*$^{-/-}$ larvae. Yellow open arrowheads denote dorsal OPCs. Yellow dashed-line denotes ventral edge of the spinal cord. (B and C) Quantifications taken from lateral images of 72 hpf *olig2:egfp lingo1a*$^{+/+}$ (n = 6), *lingo1a*$^{+/-}$ (n = 9) and *lingo1a*$^{-/-}$ (n = 4) larvae. (D) Close up images taken from lateral images in (A). Yellow arrowhead denotes OPC cell bodies. Blue arrowheads denote OPC processes. (E and F) Quantifications taken from individual cell processes in lateral images of 72 hpf *olig2:egfp lingo1a*$^{+/+}$ (n = 11), *lingo1a*$^{+/-}$ (n = 12) and *lingo1a*$^{-/-}$ (n = 9) larvae. Mean with SEM. Statistical test: 1-way ANOVA with Tukey's Multiple Comparison Test.

*lingo1a*$^{+/-}$ larvae (p = 0.019) (Figure 4-8D-E). However, no difference was observed in how long the processes persisted once they reached their longest length in *lingo1a* mutants compared to wildtype and heterozygotes (Figure 4-8F). Reduced distance between OPCs and altered process morphology implicate *lingo1a* as a mediator of CMR.

I next wanted to conduct the same *in vivo* imaging experiments in 96 hpf *olig2:egfp;lingo1a*$^{+/+}$, *lingo1a*$^{+/-}$, and *lingo1a*$^{-/-}$ larvae to see if the mutant phenotypes persisted later in development (Figure 4-9A). I found no difference in the number of dorsal OPCs when comparing *lingo1a*$^{+/+}$, *lingo1a*$^{+/-}$, and *lingo1a*$^{-/-}$ larvae (Figure 4-9B). Additionally, I found no statistically significant difference in the nearest neighbor distances between OPCs in *lingo1a*$^{+/+}$, *lingo1a*$^{+/-}$, and *lingo1a*$^{-/-}$ larvae (Figure 4-9C). However, these quantifications were taken from flattened z-stacks of 30 micron lateral views of the spinal cord, which restricts the ability to quantify nearest neighbor distances that incorporate the z-direction. More careful analysis of nearest neighbor distances could reveal increased clustering of OPCs in *lingo1a* mutants, which would support my hypothesis that *lingo1a* is a novel mediator of CMR during OPC development.

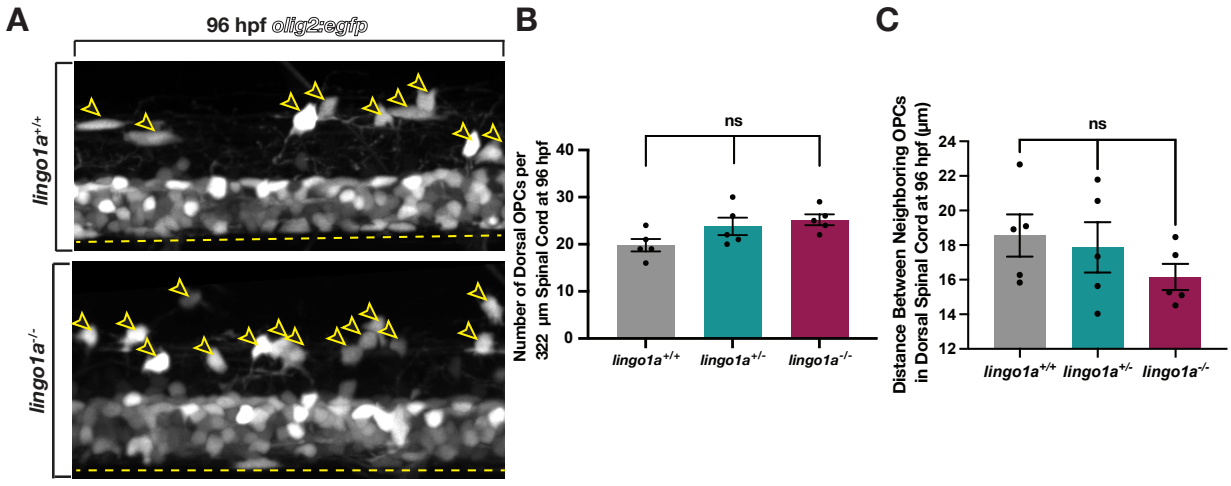


**Figure 4-9. *lingo1a* mutants exhibit altered spacing at 96 hpf. (A) Lateral images of 96 hpf *olig2:egfp lingo1a*$^{+/+}$ and *lingo1a*$^{-/-}$ larvae.** Yellow open arrowheads denote dorsal OPCs. Yellow dashed-line denotes ventral edge of the spinal cord. (B and C) Quantifications taken from lateral images of 96 hpf *olig2:egfp*

*lingo1a*$^{+/+}$(n = 5), *lingo1a*$^{+/-}$ (n = 5) and *lingo1a*$^{-/-}$ (n =5) larvae. Mean with SEM. Statistical test: 1-way ANOVA with Tukey's Multiple Comparison Test.

## Discussion

In this chapter, I sought to provide a broader understanding of OPC tiling by investigating mediators of the tiling processes of proliferation and contact-mediated repulsion. I demonstrated that *ntn1*, a traditional mediator of OPC migration, also plays a role in mediating OPC proliferation. Additionally, preliminary results from the *ntn1a* and *b* morpholino experiments indicate that Ntn1 may also mediate the rapid migration of daughter cells away from each other following cell division. This phenomenon of stalled migration following cell division was not observed in my investigation of the Met signaling pathway and its contribution to migration, which supports that notion that OPCs potentially utilize different mechanisms for migration depending on the context of migration. A previously proposed model for Ntn1 in OPC development described its role in mediating repulsion of OPCs out of the ventral spinal cord. My observation of ventral OPCs in wildtype development makes it unlikely that this mode of dispersal is universal for all OPCs. Taken together, these results support my hypothesis that OPCs utilize different methods to facilitate dispersal during developmental tiling. It remains to be determined if there are different subsets of OPCs that express different receptors at different timepoints or if each OPC expresses multiple receptors at different levels and this differential expression results in OPCs being influenced by various molecules in slightly different ways.

CMR between OPCs is also a vital process in mediating OPC dispersal throughout the spinal cord because it prevents overcrowding and facilitates the process of OPCs occupying distinct non-overlapping territories. A handful of mediators of OPC CMR have been proposed. Here, I presented my investigations into two potential mediators of CMR, *dscama* and *lingo1a*. *Dscama* was a likely mediator of CMR because of its high expression in OPCs and its role in mediating homotypic self-avoidance in the

development of retinal axons. Previous investigations into the role of *Dscam* in OPC development demonstrated no difference in CMR or OPC development (Huang, et al., 2020). My investigations into a *dscama* mutant also reveal no change in OPC development or CMR, however, I did observe the presence of peripheral OPCs in these mutants. These findings are exciting because they potentially uncover a novel mediator of contact-inhibition between OPCs and MEP glia that restrict OPCs from migrating into the PNS.

I next demonstrated that *lingo1a* mutants exhibit tiling defects that are consistent with altered CMR. The presence of an increased number of OPCs and reduced spacing between OPCs suggests that OPCs are unable to sense their nearest neighbors and maintain appropriate spacing. Additionally, it has been demonstrated that OPCs undergo apoptosis when they are kept in close contact for extended periods of time (Hughes, et al., 2013). I do not observe increased apoptosis in *lingo1a* mutants, which further supports the notion that these OPCs are unable to detect each other. More work needs to be done in these mutants using refined cell-tracking systems that are able to investigate tiling defects in the 3-dimensional cellular space. Previous studies into the role of Lingo1 primarily focused on its effect on oligodendrocyte myelination. However, the identification of OPC tiling defects in *lingo1a* mutants indicates that Lingo1 also plays a role in early OPC development.

Overall, this chapter demonstrates investigations into lesser studied aspects of OPC tiling: proliferation and contact-mediated repulsion. OPC proliferation is critical for producing enough OPCs to facilitate rapid dispersal and to produce enough oligodendrocytes to myelinate CNS axons. Contact-mediated repulsion works in tandem with proliferation to ensure that OPCs migrate rapidly away from each other following cell division and produces an even distribution of OPCs in the CNS throughout life. The studies presented here demonstrate candidate mediators of these critical processes, which fills a gap in our understanding of developmental OPC tiling.

# Chapter V

# Discussion and Future Directions

## Summary

In this dissertation research, I sought to provide greater understanding of the process of oligodendrocyte progenitor cell (OPC) tiling and described my investigations into novel mediators of the tiling-associated behaviors of migration, proliferation, and contact-mediated repulsion (CMR).

In Chapter III, I described my detailed investigation into the role of the Met signaling pathway in mediating OPC tiling. I utilized new transgenic animals that expressed a dominant negative Met (DNmet), as well as, a new *met* mutant to investigate the effect of loss-of-Met signaling on OPC development. Based on these studies, I concluded that Met signaling mediates two aspects of OPC tiling: migration and proliferation. Met signaling induces OPC migration during the initial phase of OPC tiling and predominantly affects the dorsally migrating population of OPCs. Additionally, Met signaling induces OPC proliferation following migration in both dorsal and ventral OPCs. I also demonstrated that Met is expressed by OPCs and cell-specific reduction of Met signaling in OPCs resulted in decreased OPC migration. These studies revealed that cell-autonomous Met signaling in OPCs mediates OPC migration and proliferation. I next investigated the source of the Met ligand, Hgfa, and demonstrated that it is secreted by radial glia. These results demonstrate the first *in vivo* investigation into the role of Met signaling in OPC development and the first proposed model for radial glial secretion of Hgfa in mediating Met-dependent OPC development.

The investigation of Met signaling presented in Chapter III can be used as a model for how to study other signaling pathways involved in mediating OPC tiling. A limit of many of the previous investigations into mediators of OPC development is the inability to demonstrate cell-autonomy and to propose an overall model for how the

entire signaling pathway is controlled throughout developmental tiling. This approach would help to resolve which mediators of tiling are active during developmental tiling, adult tiling, or both and allow for a better understanding of how each individual mediator contributes to tiling.

In Chapter IV, I investigated other potential mediators of OPC tiling with a focus on identifying novel mediators of OPC CMR. I first discussed my investigations into identifying unique markers of OPCs. I then demonstrated that OPC process morphology is altered when glutamate transport is inhibited. Next, I presented my investigations into the role of Netrin-1 (Ntn1), which is an established OPC chemorepellent molecule. I found that blocking *ntn1a/b* translation did not affect initial migration into the dorsal spinal cord, but instead resulted in reduced OPC proliferation in the dorsal spinal cord and impaired ability of daughter OPCs to migrate away from each other following cell division. These results implicate a novel role for *ntn1* in OPC tiling, beyond simply influencing OPC chemotaxis. More work needs to be done to reconcile the relative contributions of Met signaling and *ntn1* to OPC migration and proliferation. In comparing the results from the two studies, I found that Met signaling affects proliferation in both dorsal and ventral OPCs, while *ntn1* appears to only affect proliferation and post-mitogenic migration in dorsal OPCs. Additionally, *ntn1a* and *b* are not expressed by OPCs until 3 dpf, however, Met expression is high in OPCs from 48 hpf until 3 dpf with a rapid reduction by 4 dpf. This differential expression data indicates that the influence of various chemotactic and mitogenic molecules in OPC development is regulated by controlling when they are expressed.

Finally, I presented my investigations into mediators of OPC CMR. I first demonstrated that *dscama* is dispensable for CMR between OPCs, but may be required for OPC-glial interactions at the motor exit point that restrict OPCs to the CNS. This finding is significant because it supports previous investigations that also demonstrated that Dscam is not required for OPC CMR. However, by investigating *dscama* in

zebrafish using *in vivo* imaging, I was able to observe an unexpected phenotype of OPCs escaping into the peripheral nervous system in *dscama* mutants, which is extremely rare in wildtype development. These results further highlight the power of the zebrafish model for investigating CNS development.

I next revealed a novel role for *lingo1a* in mediating CMR between OPCs by utilizing a new mutant. These *lingo1a* mutants exhibited an increased number of OPCs in the dorsal spinal cord and closer nearest neighbor distances between OPCs compared to wildtype. These phenotypes suggest that the ability for OPCs to sense each other and maintain appropriate distances is reduced in *lingo1a* mutants. However, CMR is the least investigated process of OPC tiling, so it is unclear exactly how it contributes to development tiling and loss of CMR could result in subtle defects. Therefore, more careful analysis utilizing image processing software that is capable of measuring nearest neighbor distances and process interaction in the 3D spinal cord environment is needed to understand the full contributions of CMR to OPC tiling. The investigations presented in Chapter IV are preliminary studies that would greatly benefit from a more thorough analysis like those presented in Chapter III.

Overall, I demonstrated a number of molecular mediators that contribute to the developmental tiling behaviors of migration, proliferation, and contact-mediated repulsion. Based on the work presented here, I propose the following model of OPC tiling (Figure 5-1). At 55 hpf, Met signaling induces OPC migration out of the pMN domain both dorsally and ventrally (Figure 5-1A). During this migration, OPCs rapidly remodel their processes and make contact with the surrounding spinal cord environment. When OPCs contact the motor exit point (MEP), they are inhibited from exiting the spinal cord by Dscam-dependent contact-mediated inhibition with MEP glia (Figure 5-1B). When OPCs contact each other, they exhibit Lingo1-depedent contact-mediated repulsion (Figure 5-1C). During their migration, OPCs also exhibit robust proliferation. From 55 to 72 hpf, OPC proliferation is induced by Met signaling (Figure

5-1D). By 72 hpf, Ntn1 signaling induces OPC proliferation in the dorsal spinal cord (Figure 5-1E).

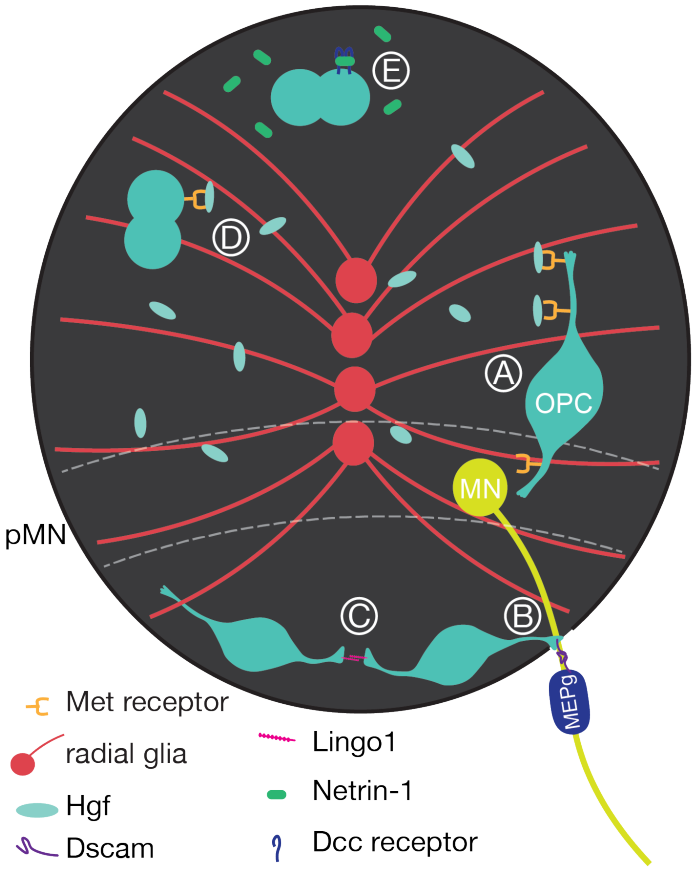


**Figure 5-1.** Novel Mediators of OPC tiling. This diagram demonstrates novel mediators of OPC tiling in the zebrafish spinal cord. (A) Met signaling induces OPC migration out of the pMN domain both dorsally and ventrally. (B) OPCs are inhibited from exiting the spinal cord by Dscam-dependent contact-mediated inhibition with MEP glia. (C) OPCs exhibit Lingo1-depedent contact-mediated repulsion. (D) From 55 to 72 hpf, OPC proliferation is induced by Met signaling. (E) By 72 hpf, Ntn1 induces OPC proliferation in the dorsal spinal cord.

Taken together, the work presented in this dissertation significantly contributes to our understanding of molecular mediators that regulate developmental OPC tiling. This work in combination with literature about OPC tiling behaviors demonstrates that there is an abundance of molecules that influence OPC tiling. I hypothesize that different contributions of each chemotactic molecule at different time points of developmental tiling results in the dispersal of OPCs throughout the spinal cord. In the

remainder of this discussion, I will propose different approaches to testing this hypothesis.

**Comprehensive approaches to determine molecular mediators of OPC tiling**

While the process of OPC tiling is well described, investigations into OPC development often focus on one proposed mediator for one behavior of tiling, most often focusing on mediators of migration. These studies demonstrate that numerous molecules influence developing OPCs, however there is little consensus regarding the timing of when these molecules influence tiling behaviors or how different mediators might interact within individual OPCs. Until recently, the majority of studies that identified mediators of tiling were conducted using *in vitro* cultures of OPCs derived from rat and mouse brain and spinal cord (Temple & Raff, 1986; Moorman, 1996; Durand & Raff, 2000; Sugimoto, et al., 2001; Yan & Rivkees, 2002; Jarjour, et al., 2003; Tsai, 2006; Ohya, et al., 2007). These studies isolated OPCs from different regions and different stages of development which makes it difficult to compare the results. Additionally, the motivation for many studies that identify mediators of tiling behaviors was to identify molecules that influence oligodendrocyte development and myelination. This further complicates the identification of mediators because it is unclear which stage of the oligodendrocyte lineage is being affected and whether or not it truly is a mediator of OPC tiling or some other process related to myelination. Given the abundance of proposed mediators of OPC tiling and the complexity therein, new approaches to determining which mediators contribute to tiling and when they actively signal in OPCs is needed.

**Systematic review and meta-analysis of mediators of OPC tiling**

One approach that is often utilized to reduce complexity and develop consensus in fields that have an abundance of research is performing systematic review and meta-

analysis of all available research that falls within a given set of criteria. Systematic reviews and meta-analyses present results by combining and analyzing data from different studies conducted on similar research topics (Ahn & Kang, 2018). A systematic review attempts to answer a defined research question by identifying and analyzing all empirical evidence available that falls within defined criteria. Meta-analysis is the statistical analysis that is conducted on the evidence gathered from a systematic review, which is used to develop a pooled estimate from published findings from different studies (Ahn & Kang, 2018). Systematic review and meta-analysis are often conducted in biomedical research to look at effect sizes of different interventions in various diseases. Additionally, a handful of systematic reviews have been conducted on various aspects of oligodendrocyte lineage cell development including OPC-endothelial interactions (Manukjan, et al., 2020), pharmacological properties of OPCs (Marinelli, et al., 2016), and OPC contribution to spinal cord injury (Fu, et al., 2018; Hassannejad, et al., 2019).

A systematic review and meta-analysis would be useful in clarifying mediators of OPC development because one of the strengths of this approach is that it requires clear criteria for which papers are included or excluded. Any systematic review that aimed to elucidate mediators of OPC tiling behaviors would have to include a few critical criteria. The first criteria for inclusion is that studies included in the review would have to have investigated mediators of tiling in developing OPCs in a wildtype background. This is necessary to determine the function of mediators of OPC tiling during development and not mediators of tiling observed in other contexts such as injury, which may not reflect basic developmental processes. The next criteria for inclusion is that studies need to have demonstrated some level of cell-autonomous signaling in OPCs that mediates a given tiling process. This is important because any conclusions about mediators of OPC tiling must include how these mediators are producing tiling behaviors.

One area of OPC tiling research that would greatly benefit from systematic review is chemotactic influences on OPCs *in vitro*. One selective criteria for a systematic review of chemotactic molecules in OPCs would be controlling for the region from which the OPCs were isolated and for the relative stage of development. These measures are often hard to glean when looking generally for mediators of OPC migration, but carefully selecting studies that show different influences on tiling by OPCs derived from the same region at the same developmental time point would allow for a powerful meta-analysis. Meta-analyses on the data gathered from this systematic review could then be used to generate pooled estimates of the effects of each chemotactic molecule, which would provide insight into the relative contribution of each molecule in influencing OPC migration. This approach would address my hypothesis that different contributions of each chemotactic molecule results in the dispersal of OPCs throughout the spinal cord.

Another systematic review that could be done in tandem with the *in vitro* OPC migration review would be to include all studies that propose *in vivo* models of OPC dispersal from the ventral spinal cord. Most studies that identify mediators of OPC migration will propose a model for how that migration then results in OPC dispersal. This has led to numerous models for OPC dispersal that have little relevance to one another. The abundance of OPC tiling and distribution models with little clarity of relatedness lends itself to the systematic review approach because compiling these models into one review allows for direct comparison and evaluation of plausibility. Both of the systematic reviews proposed here would be incredibly important for the field of OPC tiling research because they would synthesize all of the work that implicates mediators of OPC tiling. These reviews would then provide clear next steps for identifying key directions for further testing the proposed models for developmental tiling and for suggesting new, composite models.

**Utilizing hydrogels in investigating mediators of developmental OPC tiling**

Systematic reviews and meta-analyses are great approaches for identifying well-established mediators of OPC tiling. However, even with thorough analyses that detail the relative contributions of mediators of tiling, these conclusions will need to be evaluated empirically. The majority of research identifying mediators of tiling, including my work presented here, focuses on identifying individual mediators in *in vivo* models and characterizing the effects of its loss-of-function on OPC tiling behaviors. This approach, while critical for understanding the consequences of perturbing tiling mediators, is not practical or feasible for investigating the contributions of multiple mediators of tiling and observing the outcomes of different combinations of signaling molecules.

In the developing spinal cord, there is an abundance of different signaling molecules that regulate the development of various different cell-types, which creates a complex array of different signaling pathways that could be interacting to influence OPC tiling. My approach of selectively mutating individual pathways or mediators is important for isolating the contributions of individual pathways to OPC tiling, but does not address how different pathways are interacting with each other. This approach also does not allow for precise changes in the amount and distribution of the ligand, which would be necessary to determine more subtle influences of these mediators in OPC tiling. Therefore, a comprehensive approach that is able to investigate the relative contributions of different signaling molecules to different tiling behaviors is needed to resolve outstanding questions about how OPC tiling is regulated.

One approach that is a capable of investigating OPC tiling behaviors in response to different combinations of stimuli is the use of biomaterial scaffolds, such as 3D hydrogels, that mimic the environment of a developing OPC (Li, et al., 2013; Caliari & Burdick, 2016; Unal, et al., 2019). Such hydrogels have been used to investigate how different microenvironments influence OPC behaviors, including proliferation and

migration (Russell & Lampe, 2017; Unal, et al., 2020). Primarily, these studies demonstrated that different properties of these hydrogels, such as stiffness and mesh-size, influence the amount of migration and proliferation of OPCs within the hydrogel (Russell & Lampe, 2017; Unal, et al., 2020). Additionally, hydrogel systems are also porous and permeable to various signaling molecules and drugs which is useful for conducting experiments that investigate the contributions of different mediators of OPC tiling (Unal, et al., 2019).

This system would be particularly powerful for investigating the many different mediators that influence OPC migration, proliferation, and contact-mediated repulsion. The spinal cord contains many different signaling molecules, which could all be recapitulated in a controlled manner using the hydrogel system. The highly adaptable nature of hydrogels allows for the careful application of various amounts and distributions of different ligands relative to the OPCs within the hydrogel. These studies would be powerful because they would begin to elucidate how OPCs are capable of integrating signals from multiple pathways to regulate their developmental migration. Because proliferation can also be assessed within these hydrogels, these studies would also further characterize the relative contributions of chemotactic pathways to also inducing OPC proliferation. Furthermore, as new evidence emerges around mediators of CMR, these hydrogels could be impactful for investigating how OPCs lacking CMR genes disperse compared to wildtype OPCs in the same microenvironment. Taken together, the use of systematic review and meta-analysis will identify and prioritize the most salient mediators of OPC tiling. These findings can then be tested in a controlled hydrogel environment to more conclusively elucidate how these mediators facilitate OPC tiling. One limitation of the hydrogel system is that it would not contain all of the cell types present in the spinal cord that could also influence OPC tiling. However, findings from hydrogel experiments about how different mediators influence OPCs at different timepoints could then be tested using an *in vivo* model. This approach would

greatly improve our understanding of how the emergent process of OPC tiling is mediated to produce OPCs that are evenly distributed throughout the CNS.

In conclusion, the work presented in this dissertation significantly contributes to our understanding of developmental OPC tiling by first presenting a proposal for how each of the tiling behaviors of migration, proliferation, and contact-mediated repulsion are interacting to produce the uniform distribution of OPCs throughout the CNS. I then demonstrate my investigations that reveal novel molecular mediators for each of these tiling processes. Finally, I conclude by proposing different approaches that could be used to clarify the relative contributions of different mediators of tiling. These approaches would improve our overall understanding of this dynamic and important cell population and would lay a foundation for investigating OPC tiling behaviors in other regions of the CNS or in other contexts, such as adult tiling and tiling rearrangement following injury.

## References


Adams, K. L., Dahl, K. D., Gallo, V., & Macklin, W. B. (2020). Intrinsic and extrinsic regulators of oligodendrocyte progenitor proliferation and differentiation. *Seminars in Cell and Developmental Biology*. https://doi.org/10.1016/j.semcdb.2020.10.002

Ahn, E., & Kang, H. (2018). Introduction to systematic review and meta-analysis. *Korean Journal of Anesthesiology*, *71*(2), 103–112. https://doi.org/10.4097/kjae.2018.71.2.103

Ali, M. F., Latimer, A. J., Wang, Y., Hogenmiller, L., Fontenas, L., Isabella, A. J., Moens, C. B., Yu, G., & Kucenas, S. (2021). Met is required for oligodendrocyte progenitor cell migration *Danio rerio*; *BioRxiv*, 2021.05.21.445204. https://doi.org/10.1101/2021.05.21.445204

Almeida, R. G., Czopka, T., Ffrench-Constant, C., & Lyons, D. A. (2011). Individual axons regulate the myelinating potential of single oligodendrocytes in vivo. *Development*, *138*(20), 4443–4450. https://doi.org/10.1242/dev.071001

Ashton, R. S., Conway, A., Pangarkar, C., Bergen, J., Lim, K. Il, Shah, P., Bissell, M., & Schaffer, D. V. (2012). Astrocytes regulate adult hippocampal neurogenesis through ephrin-B signaling. *Nature Neuroscience*, *15*(10), 1399–1406. https://doi.org/10.1038/nn.3212

Auer, F., Vagionitis, S., & Czopka, T. (2018). Evidence for Myelin Sheath Remodeling in the CNS Revealed by In Vivo Imaging. *Current Biology*, *28*(4), 549-559.e3. https://doi.org/10.1016/j.cub.2018.01.017

Bardelli, A., Longati, P., Williams, T. A., Benvenuti, S., & Comoglio, P. M. (1999). A peptide representing the carboxyl-terminal tail of the Met receptor inhibits kinase activity and invasive growth. *Journal of Biological Chemistry*, *274*(41), 29274–29281. https://doi.org/10.1074/jbc.274.41.29274

Barres, B. A., Jacobson, M. D., Schmid, R., Sendtner, M., & Raff, M. C. (1993). Does

oligodendrocyte survival depend on axons? *Current Biology*, *3*(8), 489–497. https://doi.org/10.1016/0960-9822(93)90039-Q

Barry, D. S., Pakan, J. M. P., O'Keeffe, G. W., & McDermott, K. W. (2013). The spatial and temporal arrangement of the radial glial scaffold suggests a role in axon tract formation in the developing spinal cord. *Journal of Anatomy*, *222*(2), 203–213. https://doi.org/10.1111/joa.12006

Becker, T., & Becker, C. G. (2014). Axonal regeneration in zebrafish. In *Current Opinion in Neurobiology* (Vol. 27, pp. 186–191). Elsevier Ltd. https://doi.org/10.1016/j.conb.2014.03.019

Bergles, D. E., & Richardson, W. D. (2015). Oligodendrocyte Development and Plasticity. *Cold Spring Harbor Perspectives in Biology*, *8*(2), a020453. https://doi.org/10.1101/cshperspect.a020453

Binamé, F., Sakry, D., Dimou, L., Jolivel, V., & Trotter, J. (2013). NG2 Regulates Directional Migration of Oligodendrocyte Precursor Cells via Rho GTPases and Polarity Complex Proteins. *Journal of Neuroscience*, *33*(26).

Binari, L. A., Lewis, G. M., & Kucenas, S. (2013). Perineurial glia require notch signaling during motor nerve development but not regeneration. *Journal of Neuroscience*, *33*(10), 4241–4252. https://doi.org/10.1523/JNEUROSCI.4893-12.2013

Birchmeier, C., & Gherardi, E. (1998). Developmental roles of HGF/SF and its receptor, the c-Met tyrosine kinase. *Trends in Cell Biology*, *8*(10), 404–410. https://doi.org/10.1016/S0962-8924(98)01359-2

Birey, F., & Aguirre, A. (2015). Age-Dependent Netrin-1 Signaling Regulates NG2+ Glial Cell Spatial Homeostasis in Normal Adult Gray Matter. *The Journal of Neuroscience : The Official Journal of the Society for Neuroscience*, *35*(17), 6946–6951. https://doi.org/10.1523/JNEUROSCI.0356-15.2015

Birey, F., Kokkosis, A., & Aguirre, A. (2017). Oligodendroglia-lineage cells in brain

plasticity, homeostasis and psychiatric disorders. *Current Opinion in Neurobiology*, *47*, 93–103. https://doi.org/10.1016/j.conb.2017.09.016

Brown, T. L., & Verden, D. R. (2017). Cytoskeletal Regulation of Oligodendrocyte Differentiation and Myelination. *Journal of Neuroscience*, *37*(33). http://www.jneurosci.org/content/37/33/7797?etoc

Cai, J., Qi, Y., Hu, X., Tan, M., Liu, Z., Zhang, J., Li, Q., Sander, M., & Qiu, M. (2005). Generation of Oligodendrocyte Precursor Cells from Mouse Dorsal Spinal Cord Independent of Nkx6 Regulation and Shh Signaling. *Neuron*, *45*(1), 41–53. https://doi.org/10.1016/j.neuron.2004.12.028

Caliari, S. R., & Burdick, J. A. (2016). A practical guide to hydrogels for cell culture. In *Nature Methods* (Vol. 13, Issue 5, pp. 405–414). Nature Publishing Group. https://doi.org/10.1038/nmeth.3839

Cameron, S., & Rao, Y. (2010). Molecular mechanisms of tiling and self-avoidance in neural development. In *Molecular Brain* (Vol. 3, Issue 1, p. 28). BioMed Central. https://doi.org/10.1186/1756-6606-3-28

Carney, T. J., Dutton, K. A., Greenhill, E., Delfino-Machín, M., Dufourcq, P., Blader, P., & Kelsh, R. N. (2006). A direct role for Sox10 in specification of neural crest-derived sensory neurons. *Development*, *133*(23), 4619–4630. https://doi.org/10.1242/dev.02668

Caton, A., Hacker, A., Naeem, A., Livet, J., Maina, F., Bladt, F., Klein, R., Birchmeier, C., & Guthrie, S. (2000). The branchial arches and HGF are growth-promoting and chemoattractant for cranial motor axons. *Development*, *127*(8).

Chapman, H., Riesenberg, A., Ehrman, L. A., Kohli, V., Nardini, D., Nakafuku, M., Campbell, K., & Waclaw, R. R. (2018). Gsx transcription factors control neuronal versus glial specification in ventricular zone progenitors of the mouse lateral ganglionic eminence. *Developmental Biology*. https://doi.org/10.1016/J.YDBIO.2018.07.005

Chen, J., Poskanzer, K. E., Freeman, M. R., & Monk, K. R. (2020). Live-imaging of astrocyte morphogenesis and function in zebrafish neural circuits. *Nature Neuroscience*, *23*(10), 1297–1306. https://doi.org/10.1038/s41593-020-0703-x

Chen, T.-J., Kula, B., Nagy, B., Barzan, R., Gall, A., Ehrlich, I., & Kukley, M. (2018). In Vivo Regulation of Oligodendrocyte Precursor Cell Proliferation and Differentiation by the AMPA-Receptor Subunit GluA2. *Cell Reports*, *25*(4), 852-861.e7. https://doi.org/10.1016/j.celrep.2018.09.066

Ciccone, A. (n.d.). *Anti-LINGO-1 Fails to Meet Primary Endpoint in Multiple Sclerosis - Neurology Advisor*. Retrieved June 1, 2021, from https://www.neurologyadvisor.com/topics/multiple-sclerosis/anti-lingo-1-fails-to-meet-primary-endpoint-in-multiple-sclerosis/

Corbo, C. P., Othman, N. A., Gutkin, M. C., Alonso, A. D. C., & Fulop, Z. L. (2012). Use of different morphological techniques to analyze the cellular composition of the adult zebrafish optic tectum. *Microscopy Research and Technique*, *75*(3), 325–333. https://doi.org/10.1002/jemt.21061

Crawford, A. H., Tripathi, R. B., Richardson, W. D., & Franklin, R. J. M. (2016). Developmental Origin of Oligodendrocyte Lineage Cells Determines Response to Demyelination and Susceptibility to Age-Associated Functional Decline. *Cell Reports*, *15*, 761–773. https://doi.org/10.1016/j.celrep.2016.03.069

Cullen, C. L., O'Rourke, M., Beasley, S. J., Auderset, L., Zhen, Y., Pepper, R. E., Gasperini, R., & Young, K. M. (2021). Kif3a deletion prevents primary cilia assembly on oligodendrocyte progenitor cells, reduces oligodendrogenesis and impairs fine motor function. *GLIA*, *69*(5), 1184–1203. https://doi.org/10.1002/glia.23957

Cunliffe, V. T., & Casaccia-Bonnefil, P. (2006). Histone deacetylase 1 is essential for oligodendrocyte specification in the zebrafish CNS. *Mechanisms of Development*, *123*(1), 24–30. https://doi.org/10.1016/j.mod.2005.10.005

Dawson, M. R. L., Levine, J. M., & Reynolds, R. (2000). NG2-expressing cells in the central nervous system: Are they oligodendroglial progenitors? *Journal of Neuroscience Research*, *61*(5), 471–479. https://doi.org/10.1002/1097-4547(20000901)61:5<471::AID-JNR1>3.0.CO;2-N

De Biase, L. M., Schuebel, K. E., Fusfeld, Z. H., Jair, K., Hawes, I. A., Cimbro, R., Zhang, H.-Y., Liu, Q.-R., Shen, H., Xi, Z.-X., Goldman, D., & Bonci, A. (2017). Local Cues Establish and Maintain Region-Specific Phenotypes of Basal Ganglia Microglia. *Neuron*, *95*(2), 341-356.e6. https://doi.org/10.1016/J.NEURON.2017.06.020

de Bruijn, E., Cuppen, E., & Feitsma, H. (2009). Highly Efficient ENU Mutagenesis in Zebrafish. *Methods in Molecular Biology (Clifton, N.J.)*, *546*, 3–12. https://doi.org/10.1007/978-1-60327-977-2_1

De Castro, F., & Bribián, A. (2005). The molecular orchestra of the migration of oligodendrocyte precursors during development. *Brain Research Reviews*, *49*, 227–241. https://doi.org/10.1016/j.brainresrev.2004.12.034

Dimou, L., Simon, C., Kirchhoff, F., Takebayashi, H., & Götz, M. (2008). Progeny of Olig2-Expressing Progenitors in the Gray and White Matter of the Adult Mouse Cerebral Cortex. *Journal of Neuroscience*, *28*(41).

Dimou, L., & Simons, M. (2017). Diversity of oligodendrocytes and their progenitors. In *Current Opinion in Neurobiology* (Vol. 47, pp. 73–79). Elsevier Ltd. https://doi.org/10.1016/j.conb.2017.09.015

Dobrowolski, M., Cave, C., Levy-Myers, R., Lee, C., Park, S., Choi, B.-R., Xiao, B., Yang, W., & Sockanathan, S. (2020). GDE3 regulates oligodendrocyte precursor proliferation via release of soluble CNTFRα. *Development (Cambridge, England)*, *147*(2). https://doi.org/10.1242/dev.180695

Dubois-Dalcq, M., Behar, T., Hudson, L., & Lazzarini, R. A. (1986). Emergence of three myelin proteins in oligodendrocytes cultured without neurons. *Journal of Cell*

*Biology*, *102*(2), 384–392. https://doi.org/10.1083/jcb.102.2.384

Durand, B., & Raff, M. (2000). A cell-intrinsic timer that operates during oligodendrocyte development. *BioEssays*, *22*(1), 64–71. https://doi.org/10.1002/(SICI)1521-1878(200001)22:1<64::AID-BIES11>3.0.CO;2-Q

Egea, J., & Klein, R. (2007). Bidirectional Eph–ephrin signaling during axon guidance. *Trends in Cell Biology*, *17*(5), 230–238. https://doi.org/10.1016/j.tcb.2007.03.004

Fannon, J., Tarmier, W., & Fulton, D. (2015). Neuronal activity and AMPA-type glutamate receptor activation regulates the morphological development of oligodendrocyte precursor cells. *GLIA*, *63*(6), 1021–1035. https://doi.org/10.1002/glia.22799

Firon, M., Shaharabany, M., Altstock, R. T., Horev, J., Abramovici, A., Resau, J. H., Vande Woude, G. F., & Tsarfaty, I. (2000). Dominant negative Met reduces tumorigenicity-metastasis and increases tubule formation in mammary cells. *Oncogene*, *19*(20), 2386–2397. https://doi.org/10.1038/sj.onc.1203557

Fontenas, L., Welsh, T. G., Piller, M., Coughenour, P., Gandhi, A. V, & Prober, D. A. (2019). The Neuromodulator Adenosine Regulates Oligodendrocyte Migration at Motor Exit Point Transition Zones. *Cell Reports*, *27*, 115–128. https://doi.org/10.1016/j.celrep.2019.03.013

Frost, E. E., Zhou, Z., Krasnesky, K., & Armstrong, R. C. (2009). Initiation of oligodendrocyte progenitor cell migration by a PDGF-A activated Extracellular Regulated Kinase (ERK) signaling pathway. *Neurochemical Research*, *34*(1), 169–181. https://doi.org/10.1007/s11064-008-9748-z

Fu, H., Hu, D., Zhang, L., Shen, X., & Tang, P. (2018). Efficacy of Oligodendrocyte Progenitor Cell Transplantation in Rat Models with Traumatic Thoracic Spinal Cord Injury: A Systematic Review and Meta-Analysis. In *Journal of Neurotrauma* (Vol. 35, Issue 21, pp. 2507–2518). Mary Ann Liebert Inc.

https://doi.org/10.1089/neu.2017.5606

Fuerst, P. G., Koizumi, A., Masland, R. H., & Burgess, R. W. (2008). Neurite arborization and mosaic spacing in the mouse retina require DSCAM. *Nature*, *451*(7177), 470–474. https://doi.org/10.1038/nature06514

Gherardi, E., Birchmeier, W., Birchmeier, C., & Woude, G. Vande. (2012). Targeting MET in cancer: rationale and progress. *Nature Reviews Cancer*, *12*(2), 89–103. https://doi.org/10.1038/nrc3205

Gibson, E. M., Purger, D., Mount, C. W., Goldstein, A. K., Lin, G. L., Wood, L. S., Inema, I., Miller, S. E., Bieri, G., Zuchero, J. B., Barres, B. A., Woo, P. J., Vogel, H., & Monje, M. (2014). Neuronal activity promotes oligodendrogenesis and adaptive myelination in the mammalian brain. *Science*, *344*(6183). https://doi.org/10.1126/science.1252304

Giordano, S., Corso, S., Conrotto, P., Artigiani, S., Gilestro, G., Barberis, D., Tamagnone, L., & Comoglio, P. M. (2002). The semaphorin 4D receptor controls invasive growth by coupling with Met. *Nature Cell Biology*, *4*(9), 720–724. https://doi.org/10.1038/ncb843

Grueber, W. B., & Sagasti, A. (2010). Self-avoidance and tiling: Mechanisms of dendrite and axon spacing. In *Cold Spring Harbor perspectives in biology* (Vol. 2, Issue 9). Cold Spring Harbor Laboratory Press. https://doi.org/10.1101/cshperspect.a001750

Gudz, T. I., Komuro, H., & Macklin, W. B. (2006). Glutamate stimulates oligodendrocyte progenitor migration mediated via an αv integrin/myelin proteolipid protein complex. *Journal of Neuroscience*, *26*(9), 2458–2466. https://doi.org/10.1523/JNEUROSCI.4054-05.2006

Haines, L., Neyt, C., Gauter, P., Keenan, D. G., Bryson-Richardson, R. J., Hollway, G. E., Cole, N. J., & Currie, P. D. (2004). Met and Hgf signaling controls hypaxial muscle and lateral line development in the zebrafish. *Development*, *131*(19), 4857–

4869. https://doi.org/10.1242/dev.01374

Hassannejad, Z., Shakouri-Motlagh, A., Mokhatab, M., Zadegan, S. A., Sharif-Alhoseini, M., Shokraneh, F., & Rahimi-Movaghar, V. (2019). Oligodendrogliogenesis and Axon Remyelination after Traumatic Spinal Cord Injuries in Animal Studies: A Systematic Review. In *Neuroscience* (Vol. 402, pp. 37–50). Elsevier Ltd. https://doi.org/10.1016/j.neuroscience.2019.01.019

Hattori, D., Millard, S. S., Wojtowicz, W. M., & Zipursky, S. L. (2008). Dscam-Mediated Cell Recognition Regulates Neural Circuit Formation. *Annu. Rev. Cell Dev. Biol*, *24*, 597–620. https://doi.org/10.1146/annurev.cellbio.24.110707.175250

Hauptmann, G., & Gerster, T. (2000). Multicolor whole-mount in situ hybridization. *Methods in Molecular Biology (Clifton, N.J.)*, *137*, 139–148. https://doi.org/10.1385/1-59259-066-7:139

Hayashi, C., & Suzuki, N. (2019). *Heterogeneity of Oligodendrocytes and Their Precursor Cells* (pp. 53–62). https://doi.org/10.1007/978-981-32-9636-7_5

Horiuchi, M., Suzuki-Horiuchi, Y., Akiyama, T., Itoh, A., Pleasure, D., Carstens, E., & Itoh, T. (n.d.). Differing intrinsic biological properties between forebrain and spinal oligodendroglial lineage cells. *Journal of Neurochemistry*. https://doi.org/10.1111/JNC.14074

Hruscha, A., Krawitz, P., Rechenberg, A., Heinrich, V., Hecht, J., Haass, C., & Schmid, B. (2013). Efficient CRISPR/Cas9 genome editing with low off-target effects in zebrafish. *Development (Cambridge)*, *140*(24), 4982–4987. https://doi.org/10.1242/dev.099085

Huang, W., Bhaduri, A., Velmeshev, D., Alvarez-Buylla, A., Rowitch, D. H., Kriegstein, A. R., Wang, S., Wang, L., & Rottkamp, C. A. (2020). *Origins and Proliferative States of Human Oligodendrocyte Precursor Cells In Brief ll Origins and Proliferative States of Human Oligodendrocyte Precursor Cells.*

https://doi.org/10.1016/j.cell.2020.06.027

Hughes, E. G., Kang, S. H., Fukaya, M., & Bergles, D. E. (2013). Oligodendrocyte progenitors balance growth with self-repulsion to achieve homeostasis in the adult brain. *Nature Neuroscience*, *16*(6), 668–676. https://doi.org/10.1038/nn.3390

Hwang, W. Y., Fu, Y., Reyon, D., Maeder, M. L., Tsai, S. Q., Sander, J. D., Peterson, R. T., Yeh, J. R. J., & Joung, J. K. (2013). Efficient genome editing in zebrafish using a CRISPR-Cas system. *Nature Biotechnology*, *31*(3), 227–229. https://doi.org/10.1038/nbt.2501

Isabella, A. J., Barsh, G. R., Stonick, J. A., Dubrulle, J., & Moens, C. B. (2020). Retinoic Acid Organizes the Zebrafish Vagus Motor Topographic Map via Spatiotemporal Coordination of Hgf/Met Signaling. *Developmental Cell*, *53*(3), 344-357.e5. https://doi.org/10.1016/j.devcel.2020.03.017

Jarjour, A. A., Manitt, C., Moore, S. W., Thompson, K. M., Yuh, S.-J., & Kennedy, T. E. (2003). Netrin-1 Is a Chemorepellent for Oligodendrocyte Precursor Cells in the Embryonic Spinal Cord. *Journal of Neuroscience*, *23*(9).

Jepson, S., Vought, B., Gross, C. H., Gan, L., Austen, D., Frantz, J. D., Zwahlen, J., Lowe, D., Markland, W., & Krauss, R. (2012). LINGO-1, a transmembrane signaling protein, inhibits oligodendrocyte differentiation and myelination through intercellular self-interactions. *The Journal of Biological Chemistry*, *287*(26), 22184–22195. https://doi.org/10.1074/jbc.M112.366179

Kamen, Y., Pivonkova, H., Evans, K. A., & Káradóttir, R. T. (2021). A Matter of State: Diversity in Oligodendrocyte Lineage Cells. In *Neuroscientist* (p. 107385842098720). SAGE Publications Inc. https://doi.org/10.1177/1073858420987208

Kawakami, K. (2004). Transgenesis and gene trap methods in zebrafish by using the Tol2 transposable element. In *Methods in Cell Biology* (Vol. 2004, Issue 77, pp. 201–222). Academic Press Inc. https://doi.org/10.1016/s0091-679x(04)77011-9

Kearns, C. A., Ravanelli, A. M., Cooper, K., & Appel, B. (2015). Fbxw7 Limits Myelination by Inhibiting mTOR Signaling. *Journal of Neuroscience*, *35*(44).

Kelenis, D. P., Hart, E., Edwards-Fligner, M., Johnson, J. E., & Vue, T. Y. (2018). ASCL1 regulates proliferation of NG2-glia in the embryonic and adult spinal cord. *Glia*. https://doi.org/10.1002/glia.23344

Kilpatrick, T. J., Ortuño, D., Bucci, T., Lai, C., & Lemke, G. (2000). Rat oligodendroglia express c-met and focal adhesion kinase, protein tyrosine kinases implicated in regulating epithelial cell motility. *Neuroscience Letters*, *279*(1), 5–8. https://doi.org/10.1016/S0304-3940(99)00928-3

Kimmel, C. B., Ballard, W. W., Kimmel, S. R., Ullmann, B., & Schilling, T. F. (1995). *Stages of Embryonic Development of the Zebrafish*.

Kimura, Y., Hisano, Y., Kawahara, A., & Higashijima, S. I. (2014). Efficient generation of knock-in transgenic zebrafish carrying reporter/driver genes by CRISPR/Cas9-mediated genome engineering. *Scientific Reports*, *4*. https://doi.org/10.1038/srep06545

Kirby, B. B., Takada, N., Latimer, A. J., Shin, J., Carney, T. J., Kelsh, R. N., & Appel, B. (2006). In vivo time-lapse imaging shows dynamic oligodendrocyte progenitor behavior during zebrafish development. *Nature Neuroscience*, *9*(12), 1506–1511. https://doi.org/10.1038/nn1803

Kitada, M., & Rowitch, D. H. (2006). Transcription factor co-expression patterns indicate heterogeneity of oligodendroglial subpopulations in adult spinal cord. *Glia*, *54*(1), 35–46. https://doi.org/10.1002/glia.20354

Kucenas, S., Takada, N., Park, H. C., Woodruff, E., Broadie, K., & Appel, B. (2008). CNS-derived glia ensheath peripheral nerves and mediate motor root development. *Nature Neuroscience*, *11*(2), 143–151. https://doi.org/10.1038/nn2025

Kuhn, S., Gritti, L., Crooks, D., & Dombrowski, Y. (2019). Oligodendrocytes in

Development, Myelin Generation and Beyond. *Cells*, *8*(11), 1424. https://doi.org/10.3390/cells8111424

Kwan, K. M., Fujimoto, E., Grabher, C., Mangum, B. D., Hardy, M. E., Campbell, D. S., Parant, J. M., Yost, H. J., Kanki, J. P., & Chien, C.-B. (2007). The Tol2kit: A multisite gateway-based construction kit forTol2 transposon transgenesis constructs. *Developmental Dynamics*, *236*(11), 3088–3099. https://doi.org/10.1002/dvdy.21343

Labun, K., Montague, T. G., Krause, M., Torres Cleuren, Y. N., Tjeldnes, H., & Valen, E. (2019). CHOPCHOP v3: Expanding the CRISPR web toolbox beyond genome editing. *Nucleic Acids Research*, *47*(W1), W171–W174. https://doi.org/10.1093/nar/gkz365

Lake, B. B., Ai, R., Kaeser, G. E., Salathia, N. S., Yung, Y. C., Liu, R., Wildberg, A., Gao, D., Fung, H. L., Chen, S., Vijayaraghavan, R., Wong, J., Chen, A., Sheng, X., Kaper, F., Shen, R., Ronaghi, M., Fan, J. B., Wang, W., … Zhang, K. (2016). Neuronal subtypes and diversity revealed by single-nucleus RNA sequencing of the human brain. *Science*, *352*(6293), 1586–1590. https://doi.org/10.1126/science.aaf1204

Lalive, P., Paglinawan, R., Biollaz, G., Kappos, E., Leone, D., Malipiero, U., Relvas, J., Moransard, M., Suter, T., & Fontana, A. (2005). TGF-?-treated microglia induce oligodendrocyte precursor cell chemotaxis through the HGF-c-Met pathway. *European Journal of Immunology*, *35*(3), 727–737. https://doi.org/10.1002/eji.200425430

Latimer, A. J., & Jessen, J. R. (2008). *hgf/c-met* expression and functional analysis during zebrafish embryogenesis. *Developmental Dynamics*, *237*(12), 3904–3915. https://doi.org/10.1002/dvdy.21794

Li, H., Lu, Y., Smith, H. K., & Richardson, W. D. (2007). Olig1 and Sox10 interact synergistically to drive myelin basic protein transcription in oligodendrocytes.

*Journal of Neuroscience*, *27*(52), 14375–14382. https://doi.org/10.1523/JNEUROSCI.4456-07.2007

Li, L., Tian, E., Chen, X., Chao, J., Klein, J., Qu, Q., Sun, G., Sun, G., Huang, Y., Warden, C. D., Ye, P., Feng, L., Li, X., Cui, Q., Sultan, A., Douvaras, P., Fossati, V., Sanjana, N. E., Riggs, A. D., & Shi, Y. (2018). GFAP Mutations in Astrocytes Impair Oligodendrocyte Progenitor Proliferation and Myelination in an hiPSC Model of Alexander Disease. *Cell Stem Cell*, *23*(2), 239-251.e6. https://doi.org/10.1016/j.stem.2018.07.009

Li, X., Liu, X., Cui, L., Brunson, C., Zhao, W., Bhat, N. R., Zhang, N., & Wen, X. (2013). Engineering an in situ crosslinkable hydrogel for enhanced remyelination. *FASEB Journal*, *27*(3), 1127–1136. https://doi.org/10.1096/fj.12-211151

Linneberg, C., Harboe, M., & Laursen, L. S. (2015). Axo-Glia Interaction Preceding CNS Myelination Is Regulated by Bidirectional Eph-Ephrin Signaling. *ASN Neuro*, *7*(5), 1759091415602859. https://doi.org/10.1177/1759091415602859

Lorenzati, M., Boda, E., Parolisi, R., Bonato, M., Borsello, T., Herdegen, T., Buffo, A., & Vercelli, A. (2021). c-Jun N-terminal kinase 1 (JNK1) modulates oligodendrocyte progenitor cell architecture, proliferation and myelination. *Scientific Reports*, *11*(1), 7264. https://doi.org/10.1038/s41598-021-86673-6

Lu, Q. R., Yuk, D., Alberta, J. A., Zhu, Z., Pawlitzky, I., Chan, J., McMahon, A. P., Stiles, C. D., & Rowitch, D. H. (2000). Sonic Hedgehog–Regulated Oligodendrocyte Lineage Genes Encoding bHLH Proteins in the Mammalian Central Nervous System. *Neuron*, *25*(2), 317–329. https://doi.org/10.1016/S0896-6273(00)80897-1

Ly, A., Nikolaev, A., Suresh, G., Zheng, Y., Tessier-Lavigne, M., & Stein, E. (2008). DSCAM Is a Netrin Receptor that Collaborates with DCC in Mediating Turning Responses to Netrin-1. *Cell*, *133*(7), 1241–1254. https://doi.org/10.1016/j.cell.2008.05.030

Lyons, D. A., & Talbot, W. S. (2014). Glial cell development and function in zebrafish. *Cold Spring Harbor Perspectives in Biology*, *7*(2), a020586. https://doi.org/10.1101/cshperspect.a020586

Manukjan, N., Ahmed, Z., Fulton, D., Blankesteijn, W. M., & Foulquier, S. (2020). A Systematic Review of WNT Signaling in Endothelial Cell Oligodendrocyte Interactions: Potential Relevance to Cerebral Small Vessel Disease. *Cells*, *9*(6), 1545. https://doi.org/10.3390/cells9061545

Marinelli, C., Bertalot, T., Zusso, M., Skaper, S. D., & Giusti, P. (2016). Systematic review of pharmacological properties of the oligodendrocyte lineage. In *Frontiers in Cellular Neuroscience* (Vol. 10, Issue FEB, p. 27). Frontiers Media S.A. https://doi.org/10.3389/fncel.2016.00027

Marisca, R., Hoche, T., Agirre, E., Hoodless, L. J., Barkey, W., Auer, F., Castelo-Branco, G., & Czopka, T. (2020). Functionally distinct subgroups of oligodendrocyte precursor cells integrate neural activity and execute myelin formation. *Nature Neuroscience*, 1–12. https://doi.org/10.1038/s41593-019-0581-2

Mayor, R., & Carmona-Fontaine, C. (2010). Keeping in touch with contact inhibition of locomotion. *Trends in Cell Biology*, *20*(6), 319–328. https://doi.org/10.1016/j.tcb.2010.03.005

Mela, A., & Goldman, J. E. (2013). CD82 blocks cMet activation and overcomes hepatocyte growth factor effects on oligodendrocyte precursor differentiation. *The Journal of Neuroscience : The Official Journal of the Society for Neuroscience*, *33*(18), 7952–7960. https://doi.org/10.1523/JNEUROSCI.5836-12.2013

Meyers, J. R. (2018). Zebrafish: Development of a Vertebrate Model Organism. *Current Protocols in Essential Laboratory Techniques*, *16*(1), e19. https://doi.org/10.1002/cpet.19

Millard, S. S., Flanagan, J. J., Pappu, K. S., Wu, W., & Zipursky, S. L. (2007). Dscam2 mediates axonal tiling in the Drosophila visual system. *Nature*, *447*(7145), 720–

724. https://doi.org/10.1038/nature05855

Moorman, S. J. (1996). The inhibition of motility that results from contact between two oligodendrocytes in vitro can be blocked by pertussis toxin. *Glia*, *16*(3), 257–265. https://doi.org/10.1002/(SICI)1098-1136(199603)16:3<257::AID-GLIA8>3.0.CO;2-Z

Moransard, M., Sawitzky, M., Fontana, A., & Suter, T. (2009). Expression of the HGF receptor c-met by macrophages in experimental autoimmune encephalomyelitis. *Glia*, *58*(5), NA-NA. https://doi.org/10.1002/glia.20945

Nichols, E. L., Green, L. A., & Smith, C. J. (2018). Ensheathing cells utilize dynamic tiling of neuronal somas in development and injury as early as neuronal differentiation. *Neural Development*, *13*(1), 1–22. https://doi.org/10.1186/s13064-018-0115-8

Nishiyama, A., Boshans, L., Goncalves, C. M., Wegrzyn, J., & Patel, K. D. (2016). *Lineage, fate, and fate potential of NG2-glia.* https://doi.org/10.1016/j.brainres.2015.08.013

Noll, E., & Miller, R. H. (1993). Oligodendrocyte precursors originate at the ventral ventricular zone dorsal to the ventral midline region in the embryonic rat spinal cord. *Development*, *118*(2), 563–573. https://doi.org/10.1242/dev.118.2.563

Nord, H., Dennhag, N., Tydinger, H., & von Hofsten, J. (2019). The zebrafish HGF receptor met controls migration of myogenic progenitor cells in appendicular development. *PLOS ONE*, *14*(7), e0219259. https://doi.org/10.1371/journal.pone.0219259

Noren, N. K., & Pasquale, E. B. (2004). Eph receptor–ephrin bidirectional signals that target Ras and Rho proteins. *Cellular Signalling*, *16*(6), 655–666. https://doi.org/10.1016/j.cellsig.2003.10.006

Ohya, W., Funakoshi, H., Kurosawa, T., & Nakamura, T. (2007). Hepatocyte growth factor (HGF) promotes oligodendrocyte progenitor cell proliferation and inhibits

its differentiation during postnatal development in the rat. *Brain Research*, *1147*, 51–65. https://doi.org/10.1016/J.BRAINRES.2007.02.045

Park, H.-C., Mehta, A., Richardson, J. S., & Appel, B. (2002). olig2 Is Required for Zebrafish Primary Motor Neuron and Oligodendrocyte Development. *Developmental Biology*, *248*(2), 356–368. https://doi.org/10.1006/dbio.2002.0738

Park, H.-C., Shin, J., Roberts, R. K., & Appel, B. (2007). An olig2 reporter gene marks oligodendrocyte precursors in the postembryonic spinal cord of zebrafish. *Developmental Dynamics*, *236*(12), 3402–3407. https://doi.org/10.1002/dvdy.21365

Patel, J. R., Williams, J. L., Muccigrosso, M. M., Liu, L., Sun, T., Rubin, J. B., & Klein, R. S. (2012). Astrocyte TNFR2 is required for CXCL12-mediated regulation of oligodendrocyte progenitor proliferation and differentiation within the adult CNS. *Acta Neuropathologica*, *124*(6), 847–860. https://doi.org/10.1007/s00401-012-1034-0

Perlman, K., Couturier, C. P., Yaqubi, M., Tanti, A., Cui, Q., Pernin, F., Stratton, J. A., Ragoussis, J., Healy, L., Petrecca, K., Dudley, R., Srour, M., Hall, J. A., Kennedy, T. E., Mechawar, N., & Antel, J. P. (2020). Developmental trajectory of oligodendrocyte progenitor cells in the human brain revealed by single cell RNA sequencing. *Glia*, glia.23777. https://doi.org/10.1002/glia.23777

Peterson, S. M., & Freeman, J. L. (2009). RNA isolation from embryonic zebrafish and cDNA synthesis for gene expression analysis. *Journal of Visualized Experiments*, *30*, 1470. https://doi.org/10.3791/1470

Piller, M., Werkman, I. L., Brown, E. A., Latimer, A. J., & Kucenas, S. (2021). Glutamate signaling via the AMPAR subunit GluR4 regulates oligodendrocyte progenitor cell migration in the developing spinal cord. *The Journal of Neuroscience*, JN-RM-2562-20. https://doi.org/10.1523/JNEUROSCI.2562-20.2021

Ponzetto, C., Zhen, Z., Audero, E., Maina, F., Bardelli, A., Basile, M. L., Giordano, S., Narsimhan, R., & Comoglio, P. (1996). Specific uncoupling of GRB2 from the

met receptor: Differential effects on transformation and motility. *Journal of Biological Chemistry*, *271*(24), 14119–14123. https://doi.org/10.1074/jbc.271.24.14119

Prat, M., Crepaldi, T., Pennacchietti, S., Bussolino, F., & Comoglio, P. M. (1998). *Agonistic monoclonal antibodies against the Met receptor dissect the biological responses to HGF*. http://jcs.biologists.org/content/joces/111/2/237.full.pdf

Prestoz, L., Chatzopoulou, E., Lemkine, G., Spassky, N., Lebras, B., Kagawa, T., Ikenaka, K., Zalc, B., & Thomas, J.-L. (2004). Control of axonophilic migration of oligodendrocyte precursor cells by Eph-ephrin interaction. *Neuron Glia Biology*, *1*(1), 73–83. https://doi.org/doi:10.1017/S1740925X04000109

Rajasekharan, S., Baker, K. A., Horn, K. E., Jarjour, A. A., Antel, J. P., & Kennedy, T. E. (2009). Netrin 1 and Dcc regulate oligodendrocyte process branching and membrane extension via Fyn and RhoA. *Development*, *136*(3), 415–426. https://doi.org/10.1242/dev.018234

Rajasekharan, S., Bin, J. M., Antel, J. P., & Kennedy, T. E. (2010). A central role for RhoA during oligodendroglial maturation in the switch from Netrin-1-mediated chemorepulsion to process elaboration. *Journal of Neurochemistry*, *113*(6), 1589–1597. https://doi.org/10.1111/j.1471-4159.2010.06717.x

Ravanelli, A. M., Kearns, C. A., Powers, R. K., Wang, Y., Hines, J. H., Donaldson, M. J., & Appel, B. (2018). Sequential Specification of Oligodendrocyte Lineage Cells by Distinct Levels of Hedgehog and Notch Signaling. *Developmental Biology*. https://doi.org/10.1016/j.ydbio.2018.10.004

Richardson, W. D., Kessaris, N., & Pringle, N. (2006). Oligodendrocyte wars. *Nature Reviews Neuroscience*, *7*(1), 11–18. https://doi.org/10.1038/nrn1826

Richter-Landsberg, C. (2008). The cytoskeleton in oligodendrocytes: Microtubule dynamics in health and disease. In *Journal of Molecular Neuroscience* (Vol. 35, Issue 1, pp. 55–63). Springer. https://doi.org/10.1007/s12031-007-9017-7

Rodger, J., Salvatore, L., & Migani, P. (2012). Should I Stay or Should I Go? Ephs and Ephrins in Neuronal Migration Ephs and Ephrins in Neuronal Migration. *Neurosignals*, *20*, 190–201. https://doi.org/10.1159/000333784

Ross, E. F., Ali, M. F., Woo, L. A., Chadwick, S. R., Lee, E., Sangston, R. M., Sood, C., Zhang, Q., Zhang, X., Deppmann, C. D., Ross, E. F., Ali, M. F., Woo, L. A., Chadwick, S. R., Lee, E., Sangston, R. M., Sood, C., Zhang, Q., Zhang, X., & Deppmann, C. D. (2016). Reverse Signalling. *ELS*, *September*, 1–7. https://doi.org/10.1002/9780470015902.a0026897

Ruggieri, S., Tortorella, C., & Gasperini, C. (2017). Anti lingo 1 (opicinumab) a new monoclonal antibody tested in Relapsing Remitting Multiple Sclerosis. *Expert Review of Neurotherapeutics*, 14737175.2017.1378098. https://doi.org/10.1080/14737175.2017.1378098

Russell, L. N., & Lampe, K. J. (2017). Oligodendrocyte Precursor Cell Viability, Proliferation, and Morphology is Dependent on Mesh Size and Storage Modulus in 3D Poly(ethylene glycol)-Based Hydrogels. *ACS Biomaterials Science and Engineering*, *3*(12), 3459–3468. https://doi.org/10.1021/acsbiomaterials.7b00374

Sanchez-Rodriguez, M. A., Gomez, O., Esteban, P. F., Garcia-Ovejero, D., & Molina-Holgado, E. (2018). The endocannabinoid 2-arachidonoylglycerol regulates oligodendrocyte progenitor cell migration. *Biochemical Pharmacology*. https://doi.org/10.1016/j.bcp.2018.09.006

Shin, J., Park, H. C., Topczewska, J. M., Madwsley, D. J., & Appel, B. (2003). Neural cell fate analysis in zebrafish using olig2 BAC transgenics. *Methods in Cell Science*, *25*(1–2), 7–14. https://doi.org/10.1023/B:MICS.0000006847.09037.3a

Smith, C. J., Morris, A. D., Welsh, T. G., & Kucenas, S. (2014). Contact-Mediated Inhibition Between Oligodendrocyte Progenitor Cells and Motor Exit Point Glia Establishes the Spinal Cord Transition Zone. *PLoS Biology*, *12*(9), e1001961. https://doi.org/10.1371/journal.pbio.1001961

Soriano, J. V, Pepper, M. S., Nakamura, T., Orci, L., & Montesano, R. (1995). Hepatocyte growth factor stimulates extensive development of branching duct-like structures by cloned mammary gland epithelial cells. *Journal of Cell Science*, *108 ( Pt 2*(2), 413–430. http://www.ncbi.nlm.nih.gov/pubmed/7768990

Spassky, N., de Castro, F., Le Bras, B., Heydon, K., oise Qué raud-LeSaux, F., Bloch-Gallego, E., Ché dotal, A., Zalc, B., & on Thomas, J.-L. (2002). Directional Guidance of Oligodendroglial Migration by Class 3 Semaphorins and Netrin-1. *Journal of Neuroscience*, *22*(14), 5992–6004.

Spitzer, S. O., Sitnikov, S., Kamen, Y., & De Faria, O. (2018). Oligodendrocyte Progenitor Cells Become Regionally Diverse and Heterogeneous with Age. *Neuron*. https://doi.org/10.1016/j.neuron.2018.12.020

Sugimoto, Y., Taniguchi, M., Yagi, T., Akagi, Y., Nojyo, Y., & Tamamaki, N. (2001). Guidance of glial precursor cell migration by secreted cues in the developing optic nerve. *Development*, *128*(17).

Sun, Y., Deng, Y., Xiao, M., Hu, L., Li, Z., & Chen, C. (2017). Chondroitin sulfate proteoglycans inhibit the migration and differentiation of oligodendrocyte precursor cells and its counteractive interaction with laminin. *International Journal of Molecular Medicine*. https://doi.org/10.3892/ijmm.2017.3153

Talbot, J. C., & Amacher, S. L. (2014). A streamlined CRISPR pipeline to reliably generate zebrafish frameshifting alleles. *Zebrafish*, *11*(6), 583–585. https://doi.org/10.1089/zeb.2014.1047

Talbot, J. C., Teets, E. M., Ratnayake, D., Duy, P. Q., Currie, P. D., & Amacher, S. L. (2019). Muscle precursor cell movements in zebrafish are dynamic and require six family genes. *Development (Cambridge)*, *146*(10). https://doi.org/10.1242/dev.171421

Tallafuss, A., & Eisen, J. S. (2008). The Met receptor tyrosine kinase prevents zebrafish primary motoneurons from expressing an incorrect neurotransmitter.

*Neural Development*, *3*(1), 18. https://doi.org/10.1186/1749-8104-3-18

Tamagnone, L., & Comoglio, P. M. (1997). Control of invasive growth by hepatocyte growth factor (HGF) and related scatter factors. In *Cytokine and Growth Factor Reviews* (Vol. 8, Issue 2, pp. 129–142). Elsevier Ltd. https://doi.org/10.1016/S1359-6101(97)00007-5

Temple, S., & Raff, M. C. (1986). Clonal analysis of oligodendrocyte development in culture: Evidence for a developmental clock that counts cell divisions. *Cell*, *44*(5), 773–779. https://doi.org/10.1016/0092-8674(86)90843-3

Than-Trong, E., & Bally-Cuif, L. (2015). Radial glia and neural progenitors in the adult zebrafish central nervous system. In *GLIA* (Vol. 63, Issue 8, pp. 1406–1428). John Wiley and Sons Inc. https://doi.org/10.1002/glia.22856

Thomason, E. J., Escalante, M., Osterhout, D. J., & Fuss, B. (2020). The oligodendrocyte growth cone and its actin cytoskeleton: A fundamental element for progenitor cell migration and CNS myelination. In *GLIA* (Vol. 68, Issue 7, pp. 1329–1346). John Wiley and Sons Inc. https://doi.org/10.1002/glia.23735

Truett, G. E., Heeger, P., Mynatt, R. L., Truett, A. A., Walker, J. A., & Warman, M. L. (2000). Preparation of PCR-quality mouse genomic dna with hot sodium hydroxide and tris (HotSHOT). *BioTechniques*, *29*(1), 52–54. https://doi.org/10.2144/00291bm09

Tsai, H.-H. (2006). Netrin-1 Is Required for the Normal Development of Spinal Cord Oligodendrocytes. *Journal of Neuroscience*, *26*(7), 1913–1922. https://doi.org/10.1523/JNEUROSCI.3571-05.2006

Tsai, H.-H., Frost, E., To, V., Robinson, S., Ffrench-Constant, C., Geertman, R., Ransohoff, R. M., Miller, R. H., Anisowicz, A., Bardwell, L., Sager, R., Armstrong, R., Harvath, L., Dubois-Dalcq, M., Baggiolini, M., Baggiolini, M., Baggiolini, M., Dewald, B., Moser, B., … Littman, D. R. (2002). The chemokine receptor CXCR2 controls positioning of oligodendrocyte precursors in

developing spinal cord by arresting their migration. *Cell*, *110*(3), 373–383. https://doi.org/10.1016/S0092-8674(02)00838-3

Unal, D. B., Caliari, S. R., & Lampe, K. J. (2019). Engineering biomaterial microenvironments to promote myelination in the central nervous system. In *Brain Research Bulletin* (Vol. 152, pp. 159–174). Elsevier Inc. https://doi.org/10.1016/j.brainresbull.2019.07.013

Unal, D. B., Caliari, S. R., & Lampe, K. J. (2020). 3D Hyaluronic Acid Hydrogels for Modeling Oligodendrocyte Progenitor Cell Behavior as a Function of Matrix Stiffness. *Biomacromolecules*, *21*(12), 4962–4971. https://doi.org/10.1021/acs.biomac.0c01164

van Tilborg, E., de Theije, C. G. M., van Hal, M., Wagenaar, N., de Vries, L. S., Benders, M. J., Rowitch, D. H., & Nijboer, C. H. (2017). Origin and dynamics of oligodendrocytes in the developing brain: Implications for perinatal white matter injury. *Glia*. https://doi.org/10.1002/glia.23256

Vanderlaan, G., Tyurina, O. V., Karlstrom, R. O., & Chandrasekhar, A. (2005). Gli function is essential for motor neuron induction in zebrafish. *Developmental Biology*, *282*(2), 550–570. https://doi.org/10.1016/j.ydbio.2005.04.010

Viganò, F., & Dimou, L. (2016). *The heterogeneous nature of NG2-glia*. https://doi.org/10.1016/j.brainres.2015.09.012

Villar-Cerviño, V., Molano-Mazón, M., Catchpole, T., Valdeolmillos, M., Henkemeyer, M., Martínez, L. M., Borrell, V., Marín, O., Abercrombie, M., Abercrombie, M., Heaysman, J. E., Alcántara, S., Pozas, E., Ibañez, C. F., Soriano, E., Anderson, S. A., Eisenstat, D. D., Shi, L., Rubenstein, J. L. R., … Grove, E. A. (2013). Contact repulsion controls the dispersion and final distribution of Cajal-Retzius cells. *Neuron*, *77*(3), 457–471. https://doi.org/10.1016/j.neuron.2012.11.023

Viticchiè, G., Muller, P., Viticchiè, G., & Muller, P. A. J. (2015). c-Met and Other Cell

Surface Molecules: Interaction, Activation and Functional Consequences. *Biomedicines*, *3*(1), 46–70. https://doi.org/10.3390/biomedicines3010046

Wang, C., Wang, Y., Wang, Y., Wu, C.-T., & Yu, G. (2019). muSSP: Efficient Min-cost Flow Algorithm for Multi-object Tracking. In *Advances in Neural Information Processing Systems* (Vol. 32).

Wang, Y., Ali, M., Wang, Y., Kucenas, S., & Yu, G. (2018). Detection and tracking of migrating oligodendrocyte progenitor cells from in vivo fluorescence time-lapse imaging data. *Proceedings - International Symposium on Biomedical Imaging*, *2018-April*, 961–964. https://doi.org/10.1109/ISBI.2018.8363730

Wang, Y., Wang, C., Ranefall, P., Broussard, G. J., Wang, Y., Shi, G., Lyu, B., Wu, C. T., Wang, Y., Tian, L., & Yu, G. (2020). SynQuant: An automatic tool to quantify synapses from microscopy images. *Bioinformatics*, *36*(5), 1599–1606. https://doi.org/10.1093/bioinformatics/btz760

Warf, B. C., Fok-Seang, J., & Miller, R. H. (1991). Evidence for the ventral origin of oligodendrocyte precursors in the rat spinal cord. *Journal of Neuroscience*, *11*(8), 2477–2488. https://doi.org/10.1523/jneurosci.11-08-02477.1991

Watson, A. E. S., Goodkey, K., Footz, T., & Voronova, A. (2020). Regulation of CNS precursor function by neuronal chemokines. In *Neuroscience Letters* (Vol. 715, p. 134533). Elsevier Ireland Ltd. https://doi.org/10.1016/j.neulet.2019.134533

Wong, W. T., Faulkner-Jones, B. E., Sanes, J. R., & Wong, R. O. L. (2000). Rapid dendritic remodeling in the developing retina: Dependence on neurotransmission and reciprocal regulation by Rac and Rho. *Journal of Neuroscience*, *20*(13), 5024–5036. https://doi.org/10.1523/jneurosci.20-13-05024.2000

Wong, W. T., & Wong, R. O. L. (2001). Changing specificity of neurotransmitter regulation of rapid dendritic remodeling during synaptogenesis. *Nature Neuroscience*, *4*(4), 351–352. https://doi.org/10.1038/85987

Yamamoto, Y., Livet, J., Pollock, R. A., Garces, A., Arce, V., deLapeyriere, O., &

Henderson, C. E. (1997). Hepatocyte growth factor (HGF/SF) is a muscle-derived survival factor for a subpopulation of embryonic motoneurons. *Development*, *124*(15), 2903–2913. https://doi.org/10.1242/dev.124.15.2903

Yan, H., & Rivkees, S. A. (2002). Hepatocyte growth factor stimulates the proliferation and migration of oligodendrocyte precursor cells. *Journal of Neuroscience Research*, *69*(5), 597–606. https://doi.org/10.1002/jnr.10323

Yin, W., & Hu, B. (2014). Knockdown of Lingo1b protein promotes myelination and oligodendrocyte differentiation in zebrafish. *Experimental Neurology*, *251*, 72–83. https://doi.org/10.1016/j.expneurol.2013.11.012

Ying, Y., Yan, X., Jin, S., Liang, Y., Hou, L., Niu, W., & Luo, X. (2018). Inhibitory Effect of LPS on the Proliferation of Oligodendrocyte Precursor Cells through the Notch Signaling Pathway in Intrauterine Infection-induced Rats. *Current Medical Science*, *38*(5), 840–846. https://doi.org/10.1007/s11596-018-1951-9

Zeisel, A., Muñoz-Manchado, A. B., Codeluppi, S., Lönnerberg, P., La Manno, G., Juréus, A., Marques, S., Munguba, H., He, L., Betsholtz, C., Rolny, C., Castelo-Branco, G., Hjerling-Leffler, J., & Linnarsson, S. (2015). Cell types in the mouse cortex and hippocampus revealed by single-cell RNA-seq. *Science*, *347*(6226).

Zhang, J., & Babic, A. (2015). Regulation of the MET oncogene: Molecular mechanisms. In *Carcinogenesis* (Vol. 37, Issue 4, pp. 345–355). Oxford University Press. https://doi.org/10.1093/carcin/bgw015

Zhang, Y., Chen, K., Sloan, S. A., Bennett, M. L., Scholze, A. R., O 'keeffe, S., Phatnani, H. P., Guarnieri, X. P., Caneda, C., Ruderisch, N., Deng, S., Liddelow, S. A., Zhang, C., Daneman, R., Maniatis, T., Barres, B. A., Jia, X., & Wu, Q. (n.d.). *An RNA-Sequencing Transcriptome and Splicing Database of Glia, Neurons, and Vascular Cells of the Cerebral Cortex*. https://doi.org/10.1523/JNEUROSCI.1860-14.2014

Zhang, Y., Zhang, Y. P., Pepinsky, B., Huang, G., Shields, L. B. E., Shields, C. B., &

Mi, S. (2015). Inhibition of LINGO-1 promotes functional recovery after experimental spinal cord demyelination. *Experimental Neurology*, *266*, 68–73. https://doi.org/10.1016/j.expneurol.2015.02.006

Zhou, Q., Choi, G., & Anderson, D. J. (2001). The bHLH Transcription Factor Olig2 Promotes Oligodendrocyte Differentiation in Collaboration with Nkx2.2. *Neuron*, *31*(5), 791–807. https://doi.org/10.1016/S0896-6273(01)00414-7

Zhu, B., Nicholls, M., Gu, Y., Zhang, G., Zhao, C., Franklin, R., Song, B., Zhu, B., Nicholls, M., Gu, Y., Zhang, G., Zhao, C., Franklin, R. J. M., & Song, B. (2016). Electric Signals Regulate the Directional Migration of Oligodendrocyte Progenitor Cells (OPCs) via β1 Integrin. *International Journal of Molecular Sciences*, *17*(11), 1948. https://doi.org/10.3390/ijms17111948

Zhu, Y., Crowley, S. C., Latimer, A. J., Lewis, G. M., Nash, R., & Kucenas, S. (2019). Migratory Neural Crest Cells Phagocytose Dead Cells in the Developing Nervous System. *Cell*, *179*(1), 74-89.e10. https://doi.org/10.1016/j.cell.2019.08.001

Zimmer, M., Palmer, A., Köhler, J., & Klein, R. (2003). EphB–ephrinB bi-directional endocytosis terminates adhesion allowing contact mediated repulsion. *Nature Cell Biology*, *5*(10), 869–878. https://doi.org/10.1038/ncb1045

Zuchero, J. B., Fu, M. meng, Sloan, S. A., Ibrahim, A., Olson, A., Zaremba, A., Dugas, J. C., Wienbar, S., Caprariello, A. V., Kantor, C., Leonoudakus, D., Lariosa-Willingham, K., Kronenberg, G., Gertz, K., Soderling, S. H., Miller, R. H., & Barres, B. A. (2015). CNS Myelin Wrapping Is Driven by Actin Disassembly. *Developmental Cell*, *34*(2), 152–167. https://doi.org/10.1016/j.devcel.2015.06.011